

Glycopeptide Enrichment Workflows for Downstream  
Mass Spectrometric Analysis

by

Edward D. Bodnar

A Thesis submitted to the Faculty of Graduate Studies of  
The University of Manitoba  
in partial fulfillment of the requirements of the degree of

DOCTOR OF PHILOSOPHY

Department of Chemistry

Copyright © 2015 by Edward Bodnar

## Abstract

Mass spectrometry (MS) is a power analytical tool which is capable of analyzing biomolecules in great detail, both structurally and quantitatively. With regards to glycans, special considerations regarding sample preparation are necessary in order to achieve reproducible identification and relative quantification of these analytes. A workflow for isolation at the glycopeptide level and subsequent detection at the glycan level with phenylhydrazine, demonstrated that monoclonal antibodies (mAbs) containing a specific amino acid mutation were able to express approximately an additional 50% of the  $\alpha$ 2,6 disialylated glycan compared to their non-mutant analogues. In a second experiment using mAbs, an azide modified glycan (Ac<sub>4</sub>ManAz) was introduced both metabolically and enzymatically during mAb production. This glycan is a precursor in the sialic acid pathway and the azide moiety allows for specific chemistry post-production including the potential for highly specific enrichment. The results of this workflow demonstrated that [100  $\mu$ M] of Ac<sub>4</sub>ManAz precursor added to the cell media was necessary for metabolic expression. More complex samples however, may contain multiple sites of glycosylation. To conserve the site of attachment, these molecules are often studied at the glycopeptide level, and require enrichment of glycopeptides to improve the lower signal intensity observed in the presence of co-eluting peptides. Carboxymethyl chitosan (CMCH) as well as amine-functionalized magnetic-nanoparticles (MNP) were developed as novel materials for this purpose. CMCH is naturally occurring, and therefore is cost-effective and readily available. In a 12 protein mixture CMCH demonstrated the bulk enrichment of glycopeptides yielding an approximately 20% higher enrichment of sialylated species as compared to a commercially available glycopeptide kit through the use of tandem mass tags for relative quantification. In the same approach, amine functionalized MNP were produced and used to enrich glycopeptides from tryptic digests. This approach was fast (about 10 mins) and quantitatively demonstrated improved retention for sialylated species. Examples of these techniques and their applications are reported in this work.

## Acknowledgements

First and foremost I would like to thank my Ph.D. supervisor Dr. H          , who introduced me into the field of biological mass spectrometry and bioanalytical techniques. While allowing the freedom to pursue my own research endeavors, Dr. Perreault has provided me unconditional support and has expressed extreme interest in my research throughout the course of my Ph.D. with a welcoming demeanor and open door policy. I would also like to thank the other members of my thesis committee including Dr. Oleg Krokhin, Dr. Michael Butler , Dr. Joe O'Neil, and Dr. Doug Goltz as well as my external examiner Dr. Liang Li for their time, comments and suggestions regarding my research. Sincere appreciation is expressed towards Dr. Werner Ens, Dr. Kenneth G. Standing as well as Dr. David Shearer of the Time-of-Flight Laboratory, Department of Physics, University of Manitoba for use of instrumentation and support during my graduate studies.

I would like to thank all members of my laboratory, past and present including: Dr. S. Snovida, Dr. E. Lattova, and Emy Komatsu. To my collaborators external to the university: Dr. J. Saba, and Dr. R. Viner of Thermo Fisher Scientific, as well as, Dr. Y. Durocher and C. Raymond at the National Research Council, for suggestions, conversation and overall enjoyment throughout the course of my studies; it has been a pleasure. To my friends, Dr. Taras Babiak, Justin Jacob, Drew Hawranik, and Dr. Shaune McFarlane I thank you for your conversations and advice both personal and academic. Sincere appreciation is also expressed to my friends Brent Delaine, Shane Sauv    , and cousin Ben Davidson, for countless hours of intellectual conversation, while partaking in many beverages. Lastly, I would like to express gratitude and appreciation to my family for their unconditional love, support and understanding.

Thank you!

They say a midget standing on a giant's shoulders can see much further than the giant;

## Table of Contents

Abstract .....	ii
Acknowledgements .....	3
Table of Contents .....	5
Abbreviations .....	13
Standard Abbreviations and Masses of the 20 Common Amino Acids' Residues .....	15
List of Tables.....	16
List of Figures.....	17
Chapter 1 - Introduction .....	20
1.1    Introduction to Glycobiology .....	21
1.11    Protein Glycosylation .....	22
1.2    Implements of a Glycoprotein Analysis Workflow.....	29
1.21    Overview .....	29
1.22    Glycan Release .....	30
1.23    Enrichment of glycopeptides/glycoproteins using lectins.....	33
1.3    Mass Spectrometry .....	35
1.31    Ionization Sources in Mass Spectrometry.....	35
1.311    Electrospray Ionization (ESI).....	36

1.312	Matrix assisted laser desorption ionization (MALDI).....	38
1.32	Mass Analyzers.....	40
1.321	Quadrupole .....	40
1.322	Time of Flight (TOF).....	43
1.33	Tandem MS Fragmentation .....	49
1.4	Separation and Derivatization Techniques .....	54
1.41	Chromatography .....	54
1.42	Derivatization .....	58
1.5	Research Goals .....	63
1.6	References.....	66
Chapter 2 – Glycan Analysis of biopharmaceutical Monoclonal Antibodies.....		75
2.1	Authors Contributions.....	76
2.2	Abstract .....	77
2.3	Introduction.....	78
2.4	Experimental .....	81
2.41	Materials .....	81
2.42	Methods .....	81
2.421	Glycopeptide Preparation & Digestion .....	81
2.422	High Performance Liquid Chromatography (HPLC).....	82

2.423	Glycan Derivatization using Phenylhydrazine (PHN) .....	82
2.424	Mass Spectrometric Analysis .....	83
2.5	Results & Discussion.....	83
	<i>Isolation of Glycopeptides</i> .....	83
	<i>MS-MS determination of adducts</i> .....	86
	<i>Glycopeptide analysis of mAb sialylation</i> .....	89
	Glycan analysis of mAbs using phenylhydrazine .....	91
	<i>Incorporation of metastable ions</i> .....	95
2.6	Conclusion .....	96
2.7	Acknowledgements.....	98
2.8	References.....	99
Chapter 3 - Qualitative and Quantitative Assessment on the use of Amine Functionalized		
	Magnetic Nanoparticles for Glycopeptide Enrichment .....	101
3.1	Authors Contributions.....	102
3.2	Abstract .....	103
3.3	Introduction.....	104
3.4	Experimental .....	107
3.41	Materials .....	107
3.42	Methods .....	107

3.421	Glycopeptide Preparation & Digestion .....	107
3.422	Tandem Mass Tag (TMT) labeling .....	108
3.423	Glycopeptide Enrichment.....	108
3.424	Mass Spectrometric Analysis .....	110
3.425	Data Analysis .....	111
3.5	Results & Discussion.....	112
	<i>Method Development of MNP</i> .....	112
	<i>TMT Comparison</i> .....	114
	<i>Data Analysis</i> .....	118
3.6	Conclusions.....	121
3.7	Acknowledgements.....	123
3.8	Supporting Information.....	124
3.9	References.....	126
Chapter 4 – The Synthesis and Evaluation of Carboxymethyl Chitosan for Glycopeptide		
	Enrichment.....	130
4.1	Authors Contributions.....	131
4.2	Abstract .....	132
4.3	Introduction.....	133
4.4	Experimental .....	134



4.41	Materials .....	134
4.42	Methods .....	135
4.421	CMCH Synthesis.....	135
4.422	Glycopeptide Preparation & Digestion .....	136
4.423	Tandem Mass Tag (TMT) labeling .....	136
4.424	Glycopeptide Enrichment.....	137
4.425	Mass Spectrometric Analysis .....	138
4.426	ATR-FTIR Analysis .....	139
4.427	TEM Imaging.....	139
4.428	Data Analysis .....	139
4.5	Results and discussion.....	140
	<i>Development and characterization of CMCH .....</i>	<i>140</i>
	<i>Preliminary enrichment using CMCH .....</i>	<i>144</i>
	<i>Enrichment of 12 proteins using CMCH .....</i>	<i>147</i>
	<i>Data analysis using Byonic .....</i>	<i>148</i>
	<i>Method Comparison .....</i>	<i>151</i>
	<i>Summary .....</i>	<i>152</i>
4.6	Conclusion .....	154
4.7	Acknowledgments.....	155

4.8	References.....	156
Chapter 5 – Metabolic Glycan Engineering for the Recovery and Analysis of Sialic Acids.....		159
5.1	Authors Contributions.....	160
5.2	Abstract .....	161
5.3	Introduction.....	162
5.4	Experimental .....	165
5.41	Materials .....	165
5.42	Methods .....	165
5.421	Preparation of Azidomannosamine .....	165
5.422	Plasmids and Proteins .....	166
5.423	Cell Culture and Ac <sub>4</sub> ManNAz incorporation.....	166
5.424	Transfection.....	167
5.425	mAb Production .....	167
5.426	Synthesis of CMP-N-azidoacetylneuraminic acid (CMP-SiaNAz) .....	168
5.427	Enzymatic Addition of SiaNAz on TZMm2.....	168
5.428	Preparation & Digestion of Monoclonal Antibodies.....	169
5.429	HPLC Separation of Glycopeptides.....	169
5.430	Mass Spectrometric Analysis .....	170
5.431	Nuclear Magnetic Resonance Analysis.....	170

5.5	Results & Discussion.....	171
	<i>Enzymatic addition of CMP-SiaNAz .....</i>	<i>171</i>
	<i>Monitoring sialylation with lectins .....</i>	<i>171</i>
	<i>Isolating glycopeptides .....</i>	<i>172</i>
	<i>MS Analysis of Enzymatically attached SiaNAz .....</i>	<i>174</i>
	<i>Synthesis and characterization of Ac<sub>4</sub>ManNAz .....</i>	<i>175</i>
	<i>Metabolic incorporation of Ac<sub>4</sub>ManNAz.....</i>	<i>177</i>
	<i>MS Analysis of metabolically cultured SiaNAz mAbs.....</i>	<i>178</i>
5.6	Conclusion .....	182
5.7	Acknowledgements.....	183
5.8	References.....	184
Chapter 6 –Considerations & Future Work .....		188
6.0	Conclusions.....	189
6.01	General Overview .....	189
6.02	Analysis of Highly Sialylated Glycoproteins .....	194
6.03	Magnetic Nanoparticles for Glycopeptide Enrichment .....	196
6.04	Carboxymethyl Chitosan for Glycopeptide Enrichment .....	197
6.05	Glyco-Engineering using ManAz for the Analysis of Sialylation in Mabs.....	199
6.1	Closing Summary .....	200

6.2    References..... 202

## Abbreviations

Ac <sub>4</sub> ManNAz	per-acetylated azidomannosamine
ACN	Acetonitrile
Asn	asparagines
BNG	Bradbury-Nielson gate
CHCA	α-cyano 4-hydroxycinnamic acid
CHO	Chinese hamster ovary
CAD	collision activated dissociation
CMCH	carboxymethyl chitosan
Da	Dalton
DC	direct current
DHB	2,5-Dihydroxybenzoic Acid; Gentisic Acid
DTT	Dithiothreitol
ESI	electrospray Ionization
ETD	electron transfer dissociation
Fuc	Fucose
GAG	Glycosaminoglycan
Gal	Galactose
GalNAc	<i>N</i> -acetylgalactosamine
Glc	Glucose
GlcNAc	<i>N</i> -acetylglucosamine
GPI	glycophospholipid inositol anchor
GSL	Glycosphingolipid
h	Hour
H <sub>2</sub> O	Water
HCD	higher-energy C-trap dissociation
HILIC	hydrophilic interaction liquid chromatography
HPLC	high performance liquid chromatography
IA	Iodoacetamide
L	Liter
LC	liquid chromatography

μ	Micro; $\times 10^{-6}$
M	Molar
mAb	monoclonal antibody
MALDI	matrix-assisted laser desorption ionization
Man	Mannose
ManNAz	Azidomannosamine
MeOH	Methanol
MS	mass spectrometry
MS <sup>2</sup> ; MS/MS	tandem mass spectrometry
<i>m/z</i>	Mass to charge ratio
Neu5Ac	N-Acetylneuraminic acid
Neu5Gc	N-Glycolylneuraminic acid
NMR	nuclear magnetic resonance
PHN	phenylhydrazine
PNGaseF	peptide N-glycosidase F
PTM	post translational modification
Q	quadrupole
q	quadrupole-collision cell for MS/MS
QqQ	triple quadrupole
QqTOF	quadrupole-quadrupole time-of-flight
RF	radio-frequency
RP	reversed phase
SA	3,5-dimethoxy-4-hydroxycinnamic acid; Sinapinic Acid
TEAB	triethyl ammonium bicarbonate
TFA	trifluoroacetic acid
TMT	tandem mass tag
TOF	time-of-flight
TOF/TOF	tandem time-of-flight
UV	ultraviolet
X	any amino acid

## Standard Abbreviations and Masses of the 20 Common Amino Acids' Residues

1-letter code	3-letter code	Chemical formula	Monoisotopic (Da)	Average (Da)
A	Ala	C <sub>3</sub> H <sub>5</sub> ON	71.03711	71.0788
R	Arg	C <sub>6</sub> H <sub>12</sub> ON <sub>4</sub>	156.10111	156.1875
N	Asn	C <sub>4</sub> H <sub>6</sub> O <sub>2</sub> N <sub>2</sub>	114.04293	114.1038
D	Asp	C <sub>4</sub> H <sub>5</sub> O <sub>3</sub> N	115.02694	115.0886
C	Cys	C <sub>3</sub> H <sub>5</sub> ONS	103.00919	103.1388
Q	Gln	C <sub>5</sub> H <sub>8</sub> O <sub>2</sub> N <sub>2</sub>	128.05858	128.1307
E	Glu	C <sub>5</sub> H <sub>7</sub> O <sub>3</sub> N	129.04259	129.1155
G	Gly	C <sub>2</sub> H <sub>3</sub> ON	57.02146	57.0519
H	His	C <sub>6</sub> H <sub>7</sub> ON <sub>3</sub>	137.05891	137.1411
I	Ile	C <sub>6</sub> H <sub>11</sub> ON	113.08406	113.1594
L	Leu	C <sub>6</sub> H <sub>11</sub> ON	113.08406	113.1594
K	Lys	C <sub>6</sub> H <sub>12</sub> ON <sub>2</sub>	128.09496	128.1741
M	Met	C <sub>5</sub> H <sub>9</sub> ONS	131.04049	131.1926
F	Phe	C <sub>9</sub> H <sub>9</sub> ON	147.06841	147.1766
P	Pro	C <sub>5</sub> H <sub>7</sub> ON	97.05276	97.1167
S	Ser	C <sub>3</sub> H <sub>5</sub> O <sub>2</sub> N	87.03203	87.0782
T	Thr	C <sub>4</sub> H <sub>7</sub> O <sub>2</sub> N	101.04768	101.1051
W	Trp	C <sub>11</sub> H <sub>10</sub> ON <sub>2</sub>	186.07931	186.2132
Y	Tyr	C <sub>9</sub> H <sub>9</sub> O <sub>2</sub> N	163.06333	163.1760
V	Val	C <sub>5</sub> H <sub>9</sub> ON	99.06841	99.1326

\* Taken from the Expert Protein Analysis System (ExPASy.org)

## List of Tables

Table 1.1 - Common glycans observed on mammalian proteins .....	24
Table 1.2 – Typically encountered lectins used for glycoprotein enrichment .....	34
Table 2.1- Relative percentages of ion abundances per glycoform species obtained by MALDI positive and negative ionization modes. Peak areas are normalized to FG2.....	91
Table 2.2 - Relative percentages of ion abundances per glycan species obtained by MALDI positive and negative ionization modes. Peak areas are normalized to FG2 where possible. ....	95
Table 3.1 – 126:127 TMT reporter ion abundance ratio for selected glycopeptides from each sample.....	120
Table 4.1 - Average TMT Ratios for three individual glycoproteins and number of observed glycopeptides.....	145
Table 4.2 - Average TMT Ratios for all glycoproteins in the mixture and number of observed glycopeptides.....	151



## List of Figures

Figure 1.1 - Typically encountered mammalian N-glycoforms containing a conserved pentasaccharide core.....	25
Figure 1.2 – Microheterogeneity vs. Macroheterogeneity .....	26
Figure 1.3 – Commonly observed Core O-glycans.....	27
Figure 1.4 - Specificity of Commonly Encountered Glycosidases .....	32
Figure 1.5 – Electrospray Source with the initial formation of a Taylor Cone.....	37
Figure 1.6 - Processes associated with MALDI Ionization.....	39
Figure 1.7 – Trajectories of ions in a Quadrupole.....	41
Figure 1.8 – Tandem MS using a Triple Quadrupole Instrument .....	42
Figure 1.9 - Separation of Ions in linear Time-of-Flight analyzer.....	44
Figure 1.10 - Components of a time-of-flight reflector <sup>81</sup> .....	46
Figure 1.11 - Comparing the Resolution of Linear and Reflecting TOF .....	47
Figure 1.12 - Operations of a Bradbury-Nielson Gate .....	48
Figure 1.13 – Schematic of ESI-QqTOF hybrid mass spectrometer .....	50
Figure 1.14 - Nomenclature for the fragmentation of Carbohydrates.....	51
Figure 1.15 - Fragmentation of a Glycopeptide.....	53
Figure 1.16 – General approach to partition chromatography .....	55
Figure 1.17 - Schiff-base formation for carbohydrate derivatization.....	60
Figure 1.18 - Commonly encountered carbohydrate derivatizing agents.....	60
Figure 1.19 - Tandem Mass Tags (TMT) used in proteomic workflows.....	62

Figure 2.1- Formation of Schiff-base using phenylhydrazine .....	79
Figure 2.2 - Workflow for Glycan and Glycopeptide analysis by Mass Spectrometry. ....	80
Figure 2.3 – N-glycans observed at N <sub>297</sub> on Trastuzumab .....	84
Figure 2.4 – MALDI mass spectra of glycopeptides from samples 5-20% and 5-20% m.....	86
Figure 2.5 – MS <sup>2</sup> spectrum of over-alkylated glycopeptide at 3015.75 <i>m/z</i> (FG2+H+57) <sup>+</sup> .....	88
Figure 2.6 – MS <sup>2</sup> spectrum of glycopeptide at 2997 <i>m/z</i> (FG2+H+39) <sup>+</sup> .....	89
Figure 2.7 - Monoclonal antibody glycans labeled on target with phenylhydrazine and analyzed in positive mode.....	93
Figure 2.8 - Monoclonal antibody glycans labelled on target with phenylhydrazine in negative mode. ....	94
Figure 3.1 - MALDI spectra of glycopeptides enriched by magnetic nanoparticles, collected in positive linear mode. ....	115
Figure 3.2 - A workflow used to compare the enrichment efficiency between the EMD method and MNP protocol.....	116
Figure 3.3 – Comparison of commercial kit to MNP method for enhanced sialylation .....	117
Figure 3.4 –HPLC/ESI-MS spectra highlighting glycopeptides from the combined EMD & MNP samples (a) α1 acid human, (b) fetuin bovine, (c) Eg2 mAb, (d) IgG human.....	118
Figure 3.5 – 126:127 TMT Reporter Ion Ratios.....	119
Figure 4.1 - Attachment of carboxymethyl chitosan onto an amino silica particle.....	142
Figure 4.2 – ATR-FTIR spectra of Si-NH <sub>2</sub> and Si-CMCH .....	143
Figure 4.3 - TEM Images at 40,000x magnification of Si-NH <sub>2</sub> and Si-CMCH.....	144
Figure 4.4 - MALDI spectra of Si-CMCH enriched tryptic glycopeptides .....	146

Figure 4.5 – Workflow used to compare the enrichment efficiency between Si-CMCH and EMD on a 12 protein mixture .....	148
Figure 4.6 - (A) Selected LC-MS spectrum highlighting the elution of various enriched glycopeptides. Molecular ions of each glycopeptide triggered (B) MS <sup>2</sup> analysis as demonstrated at 1057.92 <i>m/z</i> (4+), where (C) reporter ions 126 and 127 peak areas were compared.....	150
Figure 4.7 - Enrichment ratios for selected glycoforms of the same sequon determined using TMT-based quantitation .....	153
Figure 5.1 - Synthesis & Metabolic Workflow for Introducing an azido functionality onto Monoclonal Antibodies.....	164
Figure 5.2 – Monitoring sialylation using Western Blot analysis.....	172
Figure 5.3 – Mass Spectrum of Commonly Observed Fc typtic Glycopeptides from TZMm2....	173
Figure 5.4 – N-acetyl and N-azidoneuraminic acids .....	174
Figure 5.5 – MALDI-ToF and MALDI-ToF/ToF spectra of SiaNAz introduced enzymatically .....	175
Figure 5.6 – <sup>13</sup> C NMR spectrum of synthesized Ac <sub>4</sub> ManNAz acquired on a 400mHZ NMR compared to a theoretically generated spectrum.....	176
Figure 5.7 – ESI-MS spectrum of synthesized Ac <sub>4</sub> ManNAz precursor .....	177
Figure 5.8 - Workflow to Compare SiaNAz expression .....	178
Figure 5.9 – MALDI-ToF spectra of glycopeptides from TZMm2, expressed in the presence of Ac <sub>4</sub> ManNAz in increasing concentration .....	179

## **Chapter 1 - Introduction**

## 1.1 Introduction to Glycobiology

Some would consider the field of Glycobiology to be relatively young, with its beginning in the latter quarter of the last century. First coined by Rademacher, Parekh, and Dwek in 1988, “Glycobiology” represents the union between two well known areas of research: carbohydrate chemistry and biology. Glycobiology is a growing interdisciplinary field not only incorporating chemistry, biology and biotechnology as they apply to carbohydrates, but in addition spanning the fields of enzymology, immunology, virology, physics, bioinformatics and cellular biology while employing an arsenal of methodologies and techniques to manipulate and analyze glycan moieties<sup>1,2</sup>. The term monosaccharide refers to the individual sugars (Table 1.1) found in living organisms, whereas combinations of 2 or more sugars can be referred to as a glycan or oligosaccharide. It has been determined that glycosylation is one of the most common post translational modification (PTM) on proteins, generally being observed on 50% of proteins and often in more than a single location<sup>1,3,4</sup>.

Glycans are not limited entirely to proteins, as they are part of many other molecules such as glycosphingolipids (GSL)<sup>5</sup>, glycosyl-phosphatidylinositol anchors (GPI anchors)<sup>6</sup>, and glycosaminoglycans (GAG)<sup>7</sup> to name a few. The term to describe the aforementioned species is ‘glycoconjugate’, indicating that they bear one or more glycans as part of their structure. It is generally accepted that glycoconjugates have important roles in biology, influencing many properties of proteins such as stability, protease resistance, or quaternary structure<sup>8</sup>. It is clear from X-ray data that the presence of a sugar moiety can influence protein folding as well as its ability to bind with a receptor<sup>9,10</sup>. Carbohydrates are also key in cell surface recognition, where

an important example is the ability to recruit rolling neutrophils to sites of injury. Furthermore, studies have shown that processes including carcinogenesis alter cell surface glycosylation as the cells progress towards malignancy. The therapeutic significance of glycans to serve as biomarkers to track changes in disease is therefore well recognized<sup>11,12</sup>.

### 1.11 Protein Glycosylation

To be able to entirely elucidate the structural and functional characteristics of a glycoprotein, it is best to begin with knowing how it is biosynthesized. Glycosyltransferases present in the Endoplasmic Reticulum (ER) and Golgi are enzymes responsible for the sequential addition and trimming of glycans on glycoproteins. Two main forms are produced, N-linked and O-linked. The production of N-linked glycans begin in the ER where a high-mannose precursor is synthesized onto a lipid carrier known as dolicholphosphate<sup>13</sup>. This precursor may subsequently be transferred by an oligosaccharyltransferase (OST) enzyme to a nascent protein containing an asparagine (Asn; N-linked) of a consensus motif: Asn-X-Ser/Thr (whereby X can be any amino acid except proline). The protein hence becomes post translationally modified. Further trimming of the precursor occurs in the ER as well, namely by the removal of glucose and of some mannose sugars. Next, the glycoprotein is transferred to the Golgi apparatus which contains three compartments termed *cis*, *medial*, and *trans* which together span across roughly six cisternae<sup>14</sup>. As the glycoprotein passes through each of these cisternae, various sugars may be added or removed. In particular, early cleavage enzymes such as  $\alpha$ -mannosidase-1 have been located in the *cis*-Golgi<sup>15</sup>, whereas N-acetyl glucosamine-transferase-1<sup>16</sup> and galactosyl-transferase<sup>17</sup> have been found in the *medial* and *trans*-Golgi. The abundance of each

transferase fluctuates amongst organisms and events such as pregnancy or pathological disease states, which alter the normal profile of glycans<sup>8</sup>. In mammalian N-glycans, a variety of sugars are typically observed namely glucose (Glc), fucose (Fuc), mannose (Man), N-acetylglucosamine (GlcNAc), N-acetylgalactosamine (GalNAc), galactose (Gal), N-acetyl neuraminic acid (Neu5Ac) and N-glycolyl neuraminic acid (Neu5Gc) (Table 1.1). A penta-saccharide core consisting of two GlcNAc and three Man sugars is conserved for these glycans. Depending on the glycan processing events which occur in the ER and Golgi, a variety of linkages can occur producing up to four antennae which elongate off the core. Three types of structures that are typically observed are: high-mannose glycans which contain 5-9 mannose sugars on two separate antennae, complex glycans with elongated antennae containing galactose, N-acetylglucosamine and neuraminic acid, and hybrid glycans a combination of the high-mannose and complex forms (Figure 1.1).

Microheterogeneity or site microheterogeneity, is the variability in branching, coupled with the potential for glycan epimerization that frequently yields an array of glycoforms present at the same sequon (as in the case of N-glycans). The presence of several possible isomers is one of many challenges that researchers face when elucidating and characterizing glycan structures. Closely related is the notion of macroheterogeneity (variable site occupancy), which is the variability in the number and location of attached glycans (Figure 1.2). This also constitutes a challenge for researchers.

Table 1.1 - Common glycans observed on mammalian proteins

At present no universal symbols are defined, however the ones listed below are commonly encountered.

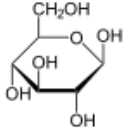

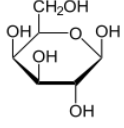

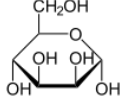

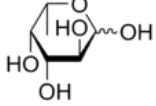

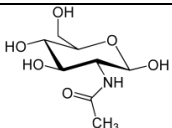

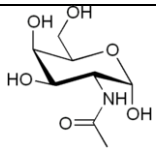

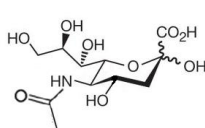

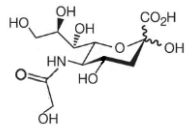

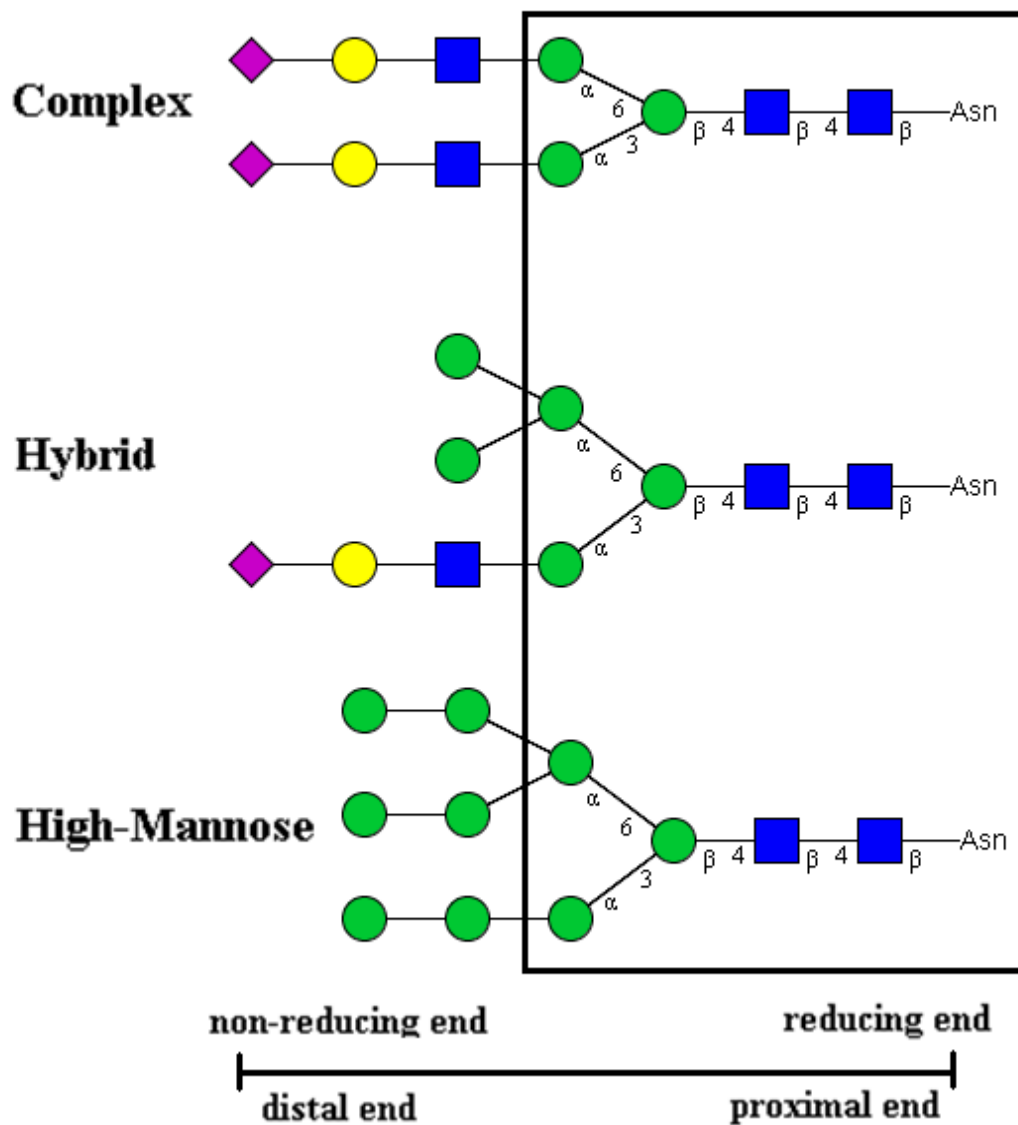
<u>Glycan</u>	<u>Abbreviation</u>	<u>Structure</u>	<u>Symbol</u>	<u>Anomer</u>	<u>Linkage</u>
D-Glucose	Glc			$\alpha$	2,3
D-Galactose	Gal			$\alpha$ $\beta$	3 3,4,6
D-Mannose	Man			$\alpha$ $\beta$	2,3,6 4
L-Fucose	Fuc			$\alpha$	2,3,4,6
N-acetyl-D-Glucosamine	GluNAc			$\beta$	2,3,4,6
N-acetyl-D-Galactosamine	GalNAc			$\alpha$ $\beta$	3 4
5(N)-acetyl neuraminic acid (a sialic acid)	Neu5Ac			$\alpha$	3,6,8
5(N)-glycolyl neuraminic acid (a sialic acid)	Neu5Gc			$\alpha$	3,6,8



Figure 1.1 - Typically encountered mammalian N-glycoforms containing a conserved pentasaccharide core

(See Table 1.1 for legend)



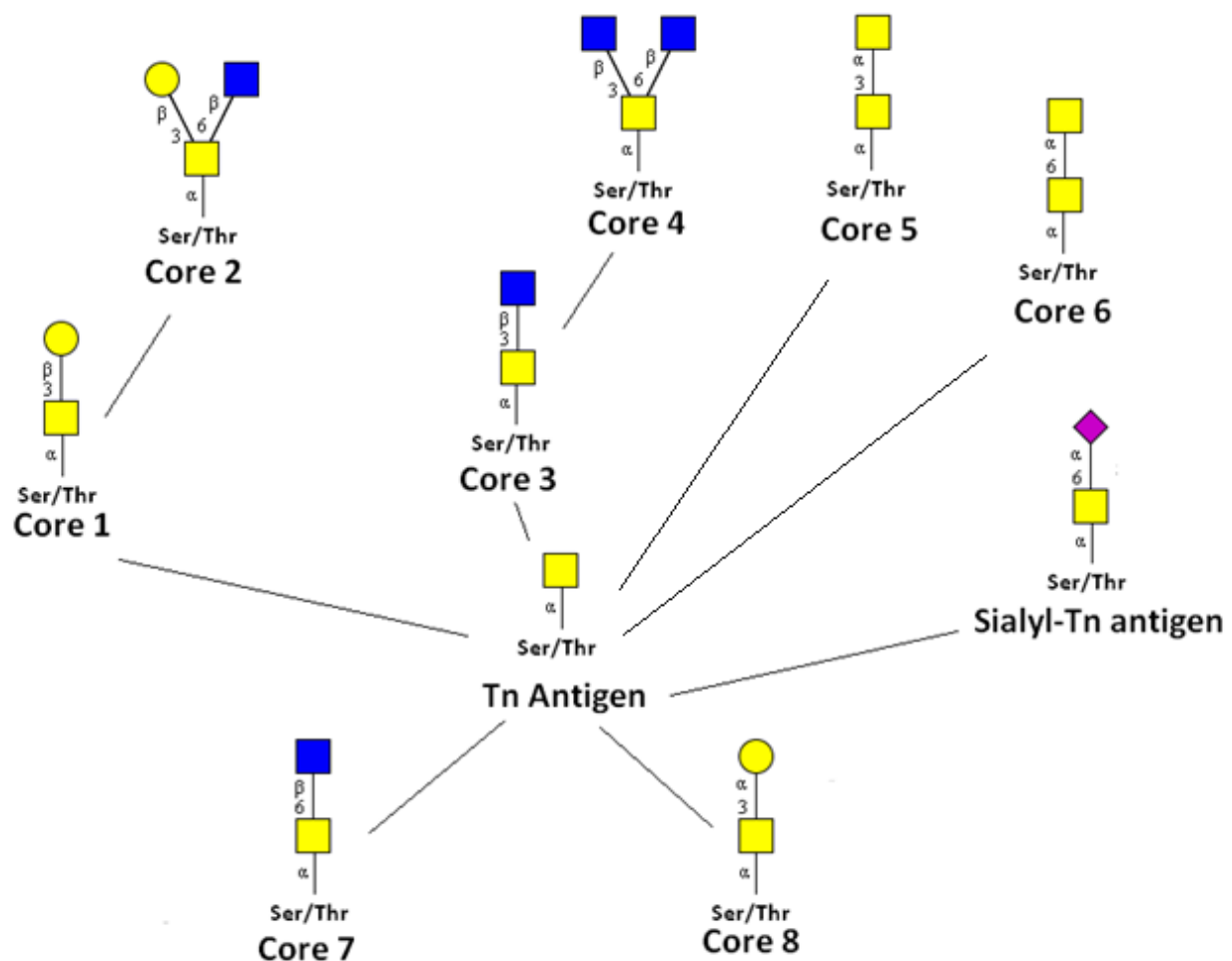
In all four molecules, the peptide sequence (R<sub>1</sub>-Asn-R<sub>2</sub>) is identical, yet microheterogeneity (observable in a,b and d) occurs as different glycoforms are present at a given sequon; in the case of macroheterogeneity (c) the glycan portion is either present or absent (c vs. a, b, d)



The second type of glycan attachment is through linkage to a serine (Ser) or threonine (Thr) (Ser/Thr); which can be in the form of O- $\alpha$ -linked (membrane and secreted proteins) or O- $\beta$ -linked (cytoplasmic and nuclear proteins)<sup>18</sup>. O-linked glycosylation occurs as a PTM in the Golgi as well, where GalNAc is the first sugar attached to the protein followed by the addition of monosaccharides to generate eight distinct “core” groups<sup>19</sup> (Figure 1.3).

Figure 1.3 – Commonly observed Core O-glycans

Common core groups of O-glycans and Sialyl-Tn antigen. These cores are the basis from which larger O-glycans are created. (Legend in Table 1.1)



The third glycan form of attachment known as C-linked, involves an  $\alpha$ -mannopyranosyl residue linked to the indole C2 position of tryptophan. This was first discovered in a protein found in human urine and known to have a sequon of WXXW<sup>20,21</sup>. Limited numbers of C-linked glycans have been described and are not as common as N- or O-linked glycans.

With respect to these forms of glycosylation, it is the highly regulated glycosyltransferases that govern the anomeric variability in the complex branching of oligosaccharides, often yielding potential  $\alpha$  and  $\beta$  glycosidic bonds (Table 1.1). N-glycans are the primary target of most glycoproteomic analyses, and this thesis will refer to N-glycans and oligosaccharides interchangeably.

## 1.2 Implements of a Glycoprotein Analysis Workflow

### 1.21 Overview

To date, there are numerous approaches that help to elucidate the structures of glycoprotein samples, such as nuclear magnetic resonance (NMR)<sup>22,23</sup>, or capillary electrophoresis (CE)<sup>24</sup>. More prevalent methods include high performance liquid chromatography (HPLC) coupled to a mass spectrometer in combination with a variety of enzymatic methods. These are known as “bottom-up” approaches, or more specifically “shotgun (glyco)-proteomics” methods<sup>25</sup>. Bottom-up approaches compare the mass spectra of (glyco)peptides purified from proteolytic digests with those predicted by sequence databases and are generally referred to as “fingerprinting”. Laborious and often time consuming, as well as requiring larger sample sizes which sometimes cannot be afforded, or entailing extensive workup, these lines of approaches remain an area in constant improvement. One noteworthy advancement includes employing tandem mass tags (TMT), a resource that aids scientists by allowing the quantification of protein samples based on the known fragmentation pattern of these tags which yield so-called “reporter ions”<sup>26</sup> in tandem mass spectrometry (MS/MS) experiments. With this tool, researchers can quantify multiple sets of peptides, by monitoring the respective reporter ions, without the need for extensive steps added to the workflow<sup>27,28</sup>. These and other approaches exist mostly owing to the use of modern mass spectrometers, including those equipped with electrospray ionization (ESI)-MS, and matrix assisted laser desorption ionization (MALDI)-MS. ESI-MS offers the advantage of enabling the on-line coupling of HPLC.

Alternatively, the “top-down” approach aims to analyze samples at the glycoprotein level rather than analyzing glycopeptides from proteolytic digests. Here, glycoproteins are isolated by lectins and purified before being characterized by ESI- or MALDI-MS. This allows for intact glycoprotein analysis, which relies on high resolution mass spectrometers to detect all glycoforms distinctly (ref). As for more detailed glycan characterization, this heavily relies on mass spectrometers equipped with unique fragmentation processes such as electron transfer dissociation (ETD)<sup>29</sup>. Through this fragmentation process, longer peptide sequences are produced which preserve labile modifications such as glycosylation. By this methodology, researchers are able to characterize glycoproteins in a few steps. These new innovations in MS provide high throughput capabilities, sensitivity, and reduced handling times, allowing the glycome to be studied in more detail<sup>30,31</sup>. With respect to the material presented in this dissertation, the work is performed as bottom up approach, aiming to study site-specific glycosylation as analyses are performed at the glycopeptide level.

## 1.22 Glycan Release

Classical bottom-up approaches start with the release of N-glycans (either chemically or enzymatically), which permits isolation of the glycan segments of a glycoprotein, generating three possible types of N-glycoforms (Figure 1.1). While this methodology does not conserve the site specific microheterogeneity, it does afford the option for high-throughput profiling of glycans by MS.

The chemical release of N- (and O-) glycans can be achieved through what is commonly referred to as  $\beta$ -elimination<sup>32</sup>. Here, the glycoconjugate is subjected to a mild (O-glycan) or

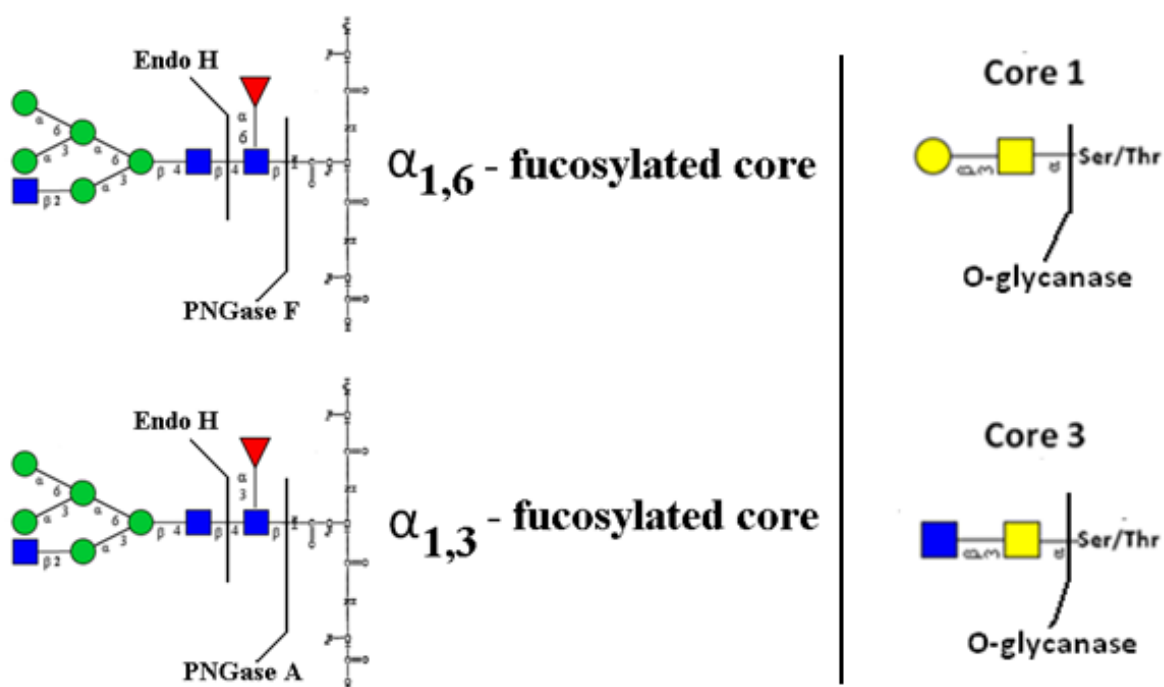
strong (N-glycan) alkaline environment which causes cleavage of the primary GlcNAc/GalNAc from the peptide to yield a glycan. Drawbacks to this approach include the potential of “peeling” (cleavage of monosaccharides from the reducing end) by which valuable information can be lost<sup>33</sup>. Peeling occurs when base removes the C2 hydrogen of the reducing end sugar, once the glycan has been released from the peptide/protein. To compensate for this, an excess of hydrazine can be employed to form a Schiff-base with the free aldehyde located at the reducing end of the glycan. In this approach, a hydrazone is formed which protects the rest of the glycan from degradation by base. Furthermore,  $\beta$ -elimination causes de-acetylation of GlcNAc residues and therefore re-acetylation must be performed prior to analysis, making this approach time consuming.

More commonly encountered, and suitable in many glycoproteomic workflows, is the enzymatic approach to the release of N-glycans. There are three glycosidases routinely used for the removal of N-glycans: endo- $\beta$ -*N*-acetylglucosaminidase (Endo H<sup>34</sup>/Endo S), peptide-*N*-glycosidase F (PNGase F)<sup>35</sup> and peptide-*N*-glycosidase A (PNGase A)<sup>36</sup>, that cleave glycans at different locations (Figure 1.4). Endo H primarily targets the release of high mannose glycoforms<sup>37</sup> and of some hybrid forms<sup>38</sup>, whereas Endo S is known to target hybrid forms. Their enzymatic activity is non-existent in the presence of an  $\alpha$ 1,6-fucosylated core. Both Endo H/Endo S cleave the glycan leaving the primary GlcNAc attached to the peptide. In contrast, PNGase A and PNGase F cleave between the primary GlcNAc and peptide backbone. PNGase A is able to cleave glycans which contain an  $\alpha$ 1,3-fucosylated core<sup>39</sup>, a common trait observed in insects and plants, whereas PNGase F is known to hydrolyze the  $\alpha$ 1,6-fucosylated core

observed in mammals. PNGase F is the standard enzyme for the release of most N-linked oligosaccharides<sup>33</sup>.

Figure 1.4 - Specificity of Commonly Encountered Glycosidases

Glycosidases for the enzymatic detachment of N-linked glycans (left), and O-linked glycans (right). Their specificities are indicated.



In regards to the enzymes available for the removal of O-linked glycans, various research groups have isolated endo- $\alpha$ -N-acetylgalactosaminidase<sup>40,41,42</sup> (O-glycanase), the enzyme responsible for cleaving between the first GalNAc and a Ser/Thr amino acid. Unfortunately, these reports have only demonstrated cleavage of core-1 glycans, with one case reported in the literature demonstrating the ability to cleave core-1 and core-3 glycans<sup>43</sup> (Figure 1.4). Due to the limited ability to detach O-glycans, studies on them have generally remained limited.



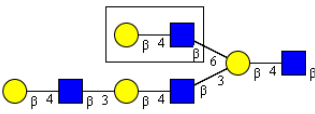
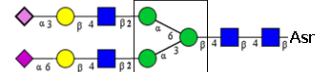

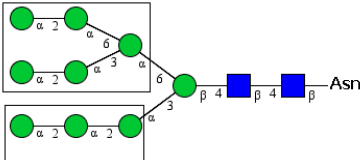
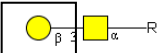
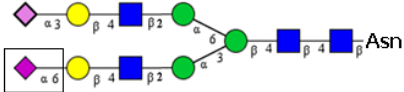
In all cases, the enzymes leave behind a so-called “footprint” that allows the de-glycosylated protein (or peptide) to be characterized for glycosylation site(s). While it is yet impossible to assign the glycans to the exact sequon they came from, evidence of their removal remains as former sugar-bearing asparagines are converted to aspartic acid (for N-glycans); this results in a mass difference of 1 Da, detectable by mass spectrometry<sup>44</sup>.

### 1.23 Enrichment of glycopeptides/glycoproteins using lectins

Widely referred to as lectins from the Latin “to gather or select”, this class of molecules are proteins capable of specific and reversible affinity towards a given pattern of glycans<sup>45</sup>. These interactions are not well understood, as some lectins have affinity for the non-reducing end of an oligosaccharide, while others appear to have a broader affinity that targets proximal or core glycans. Lectins useful in glycoproteomics are derived from plants, due to the higher concentration of soluble lectins present in plant seeds which are easy to harvest<sup>46</sup>. Commonly used lectins include Jack Bean concanavalin A (ConA)<sup>47,48</sup>, specific towards mannose-bearing glycoforms; wheat germ agglutinin (WGA)<sup>49,50</sup>, selective for polylactosamine bearing glycoforms; peanut agglutinin (PNA)<sup>51,52</sup> which targets galactose residues found in “core 1” O-type glycans, and the elderberry lectin (SNA)<sup>53</sup> which targets terminal N-acetyl neuraminic acid  $\alpha$ -2,6 galactose residues (Table 1.2). These lectins may be used separately, however for improved enrichment of glycoproteins they are often used together in a multi-lectin approach<sup>54,55</sup> which targets all glycoforms within samples. At present, there lacks a universal lectin for complete enrichment of all glycoforms, and as is the case, some glycoforms may not be enriched.

Table 1.2 – Typically encountered lectins used for glycoprotein enrichment

Glycans are targeted by corresponding lectins. Here, wheat germ agglutinin is known to bind polylactosamine or N-acetyl-D-glucosamine whereas concanavalin A shows affinity for a variety of mannose glycoforms. More specific lectins include peanut agglutinin known to have affinity for core 1 O-glycans, and the elderberry lectin specific for  $\alpha 2,6$  sialic acids.

Lectin	Latin Name	Glycan Recognition
Wheat Germ Agglutinin (WGA)	Triticum vulgaris	
Jack Bean concanavalin A (ConA)	Canavella ensiformis	 <p>Weak affinity</p>  <p>Moderate affinity</p>  <p>Strong affinity</p>
Peanut Agglutinin (PNA)	Arachis hypogaea	 <p>"Core 1" O-glycans</p>
Elderberry Lectin (SNA)	Sambucus Nigra	

## 1.3 Mass Spectrometry

Mass spectrometry (MS) has been an evolving field, since J.J. Thomson's first mass spectrometer in 1913 up until the present day. MS has played an important role in proteomics, with developments including notable inventions such as electrospray ionization<sup>56</sup> (ESI) and matrix assisted laser desorption ionization<sup>57</sup> (MALDI), as well as their complementary mass analyzers including quadrupoles, time-of-flight (TOF), linear ion traps, and hybrid analyzers. These systems have dramatically contributed to our understanding of biology at the present time, allowing for, and becoming the standard choice in, the analysis of large biomolecules such as oligosaccharides, glycoproteins, and lipids.

### 1.31 Ionization Sources in Mass Spectrometry

MS ionization is a process whereby the sample molecules become charged as either cations or anions. These charged ions are detected at a value referred to as ' $m/z$ ', where  $m$  denotes mass and  $z$ , charge. In biological MS, two modes of ionization are common, 'hard' and 'soft' referring to the ability of the technique to form intact ions and to the level of fragmentation produced. Hard techniques produce higher numbers of smaller fragment ions, as observed using electron impact (EI). However, when studying labile structures such as glycoproteins, researchers are interested in the masses of larger intact structures, and hence the need for softer ionization processes. Both ESI-MS and MALDI-MS are two such processes. Each offers many advantages, and involves different principles such that they can provide complementary information in the area of glycoproteomics.

### 1.311 Electrospray Ionization (ESI)

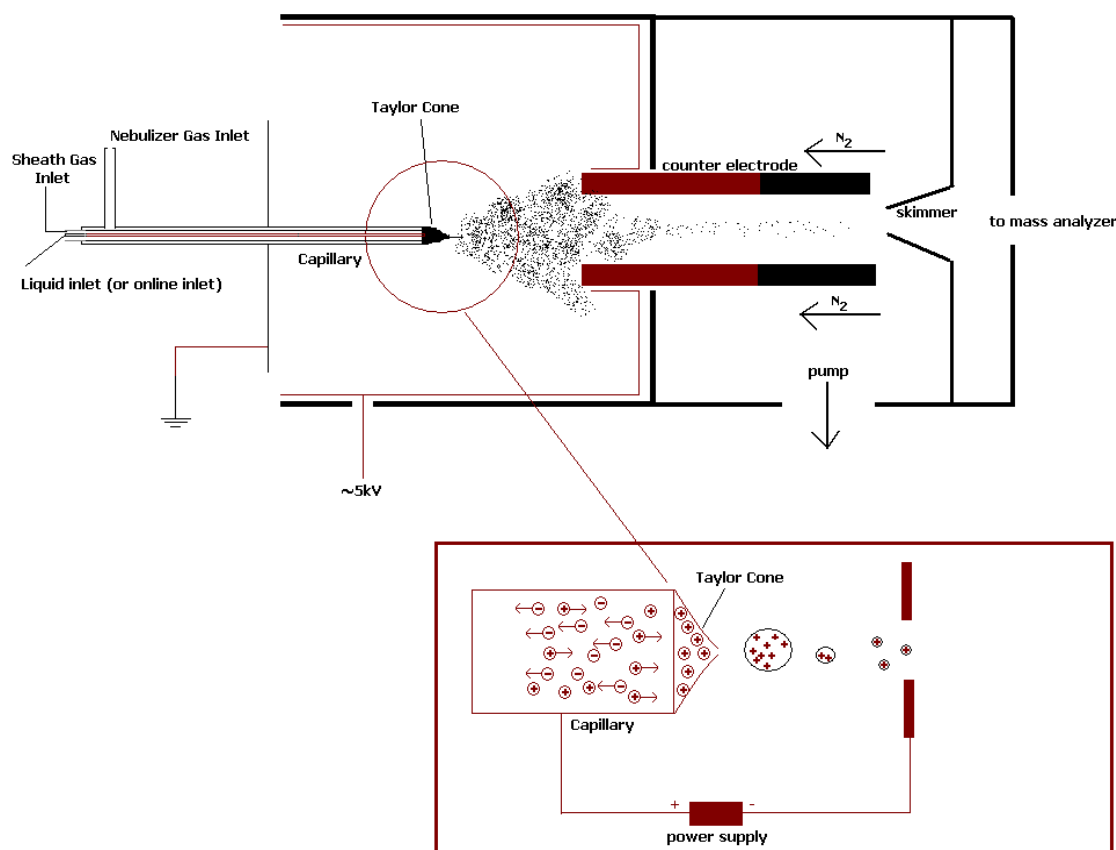
Electrospray (ES) techniques have been used since the early 1900's, when Zeleny first observed the instability of charged droplets in a fine mist<sup>58,59</sup>. In terms of MS development, Dole made the important discovery that multiply charged molecular ions are formed after solvent evaporation in the gas phase<sup>60,61</sup>. These multiply charged ions led Fenn to test ES as an ionization source for mass spectrometers. Fenn noted that it was possible to separate and measure involatile, large organic molecules as well as some that were not well suited to other ionization techniques<sup>56</sup>. Sample introduction for ES is achieved through a direct (online) connection to a continuous liquid flow system (e.g. HPLC). This has been advantageous in high throughput experiments requiring separation prior to MS analysis.

Other than online applications, a main advantage of using ESI-MS is its intrinsic ability to produce multiply charged ions resulting in smaller  $m/z$  values, allowing for a wider range of mass analyzers<sup>62</sup>. There are three proposed events that occur in ESI: the formation of droplets, followed by the evaporation of solvent from the droplet to create a highly charged droplet, and finally the process of forming the ions prior to mass analysis and detection. First, the solution containing the analyte of interest is pumped through a microcapillary with a controllable potential of ~5kV, sufficient to form a Taylor cone and initiate the ES process<sup>63</sup>. Next, the applied voltage in the capillary causes ions of the same charge polarity as the capillary to be repelled by the tip of the source, while attracting those with opposite polarity. Effectively, this polarizes a section of liquid such that when same polarity charges are exposed to an electric field, the liquid stream is destabilized into the aforementioned Taylor cone. Subsequently, high

enough voltages cause the cone to disperse as charged droplets and these are then propelled towards counter electrodes (Figure 1.5).

Figure 1.5 – Electrospray Source with the initial formation of a Taylor Cone

The top diagram is a modified schematic of an ESI source<sup>62</sup>. Below is a representation of the formation of a Taylor cone at the tip of the capillary through the action of a positive potential. Also illustrated are solvent evaporation and eventual coulombic fission of ions as they progress towards the gas phase.



From this point forward, the size of the droplets begins to decrease due to the evaporation of solvent. As a result, the  $m/z$  decreases as the charge is maintained. This

continues until the Rayleigh limit is attained, a point at which the surface tension of the droplet is overwhelmed by coulombic force. The surface undergoes coulombic fission, exploding into secondary droplets. These will undergo this process repeatedly, until the ions reach the gas phase and enter the mass analyzer.

### ***1.312 Matrix assisted laser desorption ionization (MALDI)***

Originally developed as an ultraviolet (UV) pulsed laser technique by Karas and Hillenkamp<sup>57</sup> in the late 1980s, MALDI is a 'soft ionization' technique which has become very useful for the analysis of biological samples. Both UV and infrared (IR) lasers can be used to induce the ionization process. For this technique, it is crucial that the analyte be co-mixed and spotted on a conductive target with a light absorbing weak acid or base named the matrix. The matrix spares the sample from the high energy associated with the focused laser beam<sup>64</sup>. The matrix is typically spotted first and allowed to dry, following which an equivalent amount of sample is spotted on the matrix layer prior to analysis.

Typically used acidic matrices include 2,5-dihydroxybenzoic acid (2,5 DHB or DHB),  $\alpha$ -cyano-4-hydroxycinnamic acid (CHCA), and 3,5-dimethoxy-4-hydroxycinnamic acid (sinapinic or sinapic acid; SA). Each of these boasts important characteristics, including the ability to dissolve the sample and co-crystallize with it, as well as the potential for proton transfer and absorption of UV light. While these matrices are suitable for many glycoconjugate samples, investigators have also reported on the use of various additives such as dimethylaniline (DMA) and phenylhydrazine (PHN), that have been shown to enhance ionization through the formation of a Schiff-base with the glycan<sup>65, 66</sup>. In either case, upon drying, the spot is irradiated with a

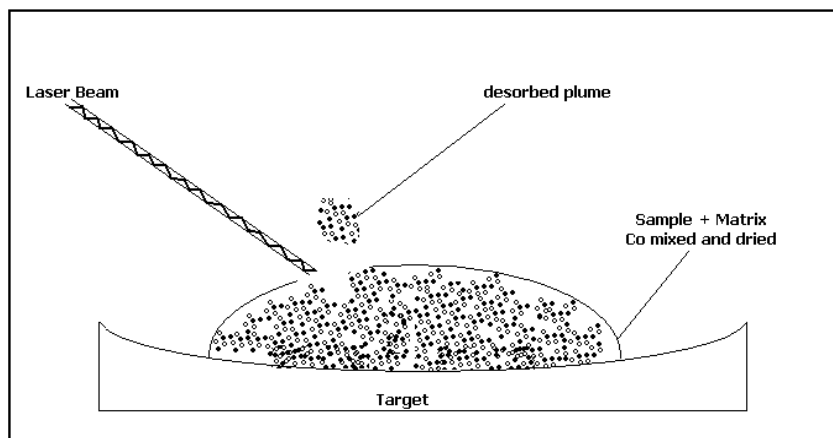
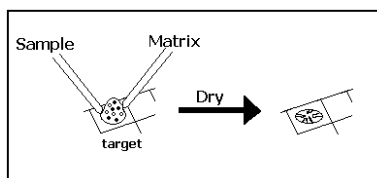
focused pulsed laser beam at a wavelength appropriate for the absorption range of the matrix.

A typical laser used in modern instruments is  $N_2$  (337nm). Next, the matrix transfers this absorbed energy to the analyte, causing a plume of excited ions to desorb from the surface.

This plume is the site of ion-molecule reactions that occur to allow transfer of protons or cations to molecules, M, forming  $(M+H^+; M+X^+)$ , where  $X = Na^+, K^+$  etc.) ions as depicted in Figure 1.6. A voltage is then applied to the target, which propels the plume towards the mass analyzer component of the mass spectrometer.

Figure 1.6 - Processes associated with MALDI Ionization

Co-spotting of an analyte and matrix onto the target (above), followed by the desorption process from a dry spot during laser irradiation (below). Typically used for MALDI are the  $N_2$  ( $\lambda = 337\text{ nm}$ ) or Nd:YAG lasers ( $\lambda = 355\text{nm}$ ) as equipped on the Bruker UltrafleXtreme MALDI-ToF/ToF.



## 1.32 Mass Analyzers

Once the sample has been ionized, the ions must be filtered or separated to allow for resolution at the detector. Two types of analyzers which have been used extensively are the quadrupole and time-of-flight (TOF) systems. Also, as will be explained in the following sections, the possibility exists to combine analyzers, as in e.g. triple quadrupoles or tandem TOF (TOF/TOF) analyzers, for the purposes of multiple stage MS. Tandem MS combinations have been found advantageous, such as in a Q-TOF instrument<sup>67,68</sup>. Each instrument, whether or not it is hybrid, has advantages and limitations according to the needs of analysis. Depending on the  $m/z$  resolution needed, on the molecular mass of the analyte, and on the ionization mode used,  $m/z$  analyzers may be selected appropriately and are crucial in the success of measurements.

### 1.321 Quadrupole

The development of the quadrupole was first reported in 1953 and the device patented by Helmut Steinwedel and Wolfgang Paul in the same year<sup>69</sup>. Since that time, quadrupole analyzers have become an integral part of mass spectrometry, later leading to the development of the linear ion trap, the idea of a circular or racetrack quadrupole geometry for the storage of ions proposed by Church in 1969<sup>70</sup>. The use of quadrupoles as independent units in mass spectrometers has led to the assembly of the tandem quadrupole instruments. For example the first triple quadrupole (QqQ) was built by Morrison and refined by Yost<sup>71,72</sup>.

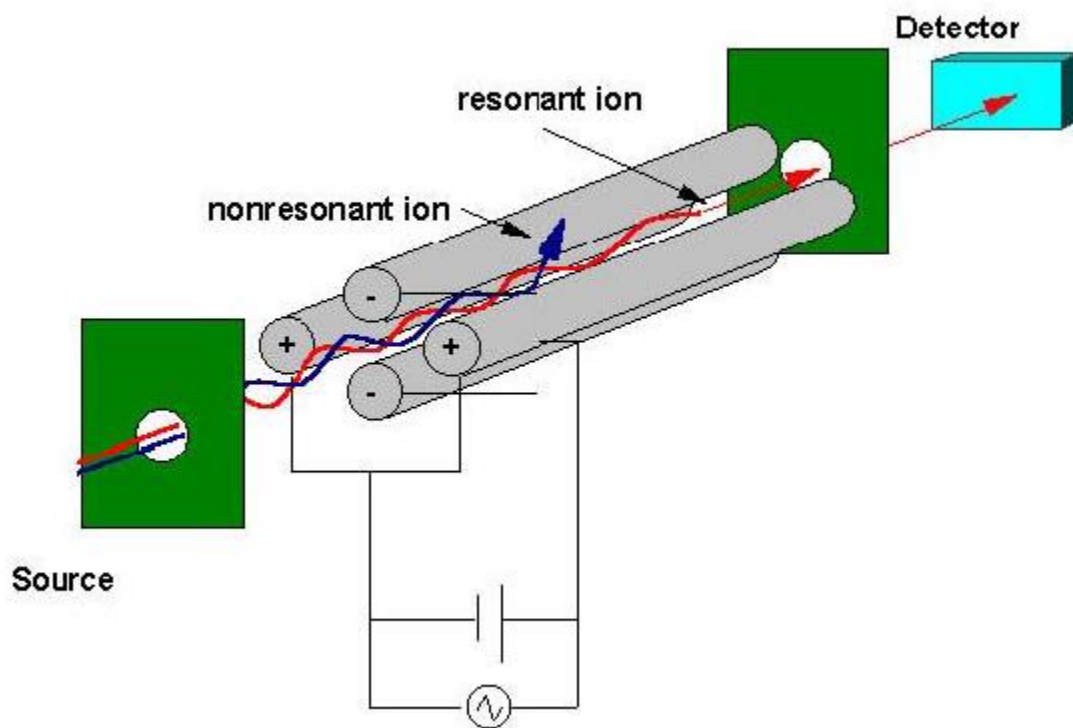
The typical design of a quadrupole consists of four equally spaced cylindrical rods between which the ions are directed by DC and RF potentials. Two of these parallel rods provide a direct current (DC) potential, and the other two provide an alternating radio



frequency (RF) oscillating potential (Figure 1.7). Quadrupoles act as mass filters. When ions enter the quadrupole, only those with stable trajectories accordant with the appropriate DC, RF and angular frequency parameters will pass through freely to reach the detector. Ions with excessive oscillating amplitudes will be grounded on one of the rods and eliminated from the filtering process.

Figure 1.7 – Trajectories of ions in a Quadrupole

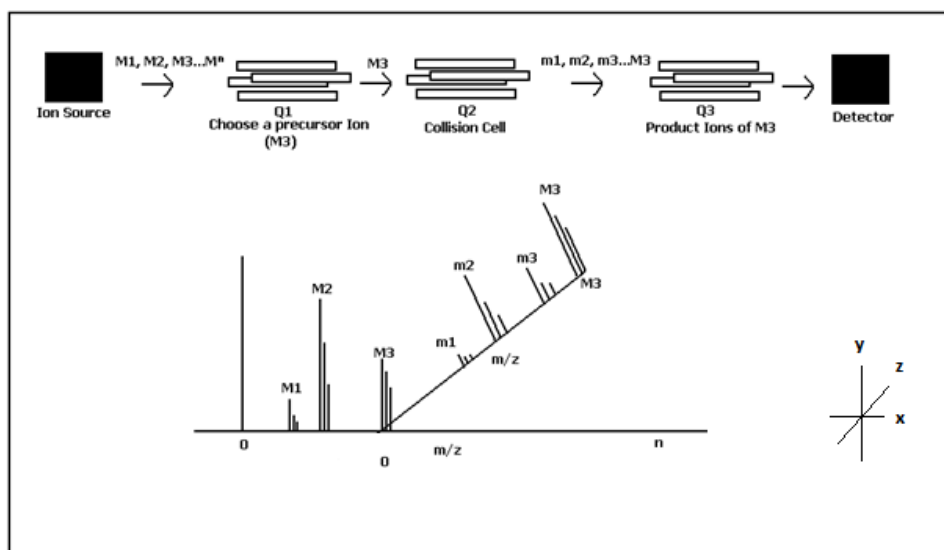
This figure compares the trajectories of two ions in a quadrupole. In one scenario, the oscillating amplitude of the ion exceeds its ability to travel through the quadrupole and hence, hits one of the rods and becomes grounded (unstable trajectory). The stable trajectory ion reaches the detector. This is an adapted figure<sup>73</sup>.



Triple quadrupoles (QqQ) are designed for tandem MS (MS/MS) experiments, which provide more structural information on a given analyte. These instruments use a process called collisional activated dissociation (CAD) to help fragment molecular parent ions. In this design, there are two quadrupoles (Q1, Q3) that precede and follow a central collision cell (q, or Q2) (Figure 1.8). The Q1 mass analyzer filters the precursor or parent ions of interest by rejecting ions of other  $m/z$  ratios with unstable trajectories. Next, the parent ions enter the collision cell where they undergo collisions with a gas such as helium, which in turn increase the internal energy of the ions, causing them to fragment or dissociate. Finally, these fragment or daughter ions enter the second mass analyzer (Q3) allowing a “daughter” ion mass spectrum to be produced.

Figure 1.8 – Tandem MS using a Triple Quadrupole Instrument

General representation of a triple quadrupole instrument (top), with a schematic explanation of tandem MS (below) where M3 precursor ions are in the form  $(M+H)^+$  and fragments have a +1 charge.



### 1.322 Time of Flight (TOF)

Noted by W.E. Stephens in the Proceedings of the American Physical Society in 1946 as 'A pulsed mass spectrometer with time dispersion', the crude [still under construction] time-of-flight (TOF) innovation then proposed a way of alleviating adjustment sensitive slits, scaffolding, as well as cumbersome magnets that lacked rapid scanning<sup>74</sup>. It was not until two years later that the first results were published by Cameron and Eggers on their TOF analyzer which they referred to as an ion 'Velocitron'<sup>75</sup>.

Mass analysis by TOF involves the separation of ions through a field free drift tube over the course of time (Figure 1.9). As all ions are accelerated with the same kinetic energy in the ionization source at the beginning of the drift tube ( $t=0$ ), those with lighter masses travel with greater velocities, reaching the detector sooner, whereas those with larger masses travel slower and arrive later. In the process, ions are thus separated and resolved by  $m/z$ . One can calculate flight time based on the following formulas:

**(Formula 1.32)**

$$KE = \frac{1}{2} mv^2 = qV$$

Where:

KE = Kinetic energy

m = mass of ion

v = velocity of ion

q = charge of ion; which also = ze;

where z = # of charges , and e = charge of an electron

V = applied acceleration potential in the ion source

The relationship between time, distance (in this case the length of the drift tube), and velocity is expressed as:

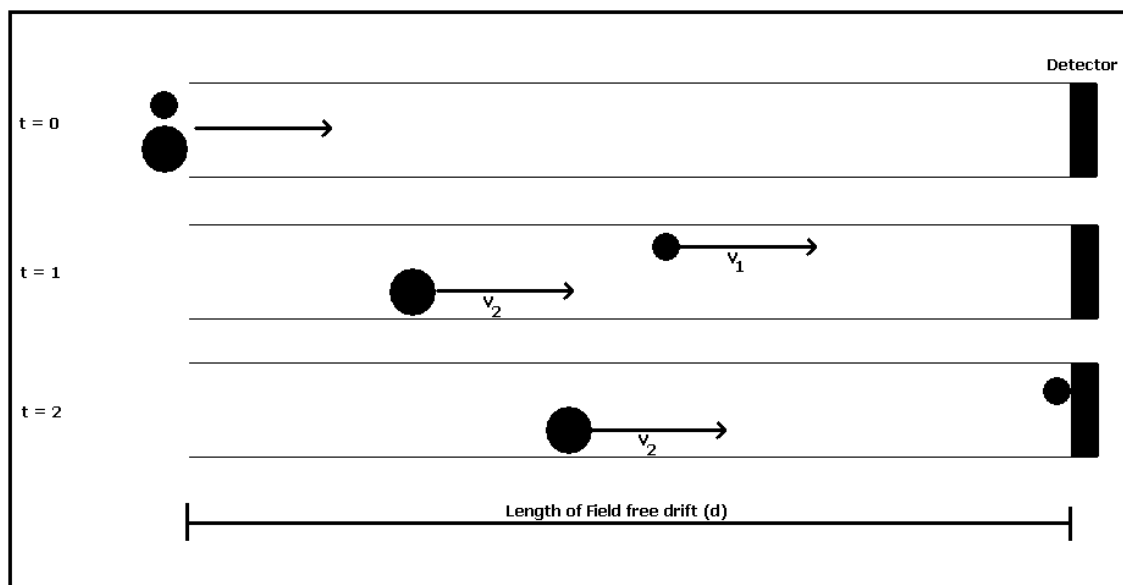
**(Formula 1.33)**  $t = d/v$

Rearranging formulas 1.32 and 1.33 for the isolation of time yields:

**(Formula 1.34)**  $m/z = (d^2/2Ve) / t^2$

Figure 1.9 - Separation of Ions in linear Time-of-Flight analyzer

At  $t=0$  both ions enter the drift region with the same kinetic energy, but due to their mass, the lighter (depicted as smaller) mass will reach the detector first, allowing the masses to be resolved over time. This is a portrayal of the linear operation of TOF. The reflective mode will be discussed later in the text.

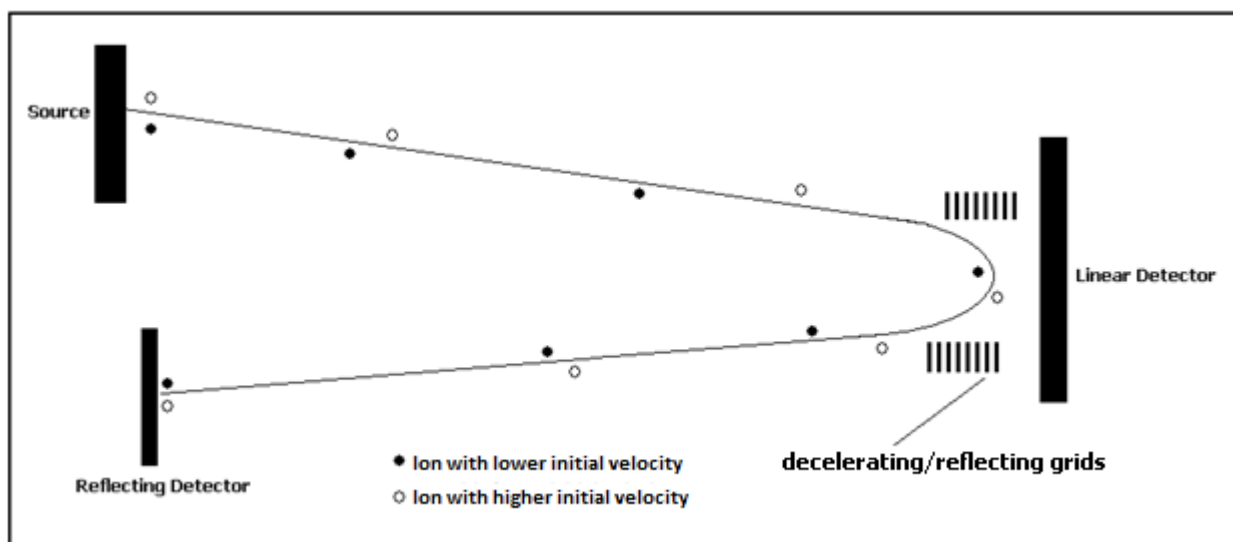


Resolution associated with TOF analyzers is also an important factor to consider. In general, resolution deteriorates as a function of mass. Ions of higher masses with lower kinetic energies experience a greater spread of kinetic energies due to their lag in the drift tube. This causes wider peaks for larger ions in the linear mode. To compensate for low resolution an ion mirror was first utilized by Mamyrin in 1973, which he referred to as a reflectron. This is more commonly called, a reflector<sup>76</sup>.

A reflector is a series of stacked metal plates, each of which supports progressively increasing voltages on a path traversed by the ions towards the detector. Ions with higher initial kinetic energies pass deeper into the reflector grid than those with lower initial kinetic energies. When the reflector grids are active, these voltages decelerate and impede the travel of ions towards the first detector (linear detector; Figure 1.10), causing them to be reflected in the opposite direction towards a detector. This process allows ions travelling with different initial kinetic energies but equal mass-to-charge ratios to be refocused (Figure 1.10). This reflecting device creates a longer drift tube, and has provided enhanced resolution in the field of TOF mass spectrometry (Figure 1.11).

Figure 1.10 - Components of a time-of-flight reflector<sup>81</sup>

Two ions (with the same  $m/z$ ) may travel with slightly different initial velocities in a TOF tube, contributing to reduced resolution. When analyzed in reflective mode, the ion mirrors aid to enhance resolution. Faster ions spend more time in the reflector as they penetrate deeper, and slower ions spend less time; the overall effect is to reduce the energy spread.



The combination of two mass analyzers can also be achieved with TOF systems. This was accomplished by Cooks *et al.* in the late 1980's<sup>77</sup>. The first TOF analyzer selects precursor ions. This is achieved by a device called an ion-shutter, unique to TOF/TOF design. Also termed Bradbury-Nielson gate (BNG) based on its developers, it is a set of two closely spaced wires interconnected with alternating polarities that are oriented orthogonally to the travel of charged ions<sup>78</sup>. When voltages equal in magnitude but opposite in polarity are applied, ions will be hindered from reaching the drift tube as the beam is caused to split, deflecting ions at an angle  $\pm\alpha$  relative to the incoming trajectory. However, when the potential is dropped to zero,

packets of ions will be allowed to traverse the BNG and reach the end of the drift tube. In order to filter ions of interest, the BNG is held closed until the packet of ions of interest reach the gate, at which point it is programmed to open and allow ions to pass into the collisional cell where they undergo CAD. Resulting fragments are then analyzed by the second TOF analyzer, completing the MS/MS analysis<sup>79,80</sup>.

Figure 1.11 - Comparing the Resolution of Linear and Reflecting TOF<sup>81</sup>

MALDI-TOF spectra of Substance P comparing linear and reflecting modes.

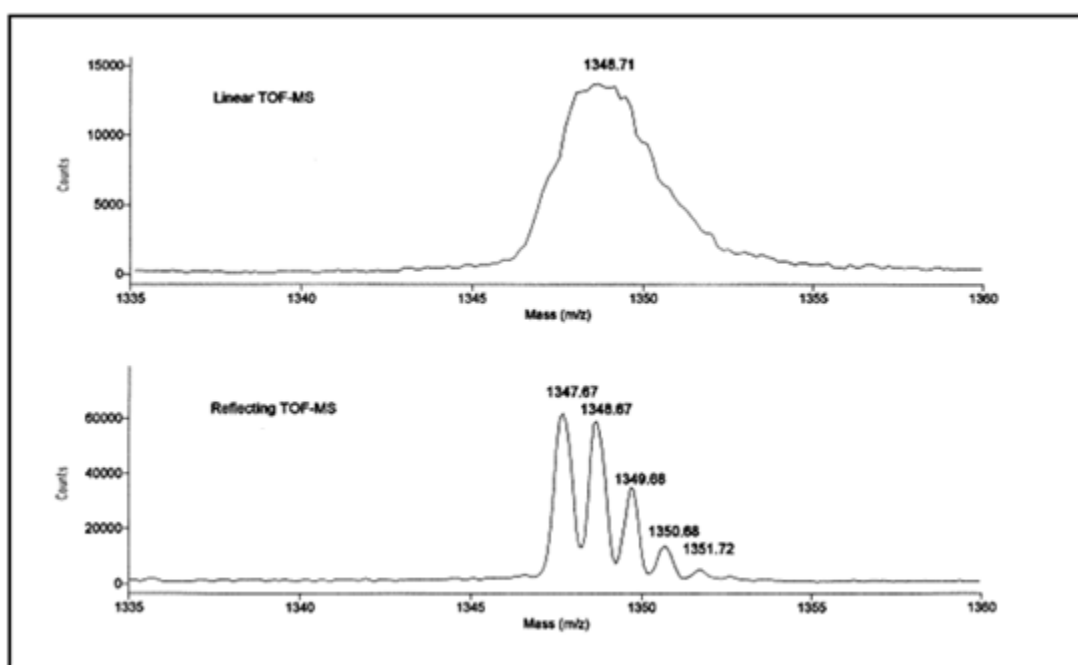
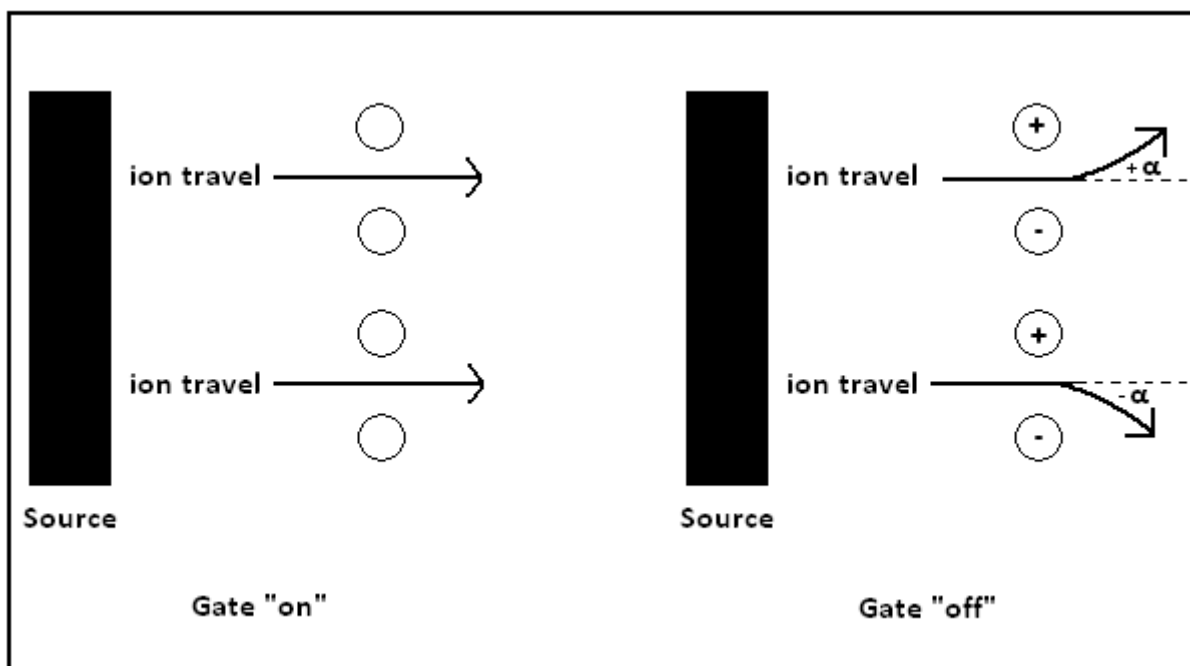


Figure 1.12 - Operations of a Bradbury-Nielson Gate

In gate “on” mode, ions are allowed to traverse the filter and proceed through, whereas in gate “off” mode, ions will be deflected from their original path. In MS/MS analysis with pulsed ion sources, the time it takes to reach the gate can be calculated, and hence it can be programmed to open for certain  $m/z$  ranges.



Considering the pulsing nature of lasers used in MALDI, and the inherent time delay incumbent to TOF analyzers, it is suitable to couple these processes. Much of the resolution quality depends on the speed of the electronics incorporated in the two processes. Each ionization event is initiated with a timed pulse, and electronics control post-ionization ion optics and detection. Therefore, the speed of response from electronic controls contributes to the final resolution obtained in the spectra.



### 1.33 Tandem MS Fragmentation

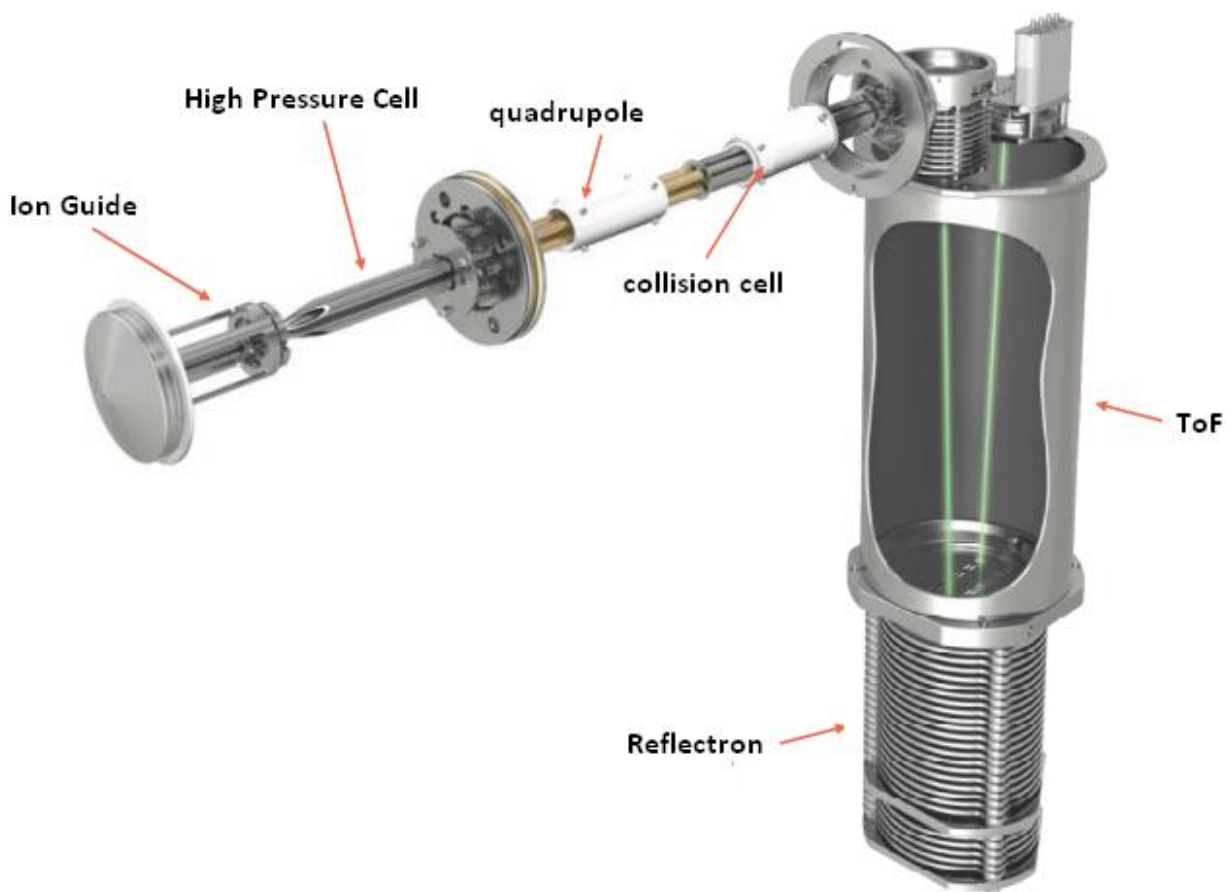
There are many forms of hybrid mass analyzers capable of performing MS/MS. This technique is important to enable identification of compounds through their fragmentation patterns. For instance, some amino acids exist as isomers (leucine and isoleucine), and some sugars are isobaric, such that a single mass spectrum would not be sufficient for identification. Furthermore, MS/MS experiments can help elucidate the branching and sequence patterns of carbohydrates and glycopeptides. For this purpose, glycan derivatization techniques such as permethylation, can lead to predictable fragments<sup>82</sup>. Understanding these fragmentation patterns allows researchers to reconstruct the structure of a glycoform.

In regards to hybrid instruments for tandem MS analysis, MALDI-ToF spectrometers have demonstrated low ppm accuracy<sup>83</sup>. These rely on post-source decay (PSD) methods within the ToF drift region to produce daughter ions from parent ions. The fragmentation of these ions however is hard to predict, and often lower in sensitivity and mass accuracy<sup>84</sup>. Alternatively, ESI hybrid quadrupole/time-of-flight (QqToF) instruments have demonstrated higher sensitivity, resolving power and mass accuracy, in part due to the ability of the ToF to record all ions in parallel without scanning<sup>85</sup>. They also comprise a collision cell (q) where CAD fragmentations occur with more predictability than with PSD. Two such hybrids combining quadrupoles and time-of-flight analyzers are the MALDI-QqTOF<sup>86</sup> and ESI-QqTOF designs (Figure 1.13). In these hybrid analyzers, ions from the source first enter into an ion guide where they are focused. Next, ions travel through a cell at higher pressure which provides more ion focusing and the ability to cool the ions. In the event of tandem MS, precursor ions are selected within the first

quadrupole mass analyzer (Q), and then fragmented within the collision cell (q). These ions are orthogonally accelerated by a pulsed electric field, pushing ions into the ToF tube where they are resolved using reflectron grids<sup>85,87</sup>.

Figure 1.13 – Schematic of ESI-QqTOF hybrid mass spectrometer

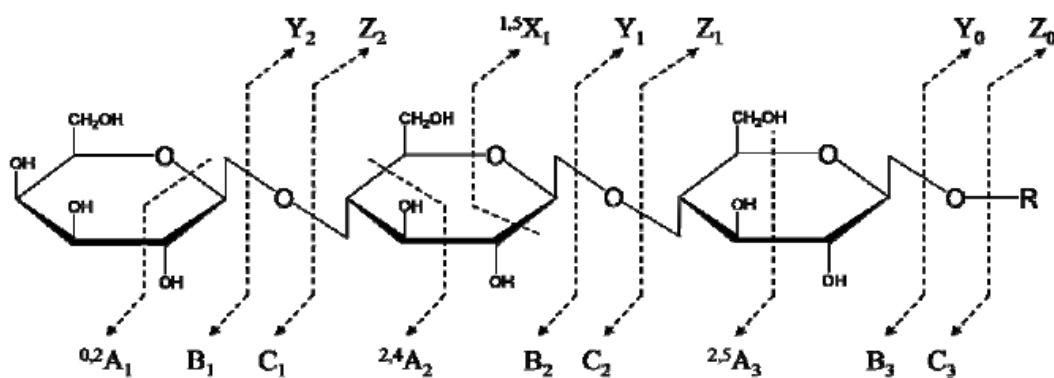
This schematic is an adaptation of the AB Sciex 5600 ESI-QqTOF mass spectrometer<sup>88</sup>. As ions enter they are focused within the ion guide and cooled in the high pressure cell. Next, parent ions may be selected in the first quadrupole and undergo CAD within the collision cell. Resulting daughter ions enter the ToF tube and are resolved by the reflectron before being detected.



While ESI-qTOF instruments have demonstrated intensive fragmentation of glycans<sup>89,90</sup>, they are prone to produce multiply charged glycans which can complicate the glycan profile and make structural elucidation more difficult<sup>91</sup>. Alternatively, MALDI-MS based instruments are often preferred as they produce singly charged ions which are capable of revealing more information in the form of cross-ring cleavages<sup>92</sup>. When carbohydrates are subjected to CAD, the energy imparted causes molecular vibrations that resonate throughout their structures. This resonance causes weaker bonds to stretch and break. Depending on the amount of energy imparted, different types of cleavages occur. For oligosaccharides, Domon and Costello<sup>93</sup> proposed a nomenclature system which is illustrated in Figure 1.14.

Figure 1.14 - Nomenclature for the fragmentation of Carbohydrates

Domon and Costello's nomenclature for the fragmentation of carbohydrates<sup>93</sup>. A,B,C are fragments that keep the charge on the non-reducing terminal and X,Y,Z are fragments keeping the charge on the reducing terminal. Subscripts indicate how many monosaccharides are being contained in the resulting ions, and in the case of cross-ring cleavages, superscripts denote which two bonds are broken when fragmentation occurs.



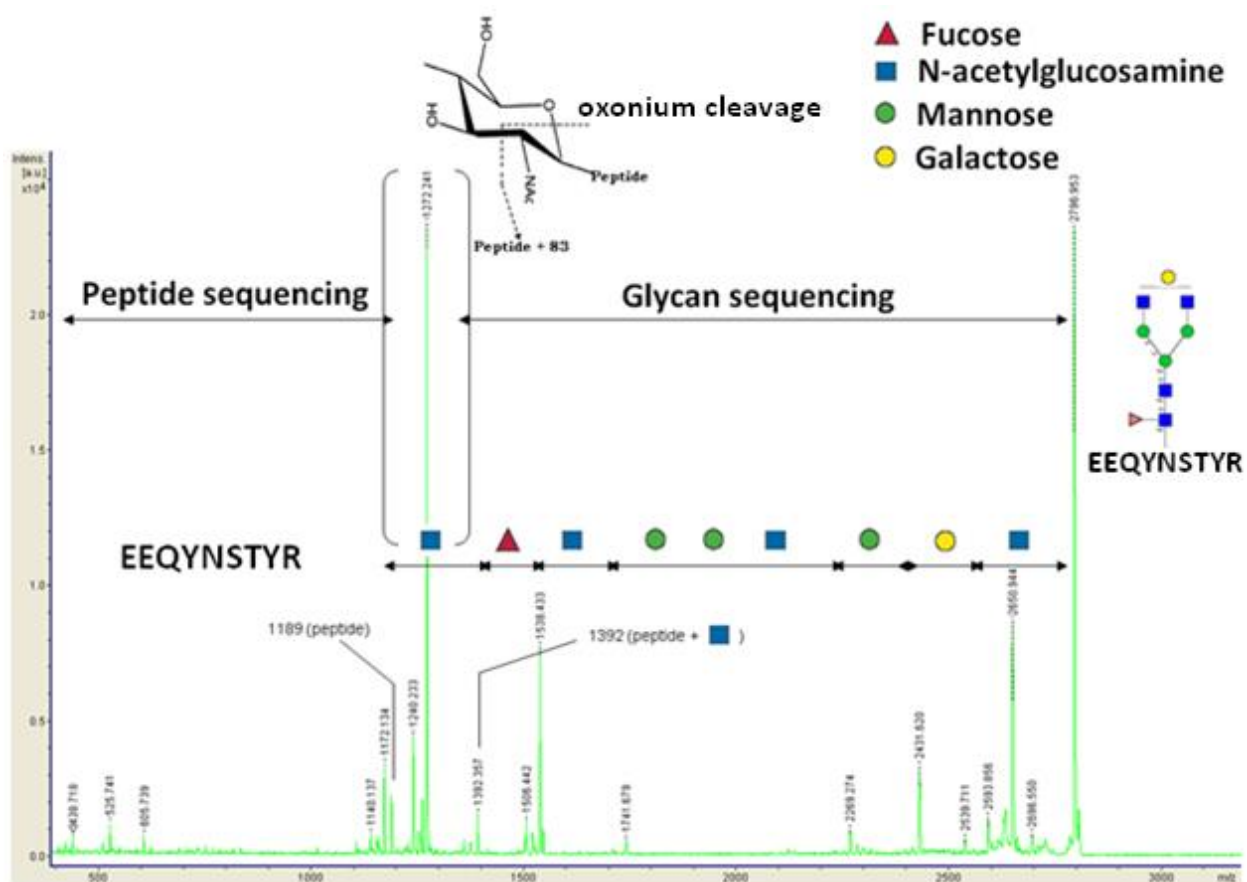
For glycopeptide analysis, CAD experiments performed on ESI-qTOF instruments have been beneficial. These instruments produce predictable cleavage patterns affecting the glycans without extensive cleavage of the peptide backbone<sup>94</sup> that yield [Peptide+GlcNAc]<sup>+</sup> ions which allow for unambiguous site-specific sequencing information<sup>95,96</sup>. However, as in the case of ionization for glycans, glycopeptides analyzed using ESI sources often ionize as multiply charged ions, and require deconvolution to the singly charged level to ease structural elucidation<sup>97</sup>.

In the case of MALDI-TOF ionization for glycopeptides, the energy imparted throughout the oligosaccharide by CAD produces a B/Y fragment ion series which involves cleavages of the glycosidic bonds. This feature simplifies glycan sequencing. MS/MS spectra are segmented into three identifiable areas: the peptide sequencing region, the glycopeptide sequencing region and the area in between. The latter features ions characteristic of the peptide + *N*-acetylglucosamine and a corresponding oxonium cross ring cleavage<sup>98</sup> (Figure 1.15). This “signature” fragmentation of glycopeptides in MALDI-MS/MS improves analysis, detection, and structural elucidation of glycopeptides providing an advantage over ESI-CAD-MS/MS, which produces mostly glycosidic cleavages and limited information about the peptide. The benefit of using Q-TOF MS/MS for analyzing glycopeptides has been demonstrated on a variety of glycoprotein samples including sialylated<sup>99,100</sup> and asialylated<sup>101</sup> glycoproteins. High mannose<sup>102</sup> and paucimannose<sup>103</sup> glycoforms have also been analyzed on these types of instruments.

Figure 1.15 - Fragmentation of a Glycopeptide

Typical cleavage pattern observed for a glycopeptide by MS/MS on a MALDI based instrument.

Three distinguishable areas are present that help in structural elucidation: the glycopeptide sequencing area (showing individual monosaccharide losses from the non-reducing end), the peptide sequencing area (aids in determining backbone sequence or any glycan fragment losses), and the area between the glycopeptide and peptide sequencing areas.



## 1.4 Separation and Derivatization Techniques

### 1.41 Chromatography

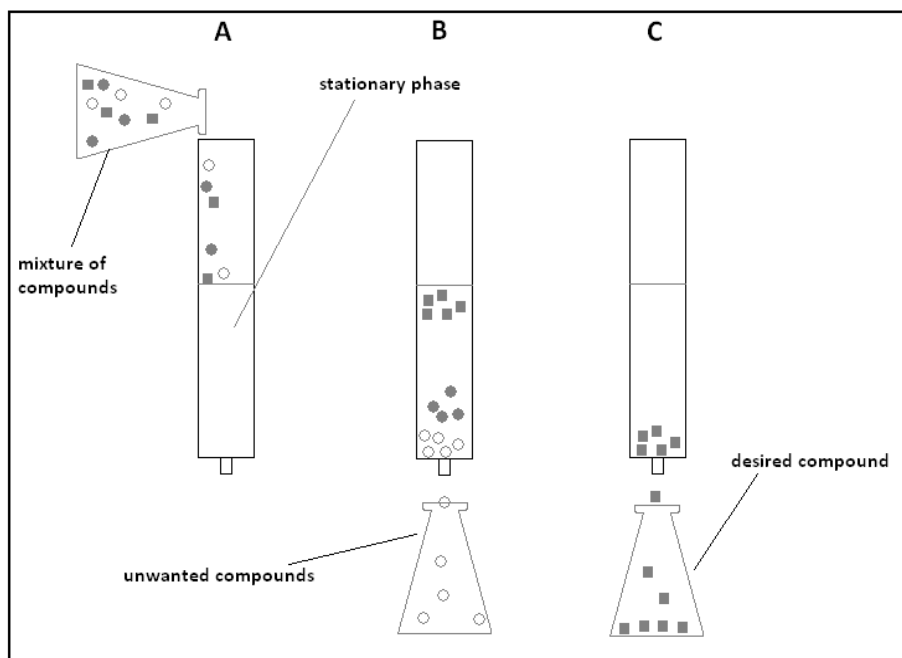
Chromatography is a method used for the separation of chemicals which is utilized in nearly every division of science. The goal of chromatography is to achieve optimal separation of compounds in a mixture, and this can be accomplished by various types of interactions such as adsorption, partitioning, ion exchange or size exclusion. Of these, partition chromatography has become the most popular, boasting both normal (hydrophilic) and reversed (hydrophobic) phase approaches, that can incorporate either liquid-liquid or liquid-solid partitioning<sup>104</sup>.

Partition chromatography involves the principle that 'like-dissolves-like', implying that in order to separate compounds of interest, a stationary phase's polarity close to that of the analytes will promote partitioning. A solvent of opposite polarity is used to elute compounds with affinity for the solvent, while the analytes of interest lag behind due to affinity for the stationary phase. Gradually, or abruptly, the polarity of the mobile phase is modified so that the analyte has more affinity for the mobile phase than the stationary phase (Figure 1.16).

Much care and consideration should be taken in the method development of partition chromatography. Depending on the complexity of the sample, compounds may interact with both the stationary and mobile phases, making separation of two analytes impossible with one method alone. Ionizable groups present on the analyte, pH of the mobile phase, incorporated detergents and buffers may contribute to separation efficacy and need to be optimized. This is important in the separation and analysis of proteolytic mixtures containing

Figure 1.16 – General approach to partition chromatography

General approach to partitioning chromatography. To begin, all compounds are loaded onto a column and allowed to adsorb onto the stationary phase designed to bind the analyte of interest - depicted as a square (A). Next, a solvent of opposite polarity to that of the stationary phase is introduced. Analytes of similar polarity to the mobile phase and with low affinity for the stationary phase (depicted as circles) elute faster. These can be collected or discarded (B). Lastly, a solvent similar in polarity to the stationary phase is introduced eluting the analytes of interest which can then be collected (C).



peptides and glycopeptides due to the limited contrast in structures between the two pools of analytes. Specifically in glycoproteomics, LC is advantageous as it can be coupled to ESI for the separation of complex samples prior to online MS analysis. This approach is extensively used to map glycoprotein biomarkers<sup>105,106,107</sup>, as well as to analyze glycans on recombinant monoclonal antibodies<sup>108,109</sup>.

In glycoprotein analysis, it is common to analyze both the glycan and the glycopeptide depending on the nature of the study. The general strategy for N-glycan analysis involves the release of the glycans by enzymes followed by the separation of glycans on graphitized carbon<sup>110</sup>, or C<sub>18</sub> to isolate glycans based on glycoform<sup>111</sup>. Glycans can also be collected in bulk<sup>112,113</sup>. Subsequently, they can be labeled using derivatization techniques as outlined in the following section. When combined with MS, this approach allows to better characterize isolated glycans in terms of structure, and to obtain glycoprofiles of samples. One of the drawbacks of this approach is the loss of site specific microheterogeneity at the protein sequon<sup>114</sup>. This type of information is important because it may offer insights into structure-function relationships. For this reason glycopeptide analysis is gaining popularity, and so are the methods developed to permit the separation of glycopeptides from peptides in proteolytic digests.

The two most routinely encountered forms of chromatography for separating glycans are reversed-phase (RP) and normal phase (NP) chromatography. With respect to RP, hydrophobic stationary phases such as C<sub>4</sub>, C<sub>8</sub>, C<sub>18</sub> or benzene attached to silica are often used. Alternatively, in NP chromatography which aims to retain hydrophilic compounds, stationary phases which emphasize hydroxyl, cyano and amino polar functional groups are often encountered. Both approaches involve water and an organic solvent such as MeOH or acetonitrile to perform the separation. With respect to RP chromatography, hydrophobic molecules partition into the stationary phase under low organic solvent and high aqueous solvent content, allowing hydrophilic analytes such as glycans to elute. In the case of NP chromatography, the opposite is true, such that hydrophilic analytes will have an affinity for the stationary phase under highly non-polar environments, requiring an increase of water content for elution.



One adaptation of normal phase chromatography which has proven fruitful for targeting glycopeptides<sup>115,116</sup> is the hydrophilic interaction liquid chromatography (HILIC) method, first purposed by Alpert<sup>117</sup>. In this method, a thin liquid layer forms around the polar stationary phase so that liquid-liquid partitioning can occur. As larger glycans will exhibit more hydrophilic character, HILIC separations have demonstrated size separation of glycans<sup>118,119</sup>. In this mode, size takes preference over charge separation when referring to retention<sup>120</sup>. For glycopeptides, HILIC methods however generally serve as enrichment protocols, as it is difficult to separate individual glycopeptides from highly polar peptides which may co-elute and compete for ionization. Instead, the enrichment of glycopeptides from other tryptic peptides enables their analysis without suppression of ionization.

Glycans are hydrophilic due to the presence of polar groups, namely hydroxyl, N-acetyl-amino, amino, carboxylate, and sometimes sulfate. The use of ion pairing reagents in both normal and reversed phase chromatography helps to improve separation selectivity by neutralizing ionic species in solution and modifying their extent of adsorption on stationary phases<sup>121</sup>. Here, an example is trifluoroacetic acid (TFA), being added to the mobile phase in amounts ranging from 0.1-1% (v/v). This is thought to accomplish two main goals. First, TFA is a relatively strong acid ( $\sim 0.23$  pKa) which implies that even in small amounts it can lower the pH enough to protonate all amino acid side chains. In the case of protonated basic side chains, the TFA anion then pairs with the side chain, neutralizing the charge in an ion-pairing fashion. As ionic interactions are suppressed, the hydrophobicity of the analyte is enhanced, allowing more compatibility with partitioning chromatography. Secondly, TFA is a very volatile acid, thus easily

removed by lyophilization. Buffers can also be used for ion pairing, but salt residues present after lyophilization can affect ionization and complicate structural elucidation by MS.

Chromatography is an important portion of a protocol. Not only does the separation of analytes prior to mass spectrometry bring more specificity to the process, but it also concentrates the sample to produce a MS signal. Often the sample must be modified prior to separation and detection. The section below discusses common types of modifications.

#### 1.42 Derivatization

Modifying a sample prior to analysis for the benefit of increased sensitivity or quantification is commonly referred to as derivatization. Among other benefits, derivatization can enhance sample volatility, reduce post ionization source decay, or aid in chromatographic separation.

An approach frequently encountered in glycoproteomics is permethylation, which converts hydroxyl groups into methoxy groups using a methylating reagent such as methyl iodide under basic conditions<sup>122</sup>. This type of derivatization has a three-fold benefit for MS applications. First, methylation reduces the polarity of the carbohydrates, thus increasing their volatility. Secondly, altering the polarity of carbohydrates is more suitable when organic solvents are used in HPLC, allowing more compatibility with online ESI interfaces. Lastly, permethylated glycans produce easily interpretable CAD MS/MS fragmentation patterns<sup>123,124</sup>.

Derivatization protocols aimed at sialylated glycans have also been employed to reduce the possibility of forming ion adducts<sup>125</sup>, and to improve the ability to distinguish between  $\alpha$ 2,3 and  $\alpha$ 2,6 sialic acid branching<sup>126</sup>.

Other forms of derivatization include tagging the reducing end of oligosaccharides with labels suitable for HPLC-UV, HPLC-fluorescence and/or MS detection. For this approach, glycans released from glycoproteins (Section 1.22 Glycan Release) are subjected to a condensation reaction called reductive amination. In this process, a UV or fluorescent-active derivatization group containing an amine reacts with the carbonyl group present at the reducing end of a glycan to yield a Schiff-base<sup>127,128</sup> (Figure 1.17). Common derivatization groups for the purpose of carbohydrate analysis include: 2-amino pyridine (2-AP)<sup>129,130</sup>, 2-aminobenzamide (2-AB)<sup>131</sup> and 8-aminonaphthalene-1,3,6-trisulfonate (ANTS)<sup>132</sup> (Figure 1.18).

Other forms of derivatization for glycan analysis include the use of hydrazides to form hydrazones. Phenylhydrazine (PHN) has been shown to react with oligosaccharides in a quantitative manner<sup>66</sup> even if peptides are present in the mixture<sup>133</sup>. Girard's reagent (carboxymethyl triethylammonium hydrazide) is another hydrazide which has been used for improved glycan analysis. By introducing a permanent positive charge on the glycan, this reaction eliminates the frequent cationization of carbohydrates in mass spectrometry as  $[M+K]^+$  and  $[M+Na]^+$  ions<sup>134</sup>. Once derivatized, glycans can be separated using LC and collected manually for MALDI-MS analysis, or detected online using HPLC-ESI-MS. One advantage of this approach is that each glycan in a pool will react stoichiometrically with each given label, allowing for direct quantification of different glycans in a sample<sup>135</sup>.

Figure 1.17 - Schiff-base formation for carbohydrate derivatization

Proposed stepwise route for Schiff base formation. R' denotes branching towards the distal end of the oligosaccharide, whereas R'' denotes the fluorescent portion of the derivatizing agent (examples in Figure 1.18).

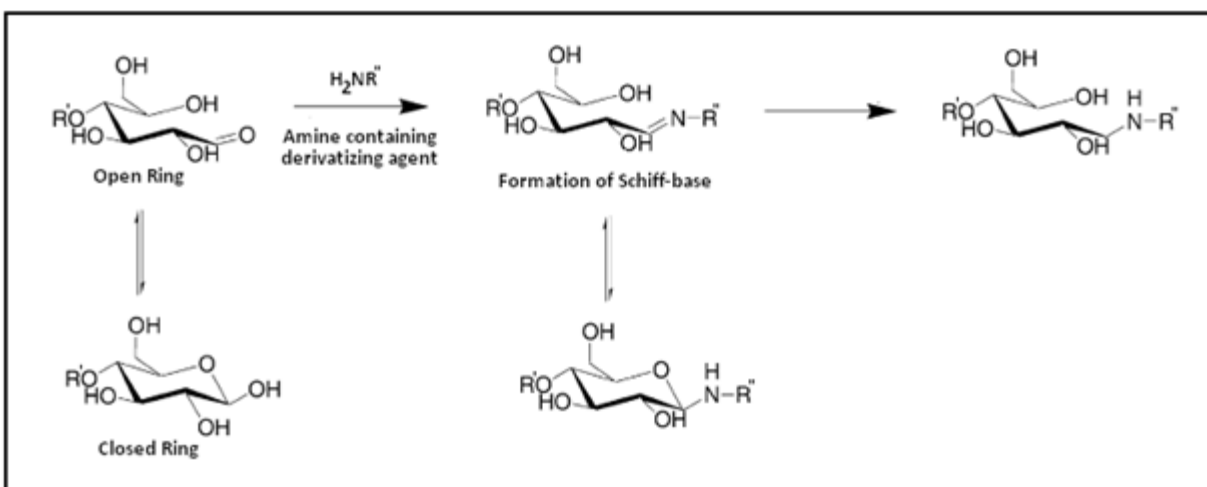
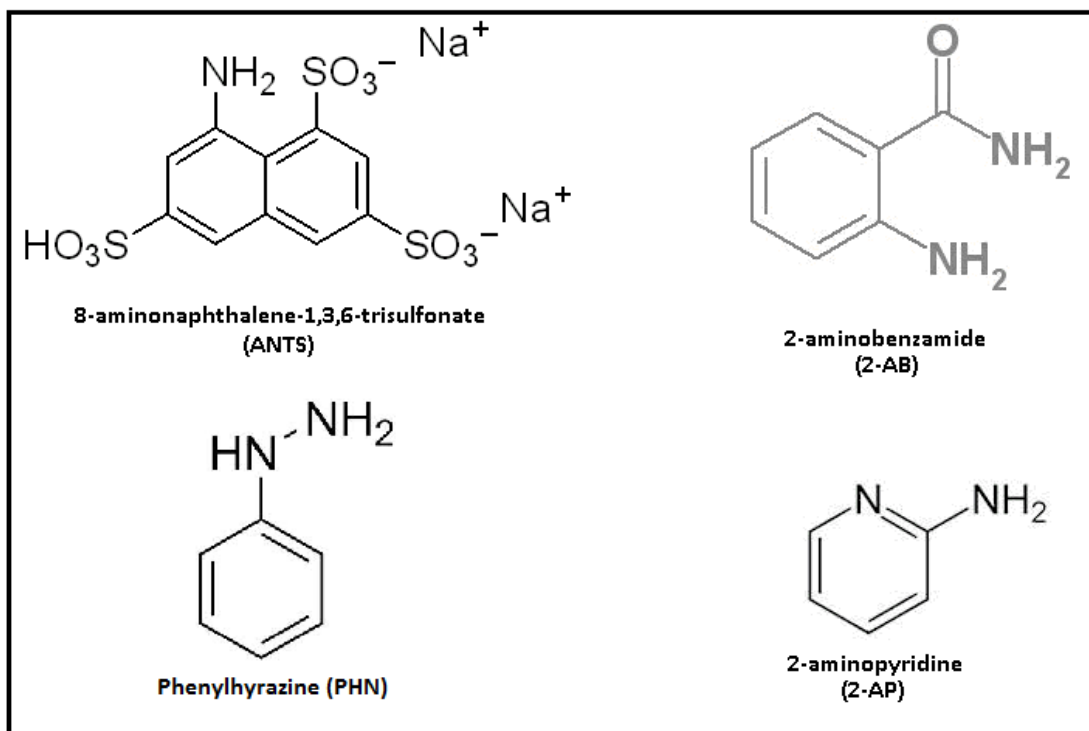


Figure 1.18 - Commonly encountered carbohydrate derivatizing agents

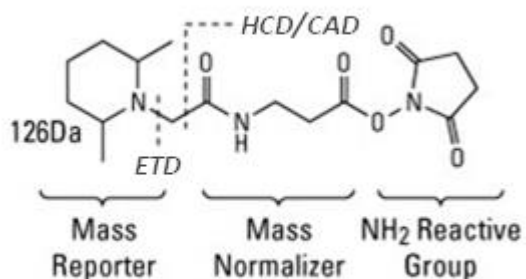


For high throughput protocols involving multiple samples, such as “control” vs. “diseased”, or for time-course studies, using one label over successive runs to quantify glycosylation is laborious. Stable isotope labels (SIL) were developed for accurate quantification of multiple samples in a single MS experiment. Examples include Tandem Mass Tags (TMTs)<sup>26</sup> and isobaric tags for relative and absolute quantitation (iTRAQ)<sup>136</sup>. These labels consist of three parts: a functional reactive group, a spacer arm, and a MS/MS reporter fragment which varies in isotopic labeling. These features allow for unique quantification owing to specific reporter ions. Also, SIL preserve similar physiochemical characteristics such as ionization efficiency for MS analysis and hydrophobicity for LC separation (Figure 1.19)<sup>137</sup>. Specific for glycoproteomic workflows, these labels contain an amine-reactive NHS-ester group which targets the side chains of lysine and N-terminal amino groups. Incomplete modification of serine, threonine, and tyrosine have however been observed<sup>138,139</sup>. This proteomic platform has been extended to the relative quantification of glycans with two distinct sets of reagents. Either hydrazide or aminoxy reactive groups are available to target the carbonyl at the reducing end of the glycan. The aminoxy approach has demonstrated better labeling efficiency and more accurate quantification than the hydrazine counterpart<sup>140</sup>.

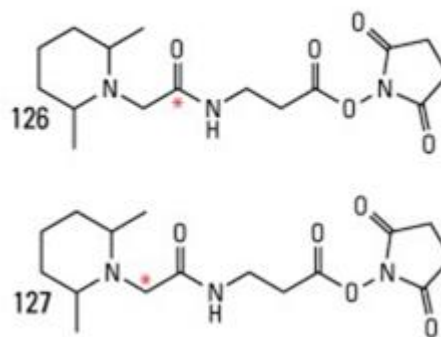
Figure 1.19 - Tandem Mass Tags (TMT) used in proteomic workflows

TMTs engineered for proteomic workflows. These labels use an amine-reactive functional group and a mass reporter region which produces cleavages specific to the mode of fragmentation used; ETD or HCD (A). These TMT tags can compare the abundances of peptides/glycopeptides from two samples as demonstrated by the duplex reagents (B). Isotope ( $^{13}\text{C}$ ) locations are indicated by an asterisk<sup>141</sup>.

**A. TMTzero Reagent (TMT<sup>0</sup>)**



**B. TMTduplex Reagents (TMT<sup>2</sup>)**



## 1.5 Research Goals

The field of Glycobiology is currently expanding as researchers probe deeper into the glycome. At present, mass spectrometry is at the forefront of instrumentation in this field. Innovations and improvements in the area of MS result in high sensitivity, high reproducibility, and high specificity in fragmentation information from glycans and glycopeptides. The work presented in this dissertation includes four independent projects that are unified by a common research objective, that is, the improvement of mass spectrometric (MS) detection and characterization of glycopeptides.

The first project (Chapter 2) was a mandated collaboration which was designed to analyze the expression of sialylation on antibodies cultured using a modified Trastuzumab construct known to generate improved yields of sialylation. In order to achieve this, HPLC methods were developed to isolate mAbs, and in depth MALDI-MS analysis at both the glycan and glycopeptide levels in the positive and negative modes were explored. Glycans were further detached from isolated glycopeptides and labeled on-target using a derivatization procedure with phenylhydrazine. Through the combination of HPLC separation, on target derivatization and optimized MS parameters, an overall workflow was established for the analysis of mAb's in general. This workflow is highly reproducible, and will allow for the separation, and glycan analysis of both mutant and non-mutant constructs.

In Chapter 3 and Chapter 4, two novel stationary phases were designed for targeted extraction of sialylated glycopeptides from tryptic digest mixtures. Since sialylation is known to be a crucial in a variety of biological processes, these approaches aimed to enrich sialylated

glycoforms for downstream MS analysis. HILIC and WAX principles were investigated for this purpose. HILIC has previously demonstrated a bulk retention of glycopeptides, and the addition of WAX interactions should aid in the retention of the negatively charged sialylated species. To evaluate the success of these two projects, a commercially available enrichment kit will be compared through the use of tandem mass tags for relative quantification.

Chapter 5 explores the metabolic expression of sialylation by varying the amount of a precursor provided to the cell culture. Mannosamine is a known precursor to sialic acid and since sialylation is a modifier of antibody efficacy, studies on the amount and location of sialic acid are important. By introducing azide-modified mannosamine, sialic acids are expected to be expressed with this azide too and could be exploited for downstream analysis to target sialylated molecules through “click-chemistry” reactions. The goal of this experiment is to determine the optimal concentrations of precursor necessary to express azide containing sialic acids. To achieve this, mAbs will be cultured with the precursor in a concentration-dependent assay and harvested prior to digestion and HPLC separation. Following this, samples will be analyzed using MALDI-MS and compared to a standard mAb which introduces the azide sialic acid enzymatically. Since the enrichment methods described in chapters 3 and 4 were not optimized for absolute enrichment prior to this experiment, moreover due to the relative simplicity of glycosylation on this antibody, HPLC separation was chosen as opposed to the developed glycopeptide enrichment protocols.

Each chapter presented in this dissertation contains a detailed introduction tailored to the specific content of the project. A section on methodology and instrumentation is also



presented, followed by discussion of the results. The work presented herein has either already been published, or is in preparation for journal submission. In Chapter 6, the work is discussed retrospectively, highlighting a variety of advantages and limitations to the methods discussed in each project as well as future research goals, and an overview of what is developing in the field of glycoproteomics.

## 1.6 References

---

- <sup>1</sup> Varki, A.; Cummings, R. D.; Esko, J. D.; Freeze, H. H.; Stanley, P.; Bertozzi, C. R.; Hart, G. W.; Etzler, M. E., *Essentials of Glycobiology, Second Edition*. CSHL Press: 2009.
- <sup>2</sup> Collins, P.; Ferrier, R., *Monosaccharides: Their Chemistry and Their Roles in Natural Products*. Wiley: 1995.
- <sup>3</sup> Geyer, H.; Geyer, R. *Biochimica et Biophysica Acta* **2006**, 1764 (2006), 1853–1869
- <sup>4</sup> Nilsson, J.; Rüetschi, U; Halim, A.; Hesse, C.; Carlsohn, E.; Brinkmalm, G.; Larson, G. *Nature Methods*. **2009**, 6 (11), 809-813.
- <sup>5</sup> Rapport, M.M.; Graf, L.; Skipski, V.P.; Alonzo, N.F. *Nature*. **1958**, 181 (4626), 1803-1804.
- <sup>6</sup> Homans, S.W.; Reguson, M.A.; Dwek, R.A.; Rademacher, T.W.; Anand, R.; Williams, A.F. *Nature*. **1988**, **333**(6170), 269-272.
- <sup>7</sup> McLean, J. *Circulation*. **1959**, 19(1), 75-78.
- <sup>8</sup> Dwek, R.A. *Chem Rev*. **1996**, 96, 683-720.
- <sup>9</sup> Weis, W.I., Drickamer, K. *Structure*. **1994**, 2, 1227-1240.
- <sup>10</sup> Sheriff, S, Chang, C.Y., Ezekowitz, R.A. *Nat. Struct. Biol*. **1994**, 1, 789–794.
- <sup>11</sup> Cazet, A., Julien, S., Bobowski, M., Krzewinski-Recchi, M., Harduin-Lepers, A., Groux-Degroote, S., Delannoy, P. **2010**, 345 (2010), 1377–1383.
- <sup>12</sup> Abbot K.L., Pierce J.M. *Methods in Enzymology*. **2010**, 480, 461-476.
- <sup>13</sup> Lennarz, W.J. *Biochemistry*. 1987. 26(23), 7205-7210.
- <sup>14</sup> Rothman, J.E. *Science*. 1981, 213(4513), 1212-9.
- <sup>15</sup> Pohlmann, R.; Waheed, A.; Haslik, A.; Von Figura, K. *J Biol Chem*. **1982**, 257, 5323-5325.
- <sup>16</sup> Dunphy, W.G.; Brands, R.; Rothman, J.E. *Cell*. **1985**, 40, 463-472.

- 
- <sup>17</sup> Roth, J.; Berger, E.G. *J Cell Biol.* **1982**, 93, 223-229.
- <sup>18</sup> Blom, N.; Sicheritz-Pontén, T.; Gupta, R.; Gammeltoft, S.; Brunak, S. *Proteomics.* **2004**, 4(6):1633-1649.
- <sup>19</sup> Kobata, A. *Eur. J. Biochem.* **1992**, 209, 483–501.
- <sup>20</sup> Furmanek, A.; Hofsteenge, J. *Acta Biochim Pol.* **2000**, 47(3):781-789.
- <sup>21</sup> Hofsteenge, J., Müller, D.R., de Beer, T., Löffler, A., Richter, W.J. & Vliegthart, J.F. *Biochemistry.* **1994**, 33, 13524-13530.
- <sup>22</sup> Yamaguchi, Y., Kato, K., Shindo, M., Aoki, S., Furusho, K., Koga, K., Takahashi N., Arata, Y., Shimada, I. *J. Biomol.NMR.* **1998**, 12, 385-394.
- <sup>23</sup> Celigoy J., Ramirez B., Tao L., Rong L., Yan L., Feng Y., Quinnan G., Broder C., Caffrey M. *J. Biological Chem.* **2011**, 286(27):23975-81.
- <sup>24</sup> Kakehi, K., Kinoshita, M., Kawakami, D., Tanaka, J., Sei, K., Endo, K., Oda, Y., Iwaki, M., Masuko, T. *Anal Chem.* **2001**, 73, 2640-2647.
- <sup>25</sup> Aebersold R., Mann M. *Nature.* **2003**, 422 (6928), 198–207
- <sup>26</sup> Thompson, A.; Schäfer, J.; Kuhn, K.; Kienle, S.; Schwarz, J.; Schmidt, G.; Neumann, T.; Hamon, C. *Anal. Chem.* **2003**, 75, 1895-1904
- <sup>27</sup> Viner, R.; Snovidá, S.; Saba, J.; Bodnar, E.; Perreault, H., A Novel Workflow for Glycopeptide Analysis Using Cellulose-based Separation Cartridges, TMT-labeling and LTQ Orbitrap ETD. ABRF 2010, Poster RP-16
- <sup>28</sup> Bodnar, E.; Snovidá, S.; Saba, J.; Viner, R.; Perreault, H, Glycopeptide Enrichment of Human Serum Using Cellulose Based Column. iHupo 2010, Poster
- <sup>29</sup> Reid, C.W.; Fulton, K.M.; Twine S.M. *Future Microbiol.* **2010**, 5(2), 267-288.

- 
- <sup>30</sup> Halim, A.; Carlsson, M.C.; Madsen, C.B.; Brand, S.; Møller, S.R.; Olsen, C.E.; Vakrushev, S.Y.; Brimnes, J.; Wurtzen, P.A.; Ipsen, H.; Petersen, B.L.; Wandall, H.H. *Mol Cell Proteomics*. **2015**, 14(1), 191-204.
- <sup>31</sup> Li, L.; Zhang, F.; Zaia, J.; Linhardt, R.J. *Anal Chem*. **2012**, 84(20), 8822-8829.
- <sup>32</sup> Cooper, C.A.; Packer, N.H.; Redmond, J.W. *Glycoconj J*. **1994**, 11(2), 163-167.
- <sup>33</sup> Triguero, A.; Cabrera, G.; Royle, L.; Harvey, D.J.; Rudd, P.M.; Dwek, R.A.; Bardor, M.; Lerouge, P.; Cremata, J.A. *Analytical Biochemistry*. **2010**, 400 (2010), 173–183.
- <sup>34</sup> Trimble R.B.; Maley F. *J. Analytical Biochem*. **1984**, 141(2), 515-522.
- <sup>35</sup> Tarentino, A.L.; Gomez G.M.; Plummer T.H. *J. Biochemistry*. **1985**, 24(17), 4665-4671.
- <sup>36</sup> Takahashi, N.; Nishibe, H. *J Biochem*. **1978**, 84(6), 1467-1473.
- <sup>37</sup> Ishihara, H.; Takahashi, N.; Ito, J.; Takeuchi, E.; Tejima, S. *Biochim Biophys Acta*. **1981**, 669(2), 216-221.
- <sup>38</sup> Maley, F.; Trimble, R.B.; Tarentino, A.L.; Plummer, T.H. Jr. *Anal Biochem*. **1989**, 180(2), 195-204.
- <sup>39</sup> Kolarich, D.; Altmann, F. *Anal Biochem*. **2000**, 285(1), 64-75.
- <sup>40</sup> Fan, J.Q.; Yamamoto, K.; Kumagai, H.; Tochikura, T. *Agric Biol Chem*. **1990**, 54, 233–234.
- <sup>41</sup> Huang, C.C.; Aminoff, D. *J Biol Chem*. **1972**, 247, 6737–6742.
- <sup>42</sup> Glasgow, L.R.; Paulson, J.C.; Hill, R.L. *J Biol Chem*. **1977**, 252, 8615–8623
- <sup>43</sup> Koutsioulis, D.; Landry, D.; Guthrie, E.P. *Glycobiology*. **2008**, (10), 799-805.
- <sup>44</sup> Carr, S.A.; Roberts, G.D.; Jurewicz, A.; Frederick, B. *Biochimie*. **1988**, 70, 1445-1454.
- <sup>45</sup> Sumner, J.B.; Howell, S.F. *J. Bacteriol*. **1936**, 32, 227–237.

- 
- <sup>46</sup> Van Damme, E. *Methods in Molecular Biology*. **2011**, 753, 289-297
- <sup>47</sup> Wang, L.; Li, F.; Sun, W.; Wu, S.; Wang, X.; Zhang, L.; Zheng, D.; Wang, J.; Gao, Y. *Mol Cell Proteomics*. **2006**, 5(3), 560-562.
- <sup>48</sup> Demelbauer, U.M.; Zehl, M.; Plematl, A.; Allmaier, G.; Rizzi, A. *Rapid Commun. Mass Spectrom*. **2004**, 18, 1575–1582
- <sup>49</sup> Gallagher, J.T.; Morris, A.; Dexter, T.M. *Biochem J*. **1985**, 231(1), 115-122.
- <sup>50</sup> Hongsachart, P.; Huang-Liu, R.; Sinchaikul, S.; Pan, F.M.; Phutrakul, S.; Chuang, Y.M.; Yu, C.J.; Chen, S.T. *Electrophoresis*. **2009**, 30(7), 1206-1220.
- <sup>51</sup> Novogrodsky, A.; Lotan, R.; Ravid, A.; Sharon, N. *J Immunol*. **1975**, 115(5), 1243-1248.
- <sup>52</sup> Lotan, R.; Skutelsky, E.; Danon, D.; Sharon, N. *J Biol Chem*. **1975**, 250(21), 8518-8523.
- <sup>53</sup> Shibuya, N.; Goldstein, I.J.; Broekaert, W.F.; Nsimba-Lubaki, M.; Peeters, B.; Peumans, W.J. *J Biol Chem*. **1987**, 262(4), 1596-1601.
- <sup>54</sup> Heo, S.H.; Lee, S.J.; Ryoo, H.M.; Park, J.Y.; Cho, J.Y. *Proteomics*. **2007**, 7, 4292–4302.
- <sup>55</sup> Kullolli, M.; Hancock, W.S.; Hincapie, M. *J Sep Sci*. **2008**, 31, 2733–2739.
- <sup>56</sup> Yamashita, M., Fenn, J.B. *J. Phys. Chem*. **1984**, 88, 4451-4459.
- <sup>57</sup> Karas, M., Hillenkamp, F. *Anal. Chem*. **1988**, 60 (20), 2299-2301
- <sup>58</sup> Zeleny, J. *Phys. Rev*. **1914**, 3, 69.
- <sup>59</sup> Zeleny, J. *Phys. Rev*. **1917**, 10, 1-8.
- <sup>60</sup> Dole, M., Mack, L.L., Hines, R.L. *J. Chem. Phys*. **1968**, 49, 2240.
- <sup>61</sup> Clegg GA, Dole M. *Biopolymers*. 1971, 10, 821–826.

- 
- <sup>62</sup> Fenn, J.B.; Mann, M.; Meng, C.K.; Wong, S.F.; Whitehouse, C.M. *Science*. **1989**, 246(4926), 64-71.
- <sup>63</sup> Taylor G. *Proc. R. Soc. Lond. A*. **1964**, 280, 383-397.
- <sup>64</sup> Hillencamp, F., Karas, M., Beavis, R.C., Chait, B.T. *Anal Chem*. **1991**, 63(24):1193A-1203A.
- <sup>65</sup> Snovida, S., Perreault, H. *Rapid Commun. Mass Spectrom*. **2007**, 21, 3711–3715
- <sup>66</sup> Lattová, E., Perreault, H. *J Chromatogr B*. **2003**, 793(1), 167-79.
- <sup>67</sup> Morris H.R., Paxton T., Dell A., Langhorne J., Berg M., Bordoli R.S., Hoyes J., Bateman R.H. *Rapid Communications in Mass Spec*. **1996**, 10, 889-896
- <sup>68</sup> Shevchenko A., Chernushevich I., Ens W., Standing K.G., Thomson B., Wilm M., Mann M. *Rapid Communications in Mass Spec*. **1997**, 11(9):1015-24.
- <sup>69</sup> Paul, W. Steinwedel, H.S.Z. *Z Naturforsch*. **1953**, 8a: 448-450.
- <sup>70</sup> Church, D.A. *J Applied Phys*. **1969**, 40: 3127–3134.
- <sup>71</sup> Morrison, J.D. *J. Organic Mass Spec*. **1991**, 26 (4): 183-194.
- <sup>72</sup> Yost, R.A., Enke, C.G. *J. American Chem. Society*. **1978**, 100:7 2274-2275
- <sup>73</sup> [http://www.ivv.fraunhofer.de/en/leistungsangebot/stoerstoffanalyse/ms\\_pages/Introduction\\_into\\_mass\\_spectrometry/ms\\_intro\\_analyzers.html](http://www.ivv.fraunhofer.de/en/leistungsangebot/stoerstoffanalyse/ms_pages/Introduction_into_mass_spectrometry/ms_intro_analyzers.html)
- <sup>74</sup> Stephens, W.E. *Phys. Rev*. **1946**, 69, 691
- <sup>75</sup> Cameron, A.E., Eggers Jr., D.F. *Rev. Sci. Instrum*. **1948**, 19, 605-607
- <sup>76</sup> Mamyrin, B.A., Karateav, V.I., Schmickk, D.V., Zagulin, V.A. *Sov. Phys. JETP*. **1973**, 37,45
- <sup>77</sup> Grix, R., Wöllnik, H., Schey, K., Cooks, R.G. *Int. J. Mass Spec. and Ion Proc*. **1987**, 77, 49-91.

- 
- <sup>78</sup> Bradbury, N.E., Nielson R.A. *Phys. Rev.* **1936**, 49, 388-393.
- <sup>79</sup> Kimmel, J.R., Engelke, F., Zare R.N. **2001**, 72, 4354-4357.
- <sup>80</sup> Vlasak, P.R., Beussman, D.J., Davenport, M.R., Enke, C.G. *Rev. Sci. Inst.* **1996**, 67, 68-72.
- <sup>81</sup> <http://www.abrf.org/ABRFNews/1997/June1997/jun97lennon.html>
- <sup>82</sup> Zaia J. *Mass Spec. Rev.* **2004**, 23, 161-227.
- <sup>83</sup> Clauser, K.R.; Baker, P.; Burlingame, A.L. *Anal Chem.* **1999**, 71, 2871.
- <sup>84</sup> Chaurand, P.; Luetzenkirchen, F.; Spengler, B. *J. Am. Soc. Mass Spectrom.* **1999**, 10, 91.
- <sup>85</sup> Chernushevich, I.V.; Loboda, A.V.; Tomson, B.A. *J Mass Spectrom.* **2001**, 36(8), 849-65.
- <sup>86</sup> Shevchenko, A.; Loboda, A.V.; Shevchenko, A.; Ens, W.; Standing, K.G. *Anal Chem.* **2000**, 72, 2132.
- <sup>87</sup> Chernushevich, I.V.; Ens, W.; Standing, K.G. *Anal Chem.* **1999**, 71(13), 452A-461A.
- <sup>88</sup> [http://www.per-form.hu/dokumentacio/intro\\_to\\_the\\_tripletof\\_5600\\_seminar\\_tf.pdf](http://www.per-form.hu/dokumentacio/intro_to_the_tripletof_5600_seminar_tf.pdf)
- <sup>89</sup> Charlwood, J.; Langridge, J.; Camilleri, P. *Rapid Commun. Mass Spectrom.* **1999**, 13(2), 107-112.
- <sup>90</sup> Harvey, D.J. *Analyst*, **2000**, **125**, 609-617
- <sup>91</sup> Harvey, D.J.; Scarff, C.A.; Crispin, M.; Scanlan, C.N.; Bonomelli, C.; Scrivens, J.H. *J Am Soc Mass Spectrom.* **2012**, 23(11), 1955-1966.
- <sup>92</sup> Orlando, R.; Bush, C.A.; Fenselau, C. *Bio Med. Environ. Mass Spectrom.* **1990**, 19(12), 747-754.
- <sup>93</sup> Domon, B., Costello, C. E. *Biochemistry.* **1988**, 27, 1534-1543 .
- <sup>94</sup> Wuhrer, M.; Isabel Cataline, M.; Deelder, A.R.M.; Hokke, C.H. *J Chrom. B.* **2007**, 849, 115-128.
- <sup>95</sup> Hui, J.P.M.; White, T.C.; Thibault, P. *Glycobiology*, **2002**, 12, 837.
- <sup>96</sup> Bateman, K.; White, R.; Yaguchi, M.; Thibault, P. J.; *Chromatogr. A* **1998**, 794, 327.
- <sup>97</sup> Nemeth, J.F.; Hochgesang, G.P. Jr.; Marnett, L.J.; Caprioli, R.M.; *Biochemistry*, **2001**, 40, 3109.

- 
- <sup>98</sup> Krokhin, O.; Ens, W.; Standing, K.G.; Wilkins, J.; Perreault, H. *Rapid Commun. Mass Spectrom.* **2004**, 18, 2020-2030.
- <sup>99</sup> Stimson, E.; Hope, J.; Chong, A.; Burlingame, A.L. *Biochemistry.* **1999**, 38, 4885-4895.
- <sup>100</sup> Harazono, A.; Kawasaki, N.; Itoh, S.; Hashii, N.; Ishii-Watabe, A.; Kawanishi, T.; Hayakawa, T. *Anal Biochem.* **2006**, 348(2), 259-268.
- <sup>101</sup> Nimtz, M.; Conradt, H.S.; Mann, K. *Biochim. Biophys. Acta.* **2004**, 1675 (1-3), 71-80.
- <sup>102</sup> Henriksson, H.; Denman, S.E.; Campuzano, I.D.; Ademark P.; Master, E.R.; Teeri, T.T.; Brumer III, H. *Biochem. J.* **2003**, 375, 61-73.
- <sup>103</sup> Marxen, J.C.; Nimtz, M.; Becker, W.; Mann, K. *Biochim. Biophys. Acta.* **2003**, 1650 (1-2), 92-98.
- <sup>104</sup> Skoog, D.A., Holler, J.F., Nieman T.A., Principles of instrumental analysis 5<sup>th</sup> Ed. Philadelphia: Saunders College, 1998.
- <sup>105</sup> Whelan, S.A.; Lu, M.; He, J; Yan, W.; Saxton, R.E.; Faull, K.F.; Whitelegge, J.P.; Chang, H.R. *J Proteome Res.* **2009**, 8(8), 4151-4160.
- <sup>106</sup> Zhao, J.; Simeone, D.M.; Heidt, D.; Anderson, M.A.; Lubman, D.M. *J Proteome Res.* **2006**, 5(7), 1792-802.
- <sup>107</sup> Kontro, H.; Joenväärä, S.; Haglund, C.; Renkonen, R. *Proteomics.* **2014**, 15, 1713-1723.
- <sup>108</sup> Du, Y.; Wang, F.; May, K.; Xu, W.; Liu, H.; *J Chromatogr B Analyt Technol Biomed Life Sci.* **2012**, 907, 87-93.
- <sup>109</sup> Du, Y.; May, K.; Xu, W.; Liu, H. *J Am Soc Mass Spectrom.* **2012**, 23(7), 1241-1249.
- <sup>110</sup> Nakano, M.; Kakehi, K.; Lee, Y.C. *J Chromatogr A.* **2003**, 1005, 13-21.
- <sup>111</sup> Lin, C.H.; Kuo, C.W.; Jarvis, D.L.; Khoo, K.H. *Proteomics.* **2014**, 14(1), 87-92.



- 
- <sup>112</sup> Pompach, P.; Chandler, K.B.; Lan, R.; Edwards, N.; Goldman, R. *J Proteome Res.* **2012**, 11(3), 1728-40.
- <sup>113</sup> Morelle, W.; Faïd, V.; Chirat, F.; Michalski, J.C. *Methods Mol Biol.* **2009**, 534, 5-21.
- <sup>114</sup> Shah, B.; Jiang, X.G.; Chen, L.; Zhang, Z. *J Am Soc Mass Spectrom.* **2014**, 25(6), 999-1011.
- <sup>115</sup> Jensen, P.H., Mysling, S., Højrup, P., Jensen, O.N. *Methods Mol Biol.* **2013**, 951:131-144.
- <sup>116</sup> Selman, M., Hemayatkar, M., Deelder, A.M., Wührer, M. *Anal. Chem.* **2011**, 83, 2492–2499
- <sup>117</sup> Alpert, A. *J. Chrom.* **1990**, 499, 177–196.
- <sup>118</sup> Mauko, L.; Pelzing, M.; Dolman, S.; Nordborg, A.; Lacher, N.A.; Haddad, P.R.; Hilder, E.F. *J Chromatogr A.* **2011**, 1218(37), 6419-6425.
- <sup>119</sup> Ahn, J.; Bones, J.; Yu, Y.Q.; Rudd, P.M.; Gilar, M. *J Chromatogr B Analyt Technol Biomed Life Sci.* **2010**, 878(3-4), 403-8.
- <sup>120</sup> Wührer, M., de Boer, A.R., Deelder, A.M.. *Mass Spec. Rev.* **2009**, 28, 192-206.
- <sup>121</sup> Mysling, S., Palmisano, G., Højrup, P., Thaysen-Anderson, M. *Anal Chem.* **2010**, 82, 5598-5609.
- <sup>122</sup> Ciucanu, I., Kerek, F. *Carbohydrate Research*, **1984**, 131, 209–217.
- <sup>123</sup> Kang, P.; Mechref, Y.; Novotny, M.V. *Rapid Commun Mass Spectrom.* **2008**, 22(5), 721-734.
- <sup>124</sup> Khoo, K.H.; Yu, S.Y. *Methods Enzymol.* **2010**, 478, 3-26.
- <sup>125</sup> Toyoda, M., Ito, H., Matsuno, Y., Narimatsu, H., Kameyama, A. *Anal Chem.* **2008**, 80, 5211-5218.
- <sup>126</sup> Reiding, K.R.; Blank, D.; Kuijper, D.M.; Deelder, A.M.; Wührer, M. *Anal Chem.* **2014**, 86(12), 5784-93

- 
- <sup>127</sup> Bigge, J.C.; Patel, T.P.; Bruce, J.A.; Goulding, P.N.; Charles, S.M.; Parekh, R.B. *Anal Biochem.* **1995**, 230, 229–238.
- <sup>128</sup> Anumula, K.R. *Anal Biochem.* **1994**, 220, 275–283.
- <sup>129</sup> Hase, S.; Ikenaka, T.; Matsushima, Y. *Biochem. Biophys. Res. Comm.* **1978**, 85, 257-263.
- <sup>130</sup> Hase, S.; Ibuki T.; Ikenaka, T. *J. Biochem.* **1984**, 95, 197-203.
- <sup>131</sup> Harvey D.J. *Analyst.* **2000**, 125, 609-617.
- <sup>132</sup> Che, F.; Jin-Fang, S.; Rong, Z.; Wang, K.; Xia, Q. *J. Chrom. A.* **1999**, 858, 229-238.
- <sup>133</sup> Lattová, E.; Perreault, H. *Mass Spectrom Rev.* **2013**, 32(5):366-85
- <sup>134</sup> Gil, G.C.; Kim, Y.G.; Kim, B.G. *Anal Biochem.* **2008**, 379, 45-59.
- <sup>135</sup> Ruhaak, L.R.; Zauner, G.; Huhn, C.; Bruggink, C.; Deelder, A.M.; Wührer, M. *Anal Bioanal Chem.* **2010**, 97, 3457-3481.
- <sup>136</sup> Ross, P.L.; Huang, Y.N.; Marchese, J.N.; Williamson, B.; Parker, K.; Hattan, S.; Khainovski, N.; Pillai, S.; Dey, S.; Daniels, S.; Purkayastha, S.; Juhasz, P.; Martin, S.; Bartlett-Jones, M.; He, F.; Jacobson, A.; Pappin, D.J. *Mol Cell Proteomics.* **2004**, 3(12), 1154-69.
- <sup>137</sup> Dayon, L.; Hainard, A.; Licker, V.; Turck, N.; Kuhn, K.; Hochstrasser, D.F.; Burkhard, P.R.; Sanchez, J.C. *Anal Chem.* **2008**, 80, 2921-2931.
- <sup>138</sup> Wiktorowicz, J. E.; English, R. D.; Wu, Z.; Kurosky, A. *J. Proteome Res.* **2012**, 11, 1512–1520.
- <sup>139</sup> Hung, C.W.; Tholey, A. *Anal. Chem.* **2012**, 84, 161–70.
- <sup>140</sup> Hahne, H.; Neubert, P.; Kuhn, K.; Etienne, C.; Bomgarden, R.; Rogers, J.C.; Kuster, B. *Anal Chem.* **2012**, 84(8), 3716-24.
- <sup>141</sup> TMT™ Mass tagging Kits and Reagents: <http://www.piercenet.com/instructions/2162073.pdf>

## **Chapter 2 – Glycan Analysis of biopharmaceutical Monoclonal Antibodies**

## 2.1 Authors Contributions

Mass spectrometric analysis, glycan separation and derivatization were performed by Edward D. Bodnar under the guidance of Dr. H. Perreault. Monoclonal antibody samples were provided by Celine Raymond at the National Research Council (NRC; Ottawa), through the Monoclonal Antibody network (MabNet). Edward D. Bodnar was also responsible for writing and generating all figures in this portion of the dissertation, while Dr. H. Perreault was responsible for editing its final version. All authors contributed equally to the final revision.

## 2.2 Abstract

Glycan moieties attached to proteins are known to influence efficacy and function of the glycoprotein. Currently, a variety of biotherapeutic compounds are being explored and developed, many of which contain varying forms of glycosylation. This study focused on determining the effect of sialyltransferase enzymes on a Trastuzumab construct in Chinese hamster ovary cells (CHO) and the ability to increase terminal  $\alpha$ 2,6 sialylation on a series of normal and mutant monoclonal antibodies. Here, we present an efficient workflow, which may be employed for streamline processing and glycan characterization of modified monoclonal antibodies. This workflow involves matrix assisted laser desorption ionization mass spectrometry (MALDI-MS) analysis in both positive and negative modes at the glycopeptide and glycan levels, including on-target derivatization with phenylhydrazine (PHN). In all mutated monoclonal antibodies, enhanced sialylation was observed as compared to their native counterparts.

## 2.3 Introduction

Glycans which are attached to proteins are known to serve a variety of physiological roles including cell-cell signaling, as well as immunological processes such as antigenicity<sup>1,2</sup>. One important family of glycoproteins are immunoglobulins (Ig) which have been found in a variety of classes including IgA, IgE, IgD, IgG, and IgM each working concertedly towards protective immunity<sup>3</sup>. Common observations regarding glycosylation of IgG include: loss of IgG effector function in the absence of glycosylation<sup>4</sup>, presence of core fucosylation which reduces FcγRII binding and ultimately antibody-dependent cell mediated cytotoxicity (ADCC)<sup>5</sup>, as well as anti-inflammatory properties in the presence of terminal sialic acids<sup>6</sup>.

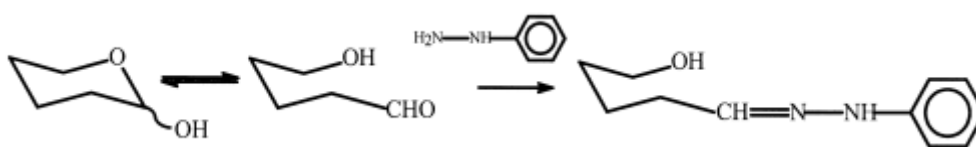
In light of this, the commercialization of recombinant monoclonal antibodies based on these constructs is of interest with special focus on glyco-engineering for enhanced efficacy and therapeutic value. One such example is Trastuzumab (Herceptin, Genentech Inc.). Trastuzumab is a highly purified humanized IgG1 monoclonal antibody which has the ability to bind with strong affinity and specificity to the extracellular domain of the human epidermal growth factor receptor 2 protein (HER2) known to be upregulated in primary breast carcinomas<sup>7</sup>.

With this considered, rigorous methodologies must be employed for strict quality control of the glycosylation profile on recombinant proteins if they are to be introduced as a therapeutic solution. To address this concern, high resolution mass spectrometric workflows have previously been employed for the complete analysis of glycans<sup>8,9,10</sup>. These approaches are performed by digesting the glycoprotein with a proteolytic enzyme such as trypsin in order to create a pool of peptides and glycopeptides. The resulting solution is then enriched or

fractionated for glycopeptides prior to MS analysis because the ionization of peptides tends to suppress that of the glycopeptides. The isolated glycopeptide fraction can also be deglycosylated to remove the sugars, which are then separated from the peptides using reversed-phase solid-phase extraction.

One beneficial method for streamline processing, is the on target derivatization of glycans using phenylhydrazine (PHN) as it allows for improved ionization of glycans in the presence of their peptide counterparts<sup>11</sup> (Figure 2.1).

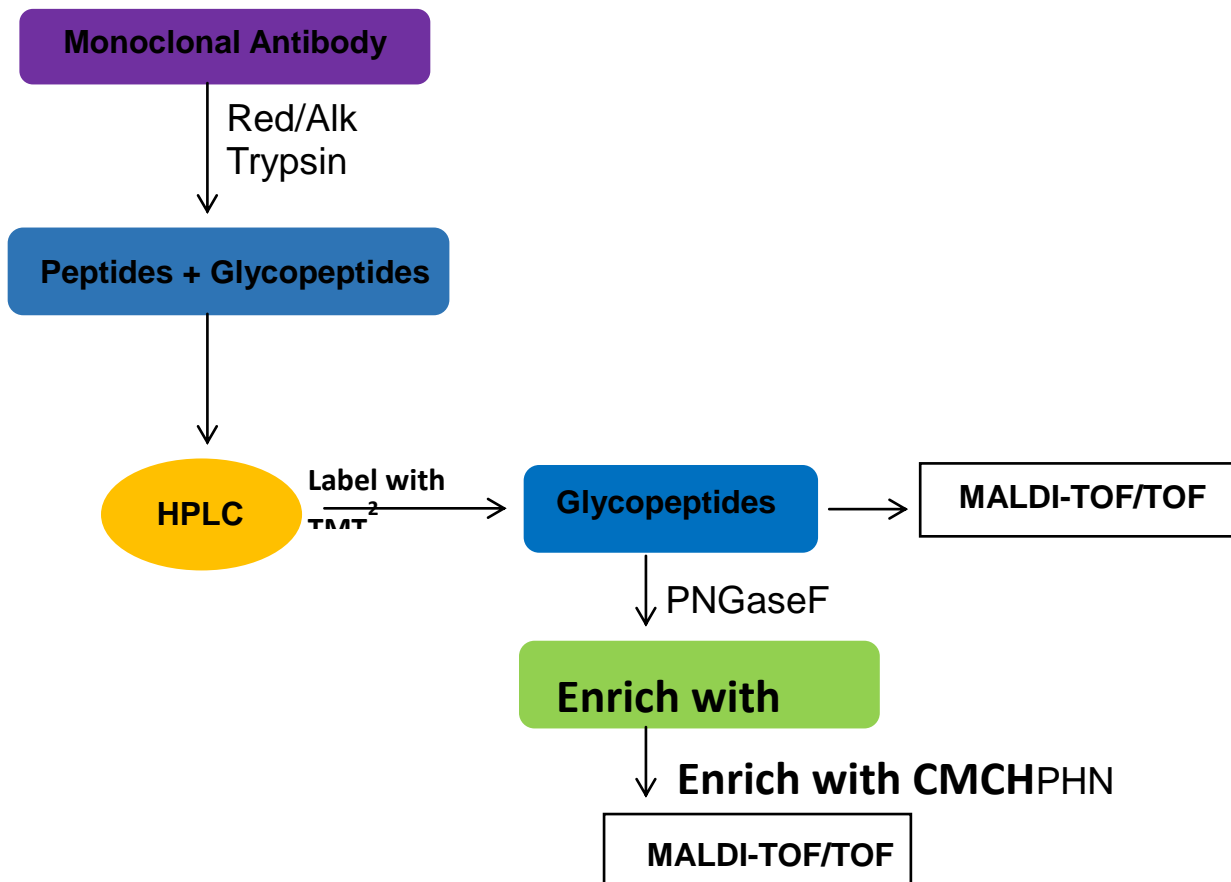
Figure 2.1- Formation of Schiff-base using phenylhydrazine



Here, we discuss an efficient approach for analyzing the glycosylation profile of two series of mAb samples at both the glycopeptide and glycan levels. The first series of three Trastuzumab samples were cultured with varying amounts of  $\alpha$  2,6 sialyl transferase, while the second series were cultured in the same manner but contain an amino acid point mutation at Phe<sub>243</sub> to alanine, which has been demonstrated to cause enhanced sialylation<sup>12</sup>. To evaluate the production and variability in glycosylation among these samples, glycopeptide fractions were isolated using high performance liquid chromatography (HPLC) for subsequent MALDI-ToF/ToF analysis. Next, these fractions were deglycosylated and derivatized using PHN (Figure 2.2).

Figure 2.2 - Workflow for Glycan and Glycopeptide analysis by Mass Spectrometry.

This illustrates a typical workflow to prepare a glycoprotein for MS analysis. Briefly, steps include reduction and alkylation of the protein, followed by proteolytic digestion with an enzyme such as trypsin. Glycopeptides are then isolated using a C<sub>18</sub> reversed phase column and analyzed with MALDI-MS. These glycopeptides can also be subjected to PNGaseF cleavage in order to remove their sugars, followed by labeling with phenylhydrazine (PHN) for improved detection with MALDI-MS.





## 2.4 Experimental

### 2.41 Materials

Dithiothreitol (DTT), iodoacetamide (IA), triethyl ammonium bicarbonate (TEAB), and tri-fluoroacetic acid (TFA) were obtained from Sigma (St. Louis, MO). Six monoclonal antibody (mAb) samples were prepared<sup>13</sup> (S2, S2m, S3, S3m, 5-20% and 5-20%m) through the Monoclonal Antibody Network (MabNet) (Winnipeg, Manitoba)<sup>14</sup>. The mAb framework was Trastuzumab<sup>TM</sup> (TMZ), also known as human IgG1. Throughout the analyses, Eg2-hFc antibody, also obtained from MabNet, was used as a control sample. Sequencing grade Trypsin was purchased from Promega (Madison, WA), while peptide-N-glycosidase (PNGaseF) was obtained from Prozyme (Hayward, CA). All solvents were HPLC-grade and obtained from Sigma (St. Louis, MO). Distilled de-ionized water was obtained using a Milli-Q<sup>TM</sup> filtration system supplied by a reverse-osmosis feedstock.

### 2.42 Methods

#### 2.421 Glycopeptide Preparation & Digestion

In these experiments, all of each sample received (estimated to a maximum of 200 µg per antibody) was used. Thus each monoclonal antibody (200 µg, 1 nmol) was dissolved in 100 µL of 50 mM triethylammonium buffer (TEAB, pH~8) and vortexed. A stock DTT sample solution (10 mM) was made, and 100 µL of this was added to each sample. The samples were vortexed and left to react at 56<sup>0</sup>C for 1 h, at which time 80 µL of IA (500 mM) was added, and the sample was left to react in the dark for 30 min. To each sample, 5 µg of trypsin was added and the mixture

was allowed to react at 37<sup>0</sup>C for approximately 18 h. To deactivate the trypsin a large volume of acetonitrile + 0.1% TFA was added and this mixture was vortexed, lyophilized and resuspended in 100 µL of Milli-Q™ water for HPLC separation.

#### ***2.422 High Performance Liquid Chromatography (HPLC)***

Separation and isolation of glycopeptides were performed using a previously reported method<sup>15</sup>. In brief, this involved equilibrating the column (Vydac 218 TP54 Protein & Peptide C<sub>18</sub> analytical column; Separation Group, Hesperia, Ca, USA), with 95:5 H<sub>2</sub>O:ACN + 0.1%TFA, for approximately 10 min. Upon injection of the sample (25 µL), the gradient used is as follows: 95:5 H<sub>2</sub>O:ACN + 0.1%TFA for (5 min), then to 90:10 H<sub>2</sub>O:ACN + 0.1%TFA (over 5 min), and finally to 70:30 H<sub>2</sub>O:ACN + 0.1%TFA (over 10 min). Prior to injection, the column was cleaned for 10 min using 50:50 H<sub>2</sub>O:ACN + 0.1%TFA, 10 min using 5:95 H<sub>2</sub>O:ACN + 0.1%TFA, and finally it was re-equilibrated with 95:5 H<sub>2</sub>O:ACN + 0.1%TFA, with a flow rate of 0.7 mL/min. Fractions were collected manually, pooled, and dried completely prior to further analysis.

#### ***2.423 Glycan Derivatization using Phenylhydrazine (PHN)***

After glycopeptide analysis by MALDI, glycans were enzymatically detached from the glycopeptides isolated during the HPLC separation. This was accomplished by lyophilizing the glycopeptide fraction to dryness, then re-suspending it in 100 µL of 25 mM TEAB with the addition of 2 µL of stock peptide-N-glycosidase (PNGaseF) and allowing it to react at 37<sup>0</sup>C overnight. On target phenylhydrazine derivatization (PHN) of glycans was accomplished by making a stock solution of 1 µL of PHN:3 µL ACN:10 µL H<sub>2</sub>O. First, 0.75 µL of matrix was spotted on target along with 0.75 µL of sample. When the spot was nearly dry, 0.4 µL of the stock

phenylhydrazine solution was spotted and left to react at 60 °C for 1 h, prior to MALDI-MS analysis.

#### **2.424 Mass Spectrometric Analysis**

MALDI-MS and MS/MS analysis was performed using an UltrafleXtreme (Bruker Daltonics, Germany) in both the positive and negative ion modes with a matrix of 2,5-dihydroxybenzoic acid (2,5 DHB; 20 mg in 1 mL of 7:3 H<sub>2</sub>O:ACN+0.1%TFA) and a scanning range of 700-4500 m/z. Each sample was prepared by spotting 0.75 µL of matrix with 0.75 µL of sample and then allowed to dry on target before loading it into the MS.

## **2.5 Results & Discussion**

### ***Isolation of Glycopeptides***

In this workflow, 6 monoclonal antibody samples (S2, S2m, S3, S3m, 5-20%, and 5-20%m, where m denotes mutant) were prepared individually and their glycopeptides were manually collected off a HPLC using a reversed-phased (RP) C<sub>18</sub> column, prior to MALDI-MS analysis. An Ala<sub>243</sub> point mutation is selected to provide accessibility to the glycosyltransferases to effect increased sialylation. The non-mutant samples contain Phe<sub>243</sub>, which is thought to provide more steric hindrance toward sialylation by the enzymes. This was investigated by co-expressing 2% β-galactosyltransferase (β -GT) and 20% of sialyltransferase 6 (ST6) in two replicate samples (S2/S2m and S3/S3m series), and then increasing the β-GT to 5% for the final series (5-20%/5-20%m).

The first step of the analysis consisted of characterizing the tryptic glycopeptides obtained for each preparation of monoclonal antibody (mAb). A control Eg2-hFc sample (200 µg) was analyzed in parallel to assess the efficiency of the method. Since the TMZ mAb contains only a single N-linked glycosylation site in its Fc region located at Asn<sub>297</sub> (EEQN<sub>297</sub>STYR), these spectra were expected to produce 5 glycoforms of EEQYNSTYR; namely FG0 (no galactose), FG1 (1 galactose), FG2 (2 galactoses), FG2S1, which bears one sialic acid, and FG2S2, which bears two sialic acids (Figure 2.3).

Figure 2.3 – N-glycans observed at N<sub>297</sub> on Trastuzumab

The five commonly expressed glycans found at asparagine 297 in IgG monoclonal antibodies, where F denotes core fucose, G represents the number of terminal galactose, and S the number of terminal sialic acids.

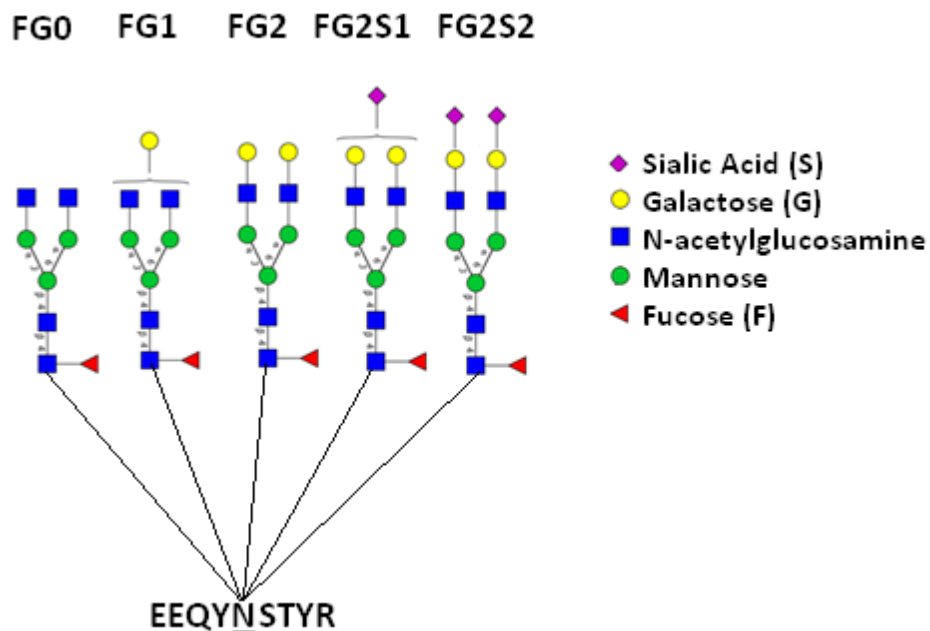
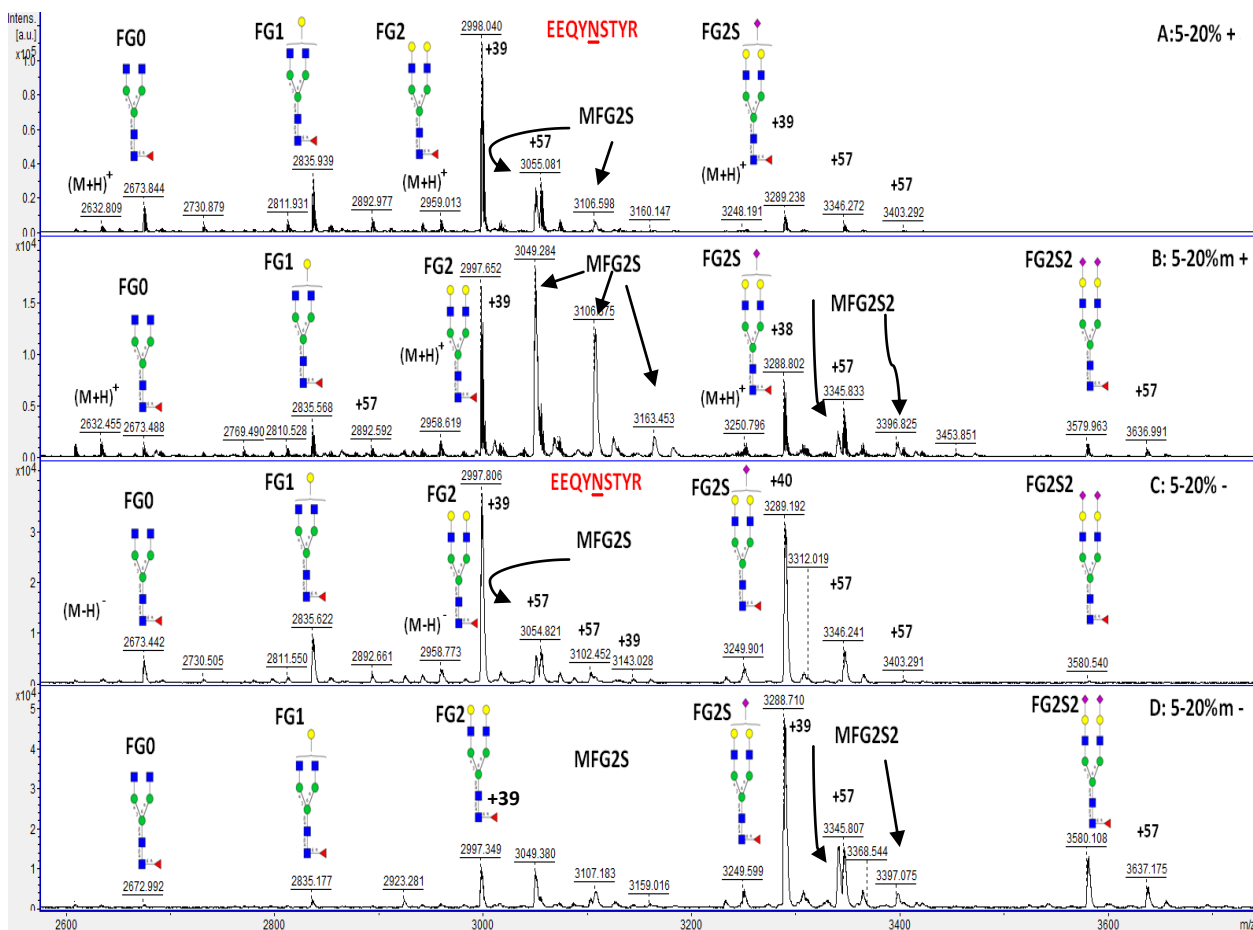


Figure 2.4 A-B shows positive mode MALDI spectra of glycopeptides acquired for samples 5-20% and 5-20%m. The  $(M+H)^+$  ions of FG0, FG1, FG2, FG2S1 and FG2S2 are predicted at nominal  $m/z$  2634, 2796, 2958, 3349 and 3540, respectively. Instead, adducts of  $[M+H+39]$  and  $[M+H+57]$  dominate. Adducts of 57 are due to overalkylation of the peptide chain. From the signals obtained in this spectrum and those of other mAb samples, it was clear that the 200  $\mu\text{g}$  quantity had been overestimated, i.e. there would have been a large excess of iodoacetamide for more probability of post-reduction alkylation. Negative mode MALDI spectra of mAb glycopeptides also showed the +57 adducts relative to  $m/z$  values of  $[M-H]^-$  ions (Figure 2.4 C-D). The adducts of 39 could be due to potassium ions present in the original sample buffer however as will be discussed below, further investigation by  $\text{MS}^2$  suggests that this adduct is also related to acetamidation. The observation of these  $M+39$  ions in the negative mode spectra (Figure 2.4 C-D), suggests a covalently attached adduct rather than  $\text{K}^+$ . In comparison, the positive and negative spectra obtained for glycopeptides of the Eg2-hFc control displayed only  $[M+H]^+$  and  $[M-H]^-$  ions and stronger signals (not shown).

Figure 2.4 – MALDI mass spectra of glycopeptides from samples 5-20% and 5-20%*m*. The spectra presented below are collected in A) & B) positive ionization mode and C) & D) negative ionization mode.



### MS-MS determination of adducts

These trends were further investigated by tandem mass spectrometry (MS/MS) to determine the source and location of these adducts, as they appeared to be the preferential form of ionization of the samples. MS/MS spectra were acquired for FG2 on (M+H+57)<sup>+</sup> precursors, and compared to the fragmentation pattern of regular FG2 (M+H)<sup>+</sup> ions (Figure 2.5). For glycopeptides typical MALDI-MS/MS spectra exhibit a characteristic fragmentation pattern

consisting of  $[P+H-17]^+$ ,  $[P+H]^+$ ,  $[P+84]^+$ , and  $[P+204]^+$  ions<sup>16</sup>, where P corresponds to the mass of the peptide without the glycan unit. However for the +57 adduct (Figure 2.5A), MS/MS produced this typical series of ions at 57  $m/z$  units higher than observed in B. This shows that the adduct is on the peptide chain and not on the glycan, confirming our assumption that overalkylation of the peptide backbone by iodoacetamide (IA) had occurred, as reported previously by another research group<sup>17</sup>. Figure 2.6, shows the spectrum of  $(M+39)^+$  ions of the FG2 glycopeptide sample from 5-20%.

Among the fragment ions all of the  $[P+H-17]^+$ ,  $[P+H]^+$ ,  $[P+84]^+$ , and  $[P+204]^+$  are observed in pairs, one corresponding to EEQYNSTYR + 39, the other to EEQYNSTYR + 57. The difference of 18 between these species suggests that the  $[M+39]^+$  ions arises from acetamidation followed by loss of water from the peptide backbone  $[P+39]^+$  or from the sugar moiety  $[P+57]^+$ . Recently, our group has investigated the nature of these adducts by alkylating synthetic peptide EEQYNSTYR<sup>18</sup>, and these preliminary data suggest that alkylation occurs on the secondary glutamic acid followed by dehydration through cyclization to the N-terminus, which has been observed for N-terminus E<sup>19</sup>. Observations such as these emphasize the importance of using cleanup and desalting protocols to simplify downstream MS spectral interpretation. As the totality of each sample had been used for digestion so far in our study of sialylated mAbs, the opportunity to re-work the samples was not afforded.

Figure 2.5 – MS<sup>2</sup> spectrum of over-alkylated glycopeptide at 3015.75 *m/z* (FG2+H+57)<sup>+</sup>

Both MS/MS spectra are derived from 5-20% mAb sample. In figure A) over-alkylation of the Peptide + HexNAc<sup>O,2</sup> cross ring cleavage is shown at mass 1330.047 *m/z*. In comparison, Figure B) from the same sample shows the Peptide + HexNAc<sup>O,2</sup> cross ring cleavage at mass 1272.789

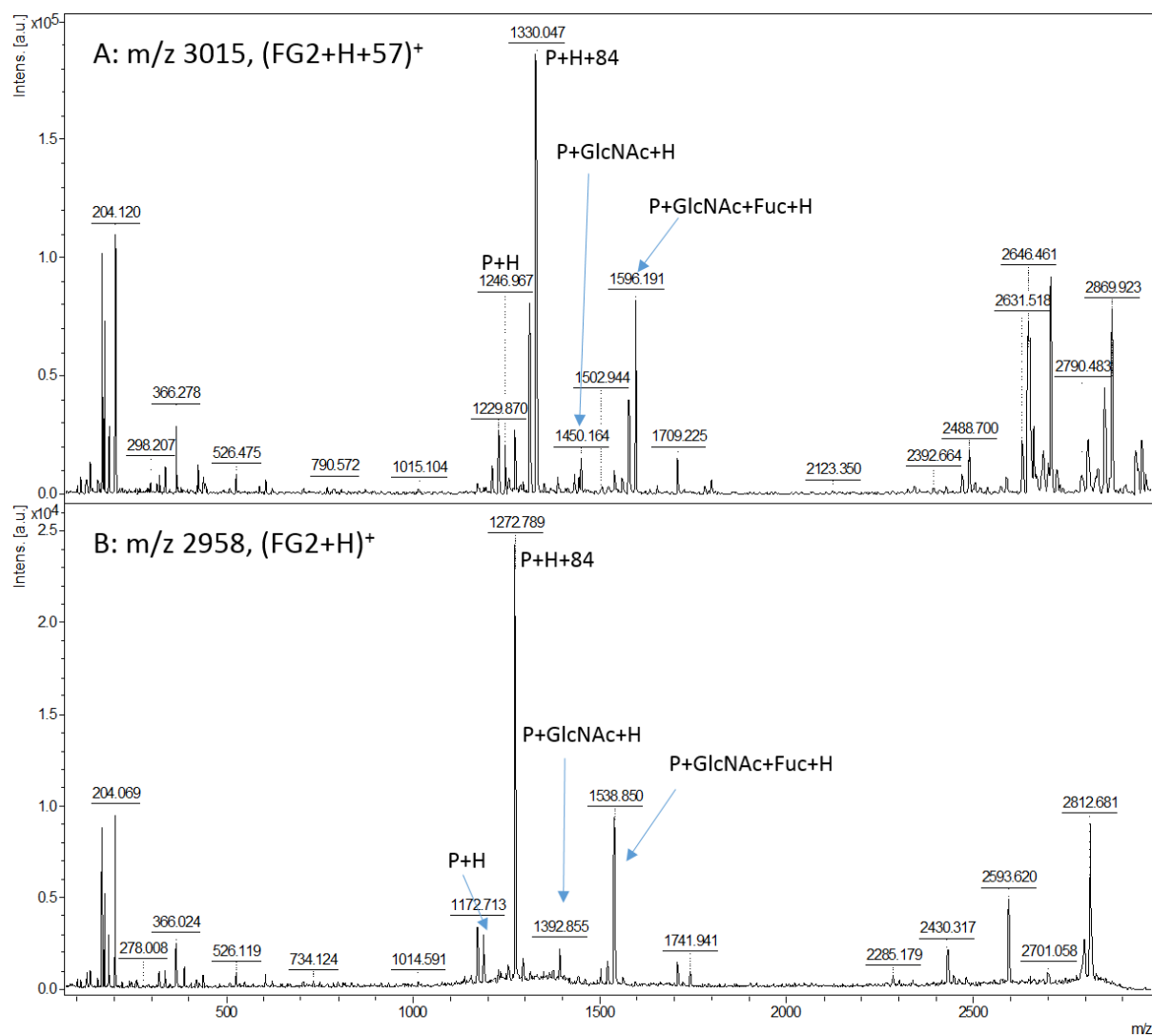
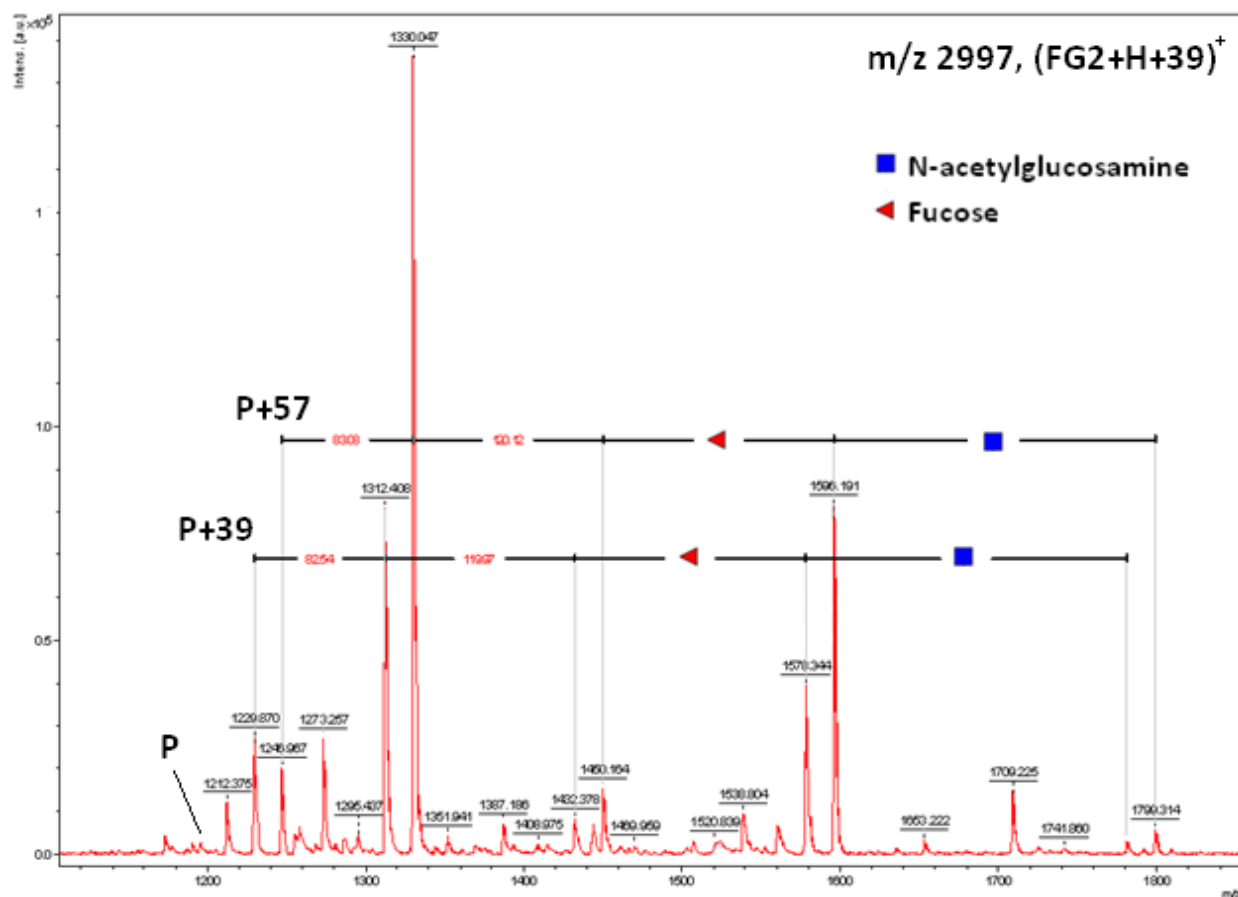




Figure 2.6 – MS<sup>2</sup> spectrum of glycopeptide at 2997 *m/z* (FG2+H+39)<sup>+</sup>

This spectrum for *m/z* 2997 is focused on the area containing the X<sup>0,2</sup> cross ring cleavage. Both P+H+39 and P+H+57 are observed as product ions. P denotes peptide.



### Glycopeptide analysis of mAb sialylation

Referring back to Figure 2.4, increases in sialylation at the glycopeptide level were observed in each of the mutant samples for both the FG2S1 and FG2S2 peaks, however the splitting of glycopeptides into different ionized species made difficult spectral interpretation and relative quantification. The latter was attempted nevertheless by summing up peak areas related to each glycoform and normalizing them to the highest peak in the spectra (FG2); these

results are presented in Table 2.2. Interestingly, in Figure 2.4 the spectra acquired in the MALDI-MS reflector mode showed metastable ions resulting from neutral losses of one sialic acid residue; FG2S ( $\text{FG2S} \rightarrow \text{FG2} + \text{S}$ ) and FG2S2 ( $\text{FG2S2} \rightarrow \text{FG2S} + \text{S}$ ) which have previously been documented<sup>20</sup>. These metastable ions are discernible from normal peaks due to their width, low resolution, and non-specific  $m/z$  values. They originate from loss of sialic acid occurring during the first part of flight, i.e. before ions arrive to the reflector. Originally accelerated from the ion source as larger sialylated ions, they pass through the reflector as smaller ions (minus 1 NeuAc) and are reaccelerated according to their new mass, explaining why they appear at  $m/z$  in between that of the ion of origin and that of the newly formed ion. They are marked with M in the figure, e.g. the label “MFG2S” refers to metastable fragmentation of FG2S through loss of S.

In Table 2.1, values reported for FG2S and FG2S2 glycoforms are the sum of (FG2S + MFG2S) and (FG2S2 + MFG2S2) peak areas, respectively. There are a few features worth noting from Table 2.2: i) FG2S2 is almost not observed in the positive mode, even for mutant samples; ii) there is a clear increment in FG2S and FG2S2 species from normal to mutant antibodies; iii) ion abundances of neutral glycoforms FG0, FG1 and FG2 remain in the same range for both + and – mode; iv) for acidic glycoforms, signals of FG2S are comparable from positive to negative, but for FG2S2 as the negative mode strongly favors ionization of these compounds; iv) the 5-20% sample shows the least increase in sialylation of all mutant samples.

Because of this discrepancy between FG2S and FG2S2 in terms of ionization efficiency, the method used here remains only qualitative, and esterification of the sialic acids into neutral

compounds would have been necessary to accurately assess the levels of sialylation in both ionization modes. Nevertheless, this portion of the study achieved its primary goal, which was to determine if the point mutation on mAbs allowed for increased sialylation, and results clearly show that it did.

Table 2.1- Relative percentages of ion abundances per glycoform species obtained by MALDI positive and negative ionization modes. Peak areas are normalized to FG2.

Ion mode\Glycoform	FG0	FG1	FG2	FG2S	FG2S2	FG2S2/FG2S
<b>S2 +</b>	34	56	100	137	0	0.00
<b>S2m +</b>	11	122	100	2189	275	0.13
<b>S2 -</b>	37	54	100	164	2	0.01
<b>S2m -</b>	18	36	100	1585	1776	1.12
<b>S3 +</b>	29	64	100	112	0	0.00
<b>S3m +</b>	50	111	100	3737	495	0.13
<b>S3 -</b>	30	67	100	149	2	0.01
<b>S3m -</b>	29	111	100	2147	2264	1.05
<b>5-20% +</b>	14	25	100	72	0	0.00
<b>5-20%m +</b>	12	16	100	562	58	0.10
<b>5-20% -</b>	12	24	100	106	1	0.01
<b>5-20%m -</b>	14	17	100	812	425	0.52

### *Glycan analysis of mAbs using phenylhydrazine*

As Figure 2.4 showed complex spectra due to adducts on the peptide chain, the next logical step was to deglycosylate the glycopeptide fractions using PNGaseF, and to subsequently derivatize glycans on target using phenylhydrazine (PHN) prior to MALDI-ToF analysis. Through this approach, the comparison of each glycoform's abundance is simpler, as the peptide has

been eliminated and there is only one peak per glycan. Figure 2.7 shows the positive mode MS spectra of glycans labeled on target with phenylhydrazine from the 6 monoclonal antibody samples. As it was the case for glycopeptides, it is easy to notice a stark increase in the FG2S1 and FG2S2 signals for each of the mutated samples, as well as lower FG0 and FG1 glycoforms (Figure 2.7; B,D,F).

Figure 2.8 contains the negative ion spectra, showing that the increase in signals of sialylated species for mutants is corroborated (B,D,F). Interestingly in the negative spectra, the ionization of neutral glycans FG0, FG1 and FG2 is almost completely suppressed by the presence of sialylated species, more so than it was the case with glycopeptides (see Table 2.1). For this reason, the values reported for the FG2S1 and FG2S2 glycoforms could not be normalized to the FG2 peak. Instead a ratio was created based on the peak areas for FG2S1 and FG2S2 (Table 2.2).

Figure 2.7 - Monoclonal antibody glycans labeled on target with phenylhydrazine and analyzed in positive mode.

Depicted are positive mode MALDI-MS spectra of glycans labeled on target with phenylhydrazine from 6 monoclonal antibodies: (a) S2 (b) S2m (c) S3 (d) S3m (e) 5-20% (f). Highlighted in rectangles is the presence of FG2S2 only for mutated samples.

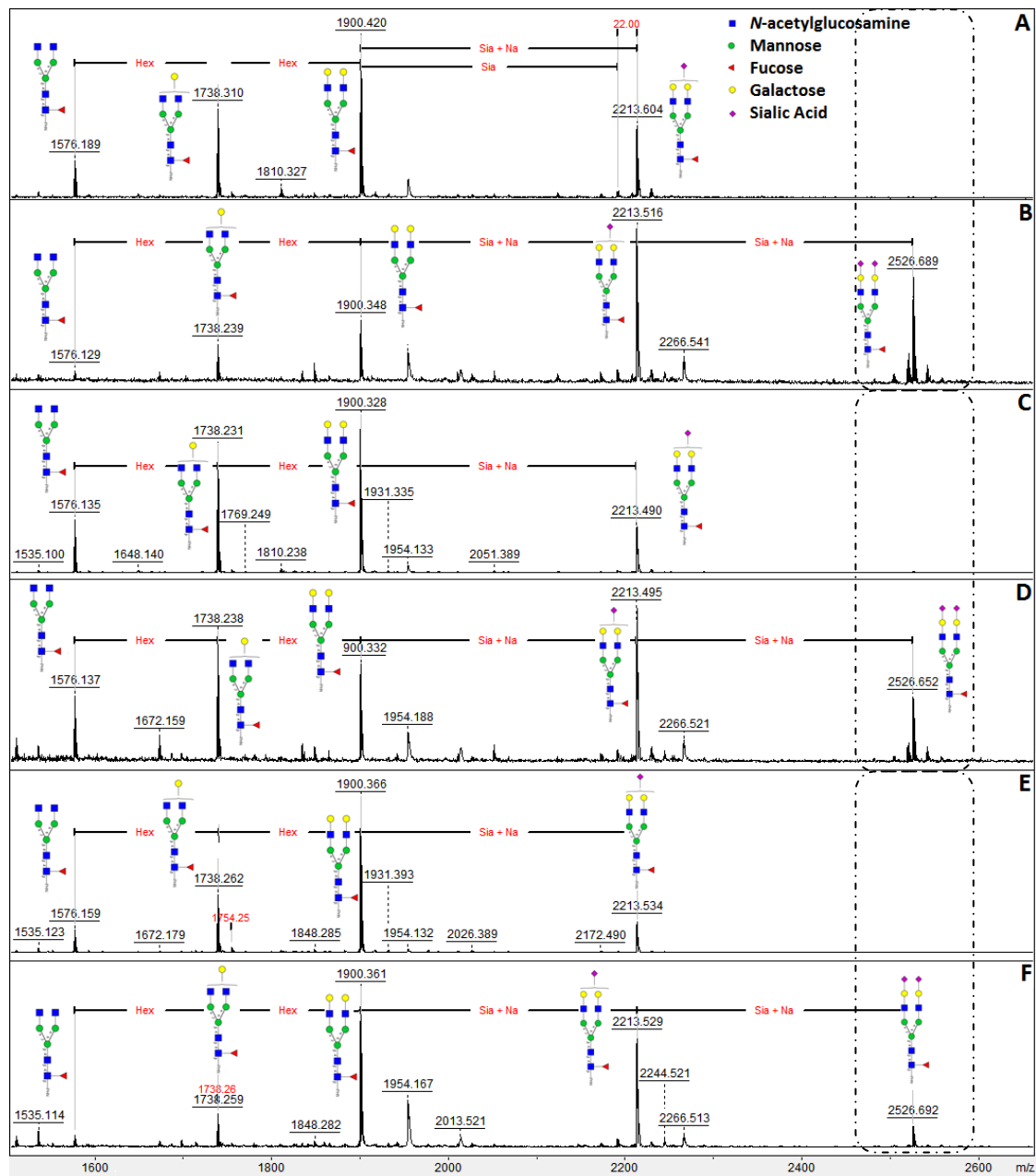


Figure 2.8 - Monoclonal antibody glycans labelled on target with phenylhydrazine in negative mode.

Depicted are negative mode MS spectra of glycans labeled on target with phenylhydrazine from 6 monoclonal antibodies (a) S2 (b) S2m (c) S3 (d) S3m (e) 5-20% (f) 5-20m.

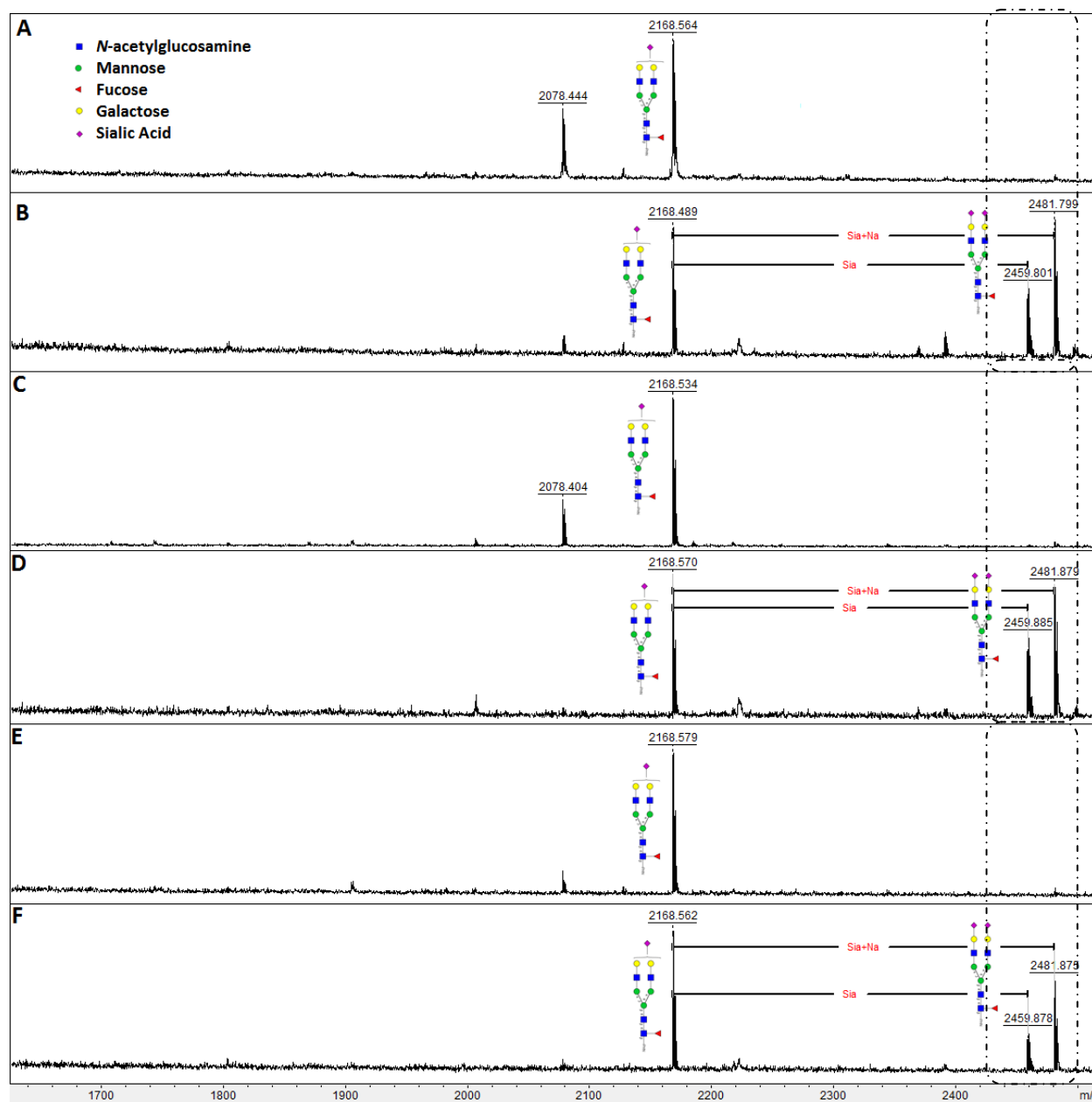


Table 2.2 - Relative percentages of ion abundances per glycan species obtained by MALDI positive and negative ionization modes. Peak areas are normalized to FG2 where possible.

Ion mode\Glycan	FG0	FG1	FG2	FG2S	FG2S2	FG2S2/FG2S
<b>S2 +</b>	21	48	100	99	0	0.00
<b>S2m +</b>	9	48	100	499	395	0.79
<b>S2 -</b>	0	0	100	3906	97	0.02
<b>S2m -</b>	0	0	0	-	-	1.79
<b>S3 +</b>	25	73	100	54	0	0,00
<b>S3m +</b>	45	92	100	288	163	0.57
<b>S3 -</b>	0	94	100	3058	97	0.03
<b>S3m -</b>	0	46	100	1055	1670	1.58
<b>5-20% +</b>	11	32	100	20	0	0.00
<b>5-20%m +</b>	5	17	100	198	38	0.19
<b>5-20% -</b>	0	109	100	4318	132	0.03
<b>5-20%m -</b>	0	0	0	-	-	0.81

### *Incorporation of metastable ions*

Metastable ions are observed for glycans as well as they lose neutral sialic acid residues before passing through the instrument's reflector, i.e. around  $m/z$  2222 in the negative mode and  $m/z$  1954 and 2226 in the positive mode. Their peak areas were included in the calculations leading to Table 2.2 which once again was normalized to highest glycan peak (FG2). The comparison of FG2S2/FG2S ratios between glycopeptides (Table 2.1) and glycans shows that the ratios are larger for glycans than for glycopeptides, i.e. double sialylation has a stronger ionization enhancement effect for glycans than glycopeptides in the negative mode. The peptide chain seemingly acts as a "buffer" and keeps a slightly more positive character than the glycan alone. As for the detection of FG2S glycans relative to FG2, in the fourth column of Table

2.2, the proportions from non-mutant to mutant are in the same range as in Table 2.1, except for samples S3-S3m for which this correlation between glycopeptides and glycan relative abundances was not followed. Altogether these observations again suggest that for accurate quantification of glycans, esterification of sialic acid would have been beneficial. But overall this second portion of the study also attained the aim of determining if point mutation of TMZ would enhance sialylation.

The study of glycans detached from mAbs eliminated all ambiguities related to the peptide chain as reported in the first portion of this work. While operating the UltraFlex<sup>TM</sup> mass spectrometer in the reflector mode, it was impossible to avoid the presence of metastable ions in the spectra; taking them into account in abundance ratios is important, as they sometimes represent a larger ion population than that detected at the predicted m/z value. To circumvent the occurrence of metastable ions, the experiments could be done in the linear mode, which was not possible in this work due to sensitivity and resolution issues.

## 2.6 Conclusion

The goal of this analysis was to determine if the mutation of a phenylalanine to alanine in a Trastuzumab construct is beneficial for increased sialylation of monoclonal antibodies (mAb). Using mass spectrometry, each of the mutant samples showed a qualitative increase in its level of sialylation, with the FG2S2 disilylated glycan only being present in mutant samples. Specifically, this increase in sialylation has been in the form of  $\alpha$ 2,6 linked sialic acids. This is a crucial glycan linkage that relates to humans in various viruses including influenza<sup>21,22</sup> which are



reported to bind through this linkage. Intuitively, the incorporation of this glycan linkage in Mabs would potentially produce higher binding affinities in humans than conventional antibodies from CHO cells which typically express  $\alpha 2,3$  sialic acids due to the lack of  $\beta$ -galactoside  $\alpha 2,6$  sialyltransferase activity<sup>23</sup>. With respect to MS, given the limited sample amount, the semi-quantitative approach used has demonstrated that if complicated glycopeptide spectra are obtained, it is possible to simplify the results through PNGase deglycosylation and elimination of the peptide chain. Future considerations should include special attention to desalting procedures in order to simplify and streamline the workflow at the glycopeptide level. For advanced quantification, tandem mass tags could be implemented for relative comparison between the mutated and non-mutated samples at either the glycan or glycopeptide levels. It would also be important to esterify the sialic acids to form non polar residues which are unbiased toward positive or negative ionization.

## 2.7 Acknowledgements

The authors would like to thank Celine Raymond and Dr. Yves Durocher at the National Research Council (NRC; Montreal) for the monoclonal antibody samples. Dr. Michael Butler and Dr. Venkata Tayi (University of Manitoba, Microbiology, Winnipeg) are thanked for provided Eg2 monoclonal. Funding acknowledgements are made to the Monoclonal Antibody Network (MabNet; Winnipeg), as well the Natural Sciences and Engineering Research Council (NSERC), Canadian Foundation for Innovation (CFI) and Manitoba Research & Innovation Fund.

## 2.8 References

---

- <sup>1</sup> Ezan, E. *Advanced drug delivery reviews*. **2013**, 65(8), 1065-1073.
- <sup>2</sup> Ghaderi, D.; Taylor, R.E.; Padler-Karavani, V.; Diaz, S.; Varki, A. *Nat. Biotechnol.* **2010**, 28(8), 863-867.
- <sup>3</sup> Butler, J.E.; Zhao, Y.; Sinkora, M.; Wertz, N.; Kacs Kovics, I. *Developmental and Comparative Immunology*. **2009**, 321-333.
- <sup>4</sup> Nose, M.; Wigzell, H. *Proc Natl Acad Sci USA*. **1983**, 80, 6632-6636.
- <sup>5</sup> Shields, R.L.; Lai, J.; Keck, R.; O'Connell, L.Y.; Hong, K.; Meng, Y.G. *et al. J Biol Chem*. **2002**, 277, 26733-26740.
- <sup>6</sup> Oefner, C.M., Winkler, A.; Hess, C.; Lorenz, A.K.; Holecska, V.; Huxdorf, M. *et al. J Allergy Clin Immunol*. **2012**, 129: 1647-55. e1613.
- <sup>7</sup> Goldenberg, M.M. *Clin Ther*. **1999**, 21(2), 309-318.
- <sup>8</sup> Restelli, V.; Wang, M.D.; Huzel, N.; Etheir, M.; Perreault, H.; Butler, M. *Biotechnol Bioeng*. **2006**, 94(3):481-494.
- <sup>9</sup> Liu, B.; Spearman, M.; Doering, J.; Lattová, E.; Perreault, H.; Butler, M. *J Biotechnol*. **2014**, 170: 17-27.
- <sup>10</sup> Saba, J.A.; Kunkel, J.P.; Jan, D.C.; Ens, W.E.; Standing, K.G.; Butler, M.; Jamieson, J.C.; Perreault, H. *Anal Biochem*. **2002**, 305(1), 16-31.
- <sup>11</sup> Lattová E.; Kapková, P.; Krokhin, O.; Perreault, H. *Anal Chem*. **2006**, 78, 2977-2984.
- <sup>12</sup> Jassal, R.; Jenkins, N.; Charlwood, J.; Camilleri, P.; Jefferis, R.; Lund, J. *Biochem Biophys Res Commun*. **2001**, 286(2), 243-249.

---

<sup>13</sup> Raymond, C.; Robotham, A.; Kelly, J.; Lattová, E.; Perreault, H.; Durocher, Y.

*Glycosylation*. **2012**, 397-418.

<sup>14</sup> Monoclonal Antibody Network: [www.mabnet.ca](http://www.mabnet.ca)

<sup>15</sup> Lattová, E.; Perreault, H. *Methods Mol Biol.* **2009**, 534, 65-77.

<sup>16</sup> Krokhin O, Ens W, Standing KG, Wilkins J, Perreault H. *Rapid Commun Mass Spectrom.* **2004**, 18(18), 2020-30.

<sup>17</sup> Boja, E.S.; Fales, H.M. *Anal Chem.* **2001**, 73(15), 3576-3582.

<sup>18</sup> Oliveira, A.; Roy, R.; Raymond, C.; Bodnar, E.; Tayi, V.; Butler, M.; Durocher, Y.; Perreault, H. *Rapid Commun Mass Spectrom.* **2015**; in submission.

<sup>19</sup> Yu, L.; Vize, A.; Huff, M.B.; Young, M.; Remmele Jr., R.L.; He, B. *J Pharm Biomed Anal.* **2006**, 42, 455.

<sup>20</sup> Harvey, D.J.; Bateman, R.H.; Bordoli, R.S.; Tyldesley, R. *Rapid Commun Mass Spectrom.* **2000**, 14(22), 2135-42.

<sup>21</sup> Mair, CM.; Ludwig, K.; Herrmann, A.; Sieben, C. *Biochim Biophys Acta.* **2014**, 1838(4), 1153-1168.

<sup>22</sup> Wei, SH.; Yang, JR.; Wu, HS.; Chang, MC.; Lin, JS.; Lin, CY.; Liu, YL.; Lo, YC.; Yang, CH.; Chuang, JH.; Lin, MC.; Chung, WC.; Liao, CH.; Lee, MS.; Huang, WT.; Chen, PJ.; Liu, MT.; Chang, FY. *Lancet Respir Med.* **2013**, 1(10), 771-778.

<sup>23</sup> Lee, KJ.; Lee, SM.; Gil, JY.; Kwon, O.; Kim, JY.; Park, SJ.; Chung, HS.; Oh, DB. *Glycoconj J.* **2013**, 30(5), 537-547.

## **Chapter 3 - Qualitative and Quantitative Assessment on the use of Amine Functionalized Magnetic Nanoparticles for Glycopeptide Enrichment**

### 3.1 Authors Contributions

All experiments pertaining to this work were designed and performed by Edward D. Bodnar under the guidance of Dr. H. Perreault. Dr. O. Krokhin was responsible for acquiring data on the AB Sciex 5600 Triple ToF instrument. Edward D. Bodnar was responsible for manuscript drafts and all figures, while Dr. H. Perreault was responsible for editing the final version of the manuscript prior to initial submission to Analytical Chemistry. Both authors contributed equally to the final revision of the manuscript prior to its publication.

### 3.2 Abstract

Glycoproteomics represent the field of study of the dynamic changes occurring among glycoconjugates within the cellular compartments. Changes in glycosylation have been linked to various diseases, including metastatic carcinomas in which the 9-carbon sialic acid moiety has been shown to play a prominent role. The common method used to study these aberrant changes most often includes a mass spectrometer at some stage in the workflow. However, serum samples contain many proteins which inhibit the analysis of these glycosylation changes, and ergo, enrichment steps are employed as a measure to help alleviate this shortcoming. Routinely, this is accomplished using lectins, either alone or in combination, to retrieve proteins with specific sugar linkages within the serum sample. This methodology, although known to be very specific, requires many washing steps, making it a cumbersome addition to a high throughput workflow. Presented here is an alternative protocol using custom-made amine functionalized magnetic nanoparticles (MNP) which are nearly 4× smaller than those used before for similar purposes. The developed protocol is based on both hydrophilic interaction and weak anion exchange principles, allowing it to target glycopeptides but, more specifically, those which contain sialylation. For quantification purposes, tandem mass tags from Thermo Scientific were utilized to compare the enrichment efficiencies between the magnetic nanoparticle method and a commercially available glycopeptide enrichment kit offered through EMD Millipore. The MNP method is fast (~10 min) and simple and can quantitatively and qualitatively enrich sialylated glycopeptides more than the commercially available kit.

### 3.3 Introduction

Regarded by many as an important post-translational modification (PTM), glycosylation has its own importance in systems biology, serving two prominent roles: providing a function to the protein, and thus allowing it to serve as a receptor or signaling scaffold for the cell<sup>1,2</sup>. Furthermore, alterations of glycans are associated with cell differentiation and have been linked to diseases such as cancer<sup>3,4</sup>. As a result, studying glycosylation can potentially serve clinicians through the use of mass spectrometric profiles of glycans as biomarkers to track these diseases and provide a more comprehensive diagnosis for the patient<sup>5,6</sup>. In particular, it has been reported that the 9 carbon sugar known as sialic acid may express at levels which differ between benign and malignant intracranial tumors<sup>7</sup>. Furthermore, sialylated glycoconjugates are known to form a so-called sialyl Lewis X epitope which is of extreme importance<sup>8,9,10</sup>, as sialic acids play prominent roles in the binding of the influenza virus as well as the binding of *Plasmodium falciparum*; the microorganism responsible for malaria disease<sup>11,12</sup>.

Commonly, glycoproteins are enriched from serum samples using lectins, including concanavalin A, wheat germ agglutinin and jacalin, to name a few<sup>13,14,15</sup>. The advantage of using lectins in the workflow however dictates their disadvantage of being highly selective towards unique and specific glycan moieties. Certain glycoforms may thus go unaccounted for (e.g. N-linked vs O-linked)<sup>16</sup>. To overcome this, alternative methods must be developed which exploit the glycan portion of the glycoprotein, while being cognizant of price, efficiency, and applicability of the method so that the researcher may quantify a glycome and establish it as a systematic tool to monitor disease stage or progression.



Recently, tandem mass tags (TMT) and isobaric tags for relative and absolute quantification (iTRAQ) have become commercially available and have been used for protein and glycoprotein quantification<sup>17,18</sup>. Briefly, these molecules allow for targeted quantification at the MS<sup>2</sup> level owing to the different positions of stable isotopes located within their so-called reporter ion region. In light of this, in order to obtain glycopeptides in sufficient abundance to be quantified, recent articles in the literature have highlighted the importance of enrichment strategies for glycopeptides prior to their analysis<sup>19, 20, 21</sup>.

Magnetic nanoparticles (MNP) are one such tool to serve this purpose and can be synthesized and functionalized accordingly<sup>22,23,24</sup>. Moreover, functionalized MNP have also shown interesting properties and applicability as isolation and enrichment tools, including the promising ability to replace traditional methods for high throughput proteomic environments<sup>25,26,27</sup>. MNP which have been reported in the literature for similar purposes have tuneability ranges of 15-220 nm<sup>28,29,30,31</sup>. As examples, boronic-acid functionalized MNP or biotinylated lectins captured on paramagnetic streptavidin beads have shown promise to be used instead of traditional agarose lectin columns<sup>27,28,32</sup>. Here, we report on the use of a novel synthetic aminosiloxane functionalized nano-particle (5-8 nm) which is ca. 4x smaller than any previously used for this purpose in the literature. The protocol described in this work is close to that recently presented by Kuo et al.<sup>33</sup>. Indeed, in their study, MNP were coated with (aminopropyl)triethoxysilane (APTS) and had sizes ranging from 30 to 150 nm. The use of smaller particles as presented here had advantages, on the basis of the greater surface area available for coating per gram of MNP. In a close pack hexagonal model, for 1 g of beads, particles with 1:4 diameter ratio would offer a 4:1 ratio in surface area. The 3- aminosiloxane

MNP used in this work were aimed at exploiting glycopeptide retention based on weak anion exchange (WAX) and hydrophilic liquid interaction liquid chromatography (HILIC) principles.

For this analysis, four glycoproteins were chosen based on varying amounts of sialylation in order to evaluate their HILIC and WAX interactions, namely  $\alpha$ 1-acid glycoprotein (human), fetuin (bovine), IgG (human), and Eg2, a monoclonal antibody (mAb)<sup>34</sup>. Hongping *et al.* have demonstrated the use of TMT quantification for bovine fetuin previously, although no enrichment strategies seemed to be apparent in their workflow<sup>35</sup>. In addition, Singh *et al.* have analyzed IgG, although no TMT labeling strategies were implemented for quantification<sup>36</sup>. Together, a workflow should contain the ability to enrich glycopeptides for downstream MS and in addition, have the capability of quantifying these results, especially if these workflows are to be used in clinical settings. The protocol presented here exemplifies both of these characteristics, and was compared to a well established commercially available glycopeptide kit offered by EMD Millipore™ which had been used extensively and successfully in our laboratory and had demonstrated a wide scale capability of enrichment according to Wohlgemuth *et al.*<sup>37,38,39</sup>. This was conducted in order to evaluate and compare the enrichment efficiencies between these two methods. Upon enrichment, all samples were profiled using matrix assisted laser desorption ionization (MALDI) and electrospray ionization (ESI) quadrupole time-of-flight (qTOF) mass spectrometry (MS) at both the MS and MS<sup>2</sup> levels to obtain qualitative and quantitative data.

## 3.4 Experimental

### 3.41 Materials

N-glycosylated  $\alpha$ 1-acid glycoprotein (human), fetuin (bovine), and IgG (human) as well as dithiothreitol (DTT), iodoacetamide (IA), triethyl ammonium bicarbonate (TEAB), formic acid (FA), and tri-fluoroacetic acid (TFA) were obtained from Sigma (St. Louis, MO) while the Eg2 monoclonal antibody (mAb) was obtained through the Monoclonal Antibody Network (MabNet) (Winnipeg, Manitoba)<sup>40</sup>. Spectra/Por membrane tubing (MWCO:6000-8000) was purchased from Spectrum Laboratories (Rancho Dominguez, CA). Sequencing grade Trypsin was purchased from Promega (Madison, WA). TMTs were acquired from Thermo Scientific as part of a TMT<sup>2</sup> Isobaric Mass Tagging Kit and the commercially available Novagen® ProteoExtract® Glycopeptide Enrichment Kit was purchased from EMD Millipore™. All solvents were HPLC-grade and obtained from Sigma (St. Louis, MO, USA). Distilled de-ionized water was obtained using a Milli-Q™ filtration system supplied by a reverse-osmosis feedstock.

### 3.42 Methods

#### 3.421 Glycopeptide Preparation & Digestion

Each glycoprotein (1 mg) was added to 100  $\mu$ L of 25 mM TEAB (pH~8) and the Eppendorf™ tube was vortexed until the sample dissolved. A stock DTT sample solution (0.5 mg/mL) was made, and 500  $\mu$ L of this was added to each sample; samples were vortexed and left to react at 56 °C for 1 h, at which time 400  $\mu$ L of IA (0.092 g/mL) was added. Vortexing was applied, and the sample was left to react in the dark for 30 min. These samples were then dialyzed against 4

L of water for 24 h using 6-8000 MWCO membranes, and lyophilized to dryness. To obtain glycopeptides, each sample was then re-suspended in 250  $\mu$ L of 25 mM TEAB buffer; 20  $\mu$ L of a  $\sim$ 1 mg/mL solution of trypsin were added and the mixture was allowed to react overnight at 37  $^{\circ}$ C for approximately 18 h. To deactivate the trypsin a large volume of acetonitrile (ACN) was added and this mixture was vortexed, lyophilized and re-suspended in 1 mL of Milli-Q<sup>TM</sup> water to create glycopeptide standards.

### *3.422 Tandem Mass Tag (TMT) labeling*

To quantify and compare the enrichment efficiency between techniques, tandem mass tags (TMT) were purchased from Pierce Thermo Scientific (Rockford, IL). Manufactures protocols were followed<sup>41</sup>, which in brief involves adding 41  $\mu$ L of acetonitrile to the stock TMT vial, followed by vortexing for  $\sim$ 5 min, at which point the amount of TMT label is sufficient for 100  $\mu$ g of sample. Each TMT label was evenly distributed amongst all four of the 20  $\mu$ g samples followed by a 1 h incubation period at room temperature, at which time the reaction was quenched by adding 2  $\mu$ L of 5% hydroxyquinilone. In order to minimize sample loss, each vial was washed 3 x with 20  $\mu$ L of ACN and transferred to the appropriate enrichment regime prior to enrichment.

### *3.423 Glycopeptide Enrichment*

In order to compare the enrichment efficiency between methods, a commercially available glycopeptides kit was purchased from EMD Millipore<sup>TM</sup>. The manufacturer's protocols were followed<sup>42</sup>, which briefly included centrifuging the stationary phase at  $\sim$ 2500 g for 2 min to

remove excess storage reagent. This was followed by dissolving the sample in a proprietary binding buffer, then by adding it to the stationary phase and allowing to incubate for up to ~20 min with end-over-end mixing. Next, the vial was centrifuged again and the supernatant was once again removed, which was assumed to contain the majority of unbound peptides. The solution was then washed with a proprietary wash solution for ~10 min and centrifuged, and the supernatant was once again removed; this was repeated 2 x to aid in removing the remainder of unbound peptides. Finally, to elute the bound glycopeptides, a proprietary elution solution was applied and allowed to react for ~2 min, followed by centrifugation and collection of the supernatant, which was then centrifuged again at 10,000 g to sequester any stationary phase particles that may have been accidentally transferred.

For the enrichment protocol presented here, 3-aminosiloxane magnetic nanoparticles (MNP) were synthesized and characterized previously<sup>43,44</sup>. To test this method's ability to enrich glycopeptides for MS analysis, 5  $\mu$ L of MNP were added to a 1.5 mL Eppendorf™ tube followed by adding 20  $\mu$ g of stock TMT labeled glycopeptide standard, to which 30  $\mu$ L of a 9:1 ACN:H<sub>2</sub>O + 0.1% TFA solution was added. The samples were vortexed periodically over the course of ~2 min. Subsequently, a magnet was applied at the bottom of the tube to sequester the MNPs from solution, and the supernatant was removed. Next, 30  $\mu$ L of a 3:7 ACN:H<sub>2</sub>O + 0.1% TFA solution was added to remove hydrophobic peptides, and once again, a magnet pulled the MNPs and supernatant was removed. Lastly, to remove bound glycopeptides, a 30  $\mu$ L solution of 3:7 ACN:H<sub>2</sub>O + 2% NH<sub>4</sub>OH was added and the supernatant was collected 3 x. These samples were then lyophilized to dryness to remove volatile ammonium and re-suspended to their initial volume of 20  $\mu$ L in 3:7 ACN:H<sub>2</sub>O + 0.1% TFA. Mass spectra of all of the samples were

collected, at which time the samples from both enrichment schemes (magnetic and commercial) were pooled in order to evaluate their efficiencies using tandem mass spectrometric TMT reporter ions.

#### *3.424 Mass Spectrometric Analysis*

For MALDI analysis an UltrafleXtreme (Bruker Daltonics, Germany) equipped with LID-LIFT™ technology for tandem MS experiments was used as well as a Manitoba/Sciex Prototype quadrupole quadrupole time of flight instrument (MALDI-QqTOF). Unless otherwise stated, these instruments were utilized in positive ion mode with a matrix of 2,5 dihydroxybenzoic acid (2,5 DHB) and a scanning range of 600-8000 m/z. Each sample was prepared whereby 0.75 µL of matrix was spotted and co-mixed with 0.75 µL of sample and then allowed to dry on target before loading it into the MS.

HPLC-MS spectra were acquired on an AB Sciex 5600 Triple TOF™ equipped with a NanoSprayIII source, operated in standard MS<sup>2</sup> data-dependent acquisition mode. The samples were diluted 1:10 with H<sub>2</sub>O + 0.1% FA. A nano-flow 2D LC Ultra system (Eksigent – Ab Sciex, Dublin, CA) with 10 µL injection via a 300 µm x 5 mm PepMap100 (Thermo FisherScientific, Rockford, IL) trap-column and 100 µm x 200 mm analytical column packed with 5 mm Luna C<sub>18</sub> were used for separation. The gradient employed started at 0% H<sub>2</sub>O + 0.1% FA and went to 30% ACN + 0.1% FA over 30 min.

### 3.425 Data Analysis

Glycopeptide MALDI data were analyzed using Bruker's FlexAnalysis software to view and interpret data by hand. In each case, the glycopeptide was further corroborated by MALDI-MS/MS, where the presence of the characteristic MALDI-specific oxonium ion cross ring cleavage ( $^{0,2}X_0$ ) (Figure 1.15) which occurs between the first HexNAc and the peptide backbone<sup>45</sup>.

To de-convolute and elucidate glycopeptide structures from HPLC-MS data, the Byonic™ software (Protein Metrics Inc., San Carlos, CA) was used, as other studies had also shown its advantages<sup>46,47,48</sup>. Specific to this analysis, in silico lysine and arginine tryptic cleavages with a maximum of 2 missed cleavages were employed. The precursor mass tolerance was set to 20 ppm, and the fragment mass tolerance was 0.1 Da using a QToF/HCD type of fragmentation. For the aforementioned sample preparation, the following protein modifications were included in the Byonic™ search: carbamidomethylation for cysteines and N-terminal and lysine TMT<sup>2</sup> tag as fixed modifications, as well as variable methionine oxidation. Moreover, Byonic™ contains a "common human/mammalian" glycan database of 350 N-linked glycans with masses up to 6000 Da for which only one glycan is allowed per peptide sequon. These options were selected for precursor ions with charges 2-5, and MS<sup>2</sup> spectra were then ranked in the software from 0 to 1000, whereby only those entries above 500 (demonstrating a "good match") were considered. These matches were then manually verified in the MS<sup>2</sup> spectra by the presence of a glycan fragment ion such as the HexNAc oxonium ion at 204.087 Da.

## 3.5 Results & Discussion

### *Method Development of MNP*

Using the amine functionalized magnetic nanoparticle (MNP) approach, it was presumed that this functionalized ligand could utilize both hydrophilic and weak anion exchange (WAX) interactions to selectively enrich for sialylated glycopeptides. Due to the large proportion of the glycopeptide being the glycan moiety, which is polar in nature, a workflow designed around HILIC principles would allow an enrichment procedure which can exploit this inherent property; that is, isolating the hydrophilic glycopeptides from the lesser hydrophobic peptides of the mixture<sup>49</sup>. Furthermore, to enhance this specific binding, the positively charged amine moiety serves as a site through which electrostatic interactions can occur with negatively charged species such as sialylated, phosphorylated or sulfated peptides; an interaction which can easily be manipulated through changes in pH according to the compound's pKa's<sup>50</sup>. These principles served as the basis by which a protocol was developed using  $\alpha$ 1-acid glycoprotein (AGP) from human and fetuin from bovine, as both samples are known to be highly sialylated species<sup>51,52</sup>.

From the onset, HILIC parameters were tested in order to emulate the protocol described in the glycopeptide enrichment kit, which meant optimizing the solvent ratios for the removal of non-glycosylated peptides. SI-Figure 2b gives an overview of the method. As peptides are typically hydrophobic in nature, higher ratios of ACN:H<sub>2</sub>O + 0.1% TFA were tested as wash solutions to remove most of peptides from the tryptic digest. The addition of TFA in this protocol serves two purposes: first, it has been reported that TFA as an ion pairing agent



helps to increase the hydrophilicity difference between glycopeptides and non-glycosylated peptides for HILIC conditions<sup>53</sup>; and secondly, acidic conditions must be employed to manipulate the electrostatic interactions between the amine functionalized MNP and the sialylated glycopeptides. It was concluded that one 30  $\mu$ L wash of 9:1 ACN:H<sub>2</sub>O + 0.1% TFA was sufficient to diminish the number of peptides while still retaining glycopeptides for analysis. Next, to extract the isolated glycopeptides, a reverse solution of 3:7 ACN:H<sub>2</sub>O + 0.1% TFA was employed, effectively increasing the overall polarity of the solvent in an attempt to release neutral glycopeptides which may have been bound through HILIC principles. This alone did not appear to relinquish an abundance of glycopeptides. To overcome this and inhibit the WAX interactions which were assumed to still be in effect, a 3:7 ACN:H<sub>2</sub>O + 2% NH<sub>4</sub>OH was implemented. Subsequently, the samples were washed in this manner twice more and pooled together where they were lyophilized to dryness followed by a re-suspension in 3:7 ACN:H<sub>2</sub>O + 0.1% TFA to their initial volume. This protocol is similar to one which has previously been reported in the literature<sup>33</sup>. SI-Figure 2a summarizes the interactions relating to chemical structures. To confirm that glycopeptides had been enriched and released, positive linear mode spectra were scrutinized for both AGP human and fetuin bovine (Figure 3.1). The spectra were passed in review for common glycan specific differences between parent ions such as 291 or 366 m/z, pin-pointing the difference of glycopeptides bearing N-acetylneuraminic acids or Hex-HexNAc moieties.

As an initial indicator of the method's enrichment efficiency relative to that of the commercial kit, spectra from AGP as well as fetuin from both enrichment modes were overlaid and relative ion abundances were calculated for ions which corresponded to characteristic

glycan  $m/z$  differences as aforementioned (not shown). The initial data corroborated that for many ions showing sialic acid residue differences (291  $m/z$ ), the MNP method was more efficient than the EMD commercial kit, based on a qualitative comparison of ion abundances.

Next, the MNP protocol was performed on two additional glycoproteins to evaluate its ability to exploit hydrophilic and weak anion exchange interactions. IgG (human) and Eg2 (mAb) were used for this purpose. Some glycopeptides were identified through glycan  $m/z$  differences, and the population of IgG glycans containing one terminal sialic acid is ~10-12%, whereas disialylated structures exist in only trace amounts<sup>54,55</sup>; so their lower level of enrichment was not surprising. These two glycoproteins were included in the efficiency analysis as control samples due to these low levels of sialylation. In this manner, it was possible to assess the MNPs ability to enrich glycopeptides based on either HILIC or WAX principles.

### *TMT Comparison*

To compare the efficiency between the MNP and EMD methods, tandem mass tags (TMTs) were implemented into the workflow. Here, samples to be enriched using the MNP protocol were first labeled with TMT-127, while samples to be enriched using the commercial method were labeled with TMT-126 (Figure 1.19). As opposed to label-free quantitation, this method allows one to track the origin of signals obtained from a sample pooled from two different but parallel preparations. From the mass spectra of TMT-labeled species, no incomplete derivatization products were observed; i.e., no peaks were detected at  $m/z$  values lower by 225, 450 u. Equal amounts of sample were enriched separately, pooled, and subsequently subjected to HPLC-MS analysis (Figure 3.2). Both HPLC-MS and MALDI-MS were utilized in this analysis. MALDI was employed during method development of the protocol;

generally as a screening technique to determine if enrichment was successful, whereas HPLC/ESI-MS was employed for quantification purposes. The reasoning for this stems from the micro-heterogeneity exhibited within the glycan portion of each glycopeptide. HPLC-MS serves as a superior approach in this regard since it can provide separation of glycopeptides prior to MS, effectively allowing for accurate quantification of the TMT tag at the MS<sup>2</sup> level.

**Figure 3.1 - MALDI spectra of glycopeptides enriched by magnetic nanoparticles, collected in positive linear mode.**

a)  $\alpha$ 1-acid glycoprotein , b) bovine fetuin bovine. Each spectrum shows characteristic glycan  $m/z$  differences, and prominent sialylation can be observed. See **SI-Figure 1** for EMD spectra.

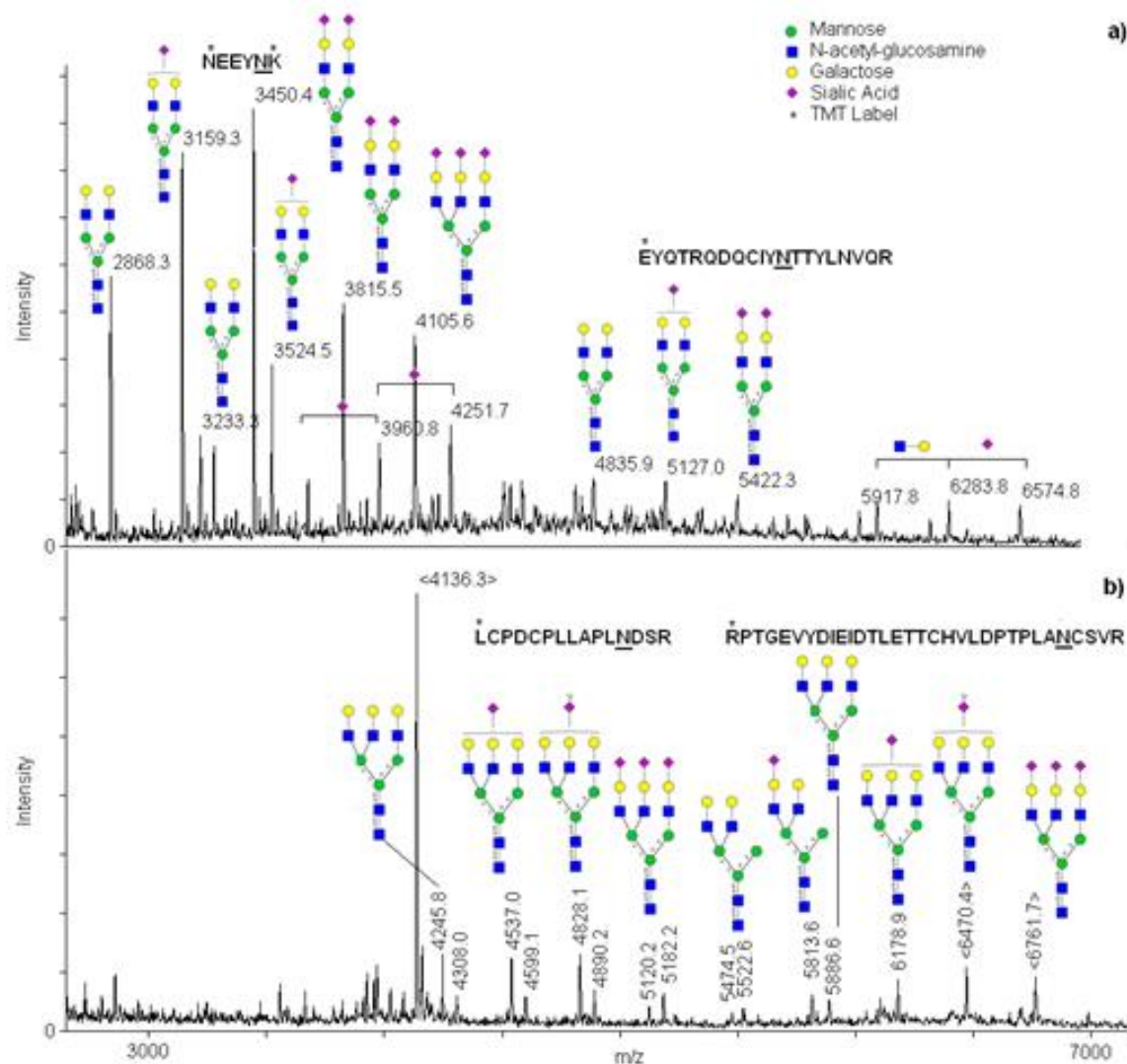
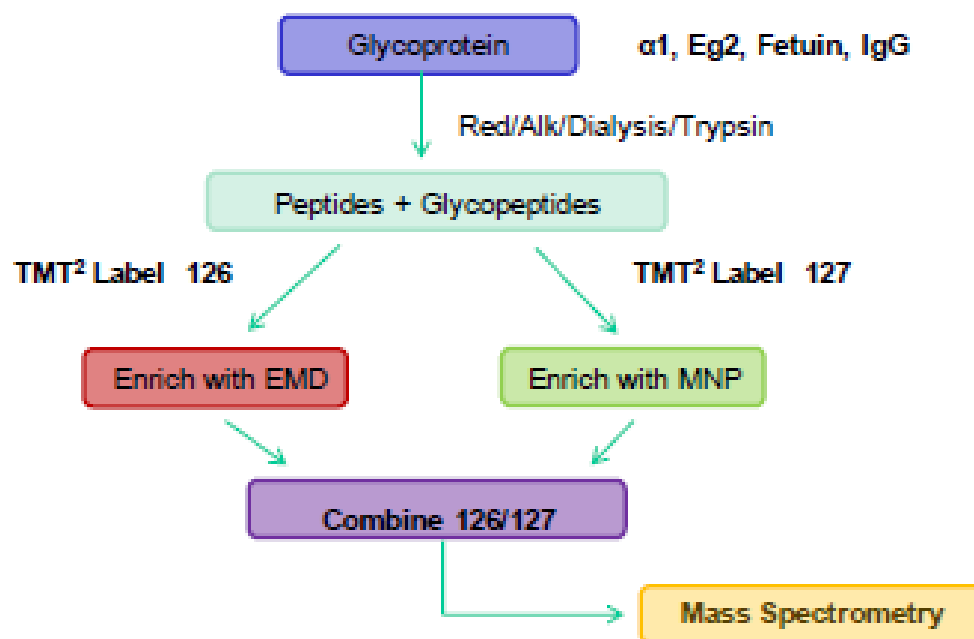


Figure 3.2 - A workflow used to compare the enrichment efficiency between the EMD method and MNP protocol.

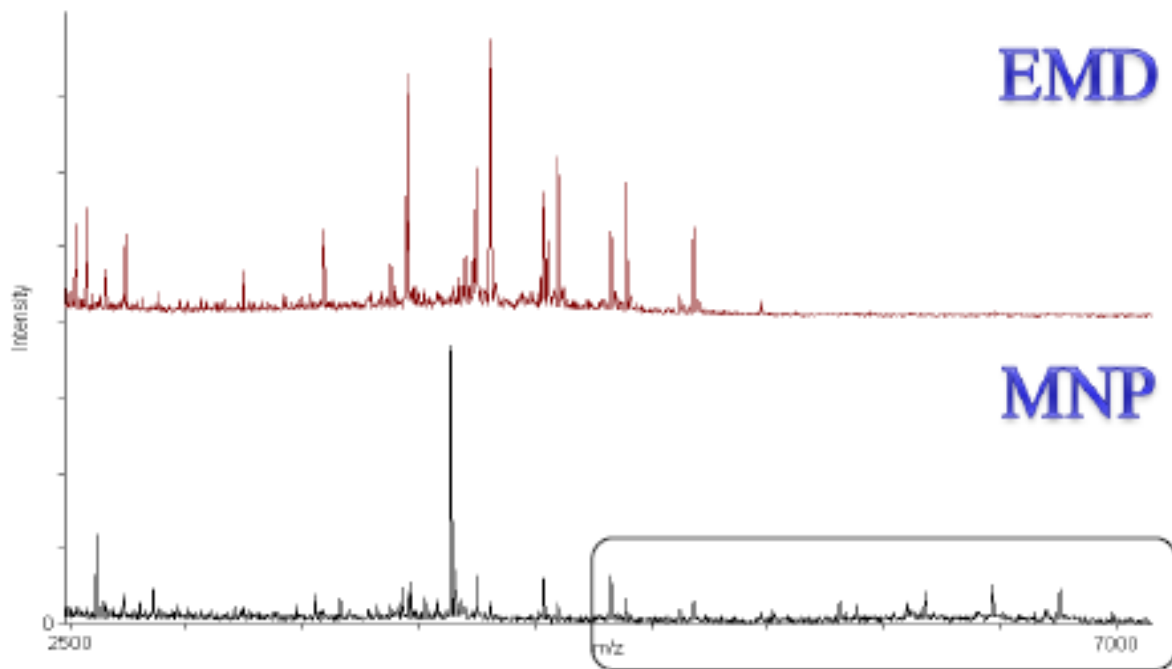
Briefly, after the tryptic digests are prepared, equal aliquots are labeled separately with a unique TMT<sup>2</sup> and enriched by their respective methods. The enriched samples are then pooled and subjected to mass spectrometric analysis. See **SI-Figure 2** for additional information.



Prior to pooling the TMT enriched samples, each isolate was analyzed by MALDI-TOF for qualitative purposes. Confirming the initial hypothesis, MALDI *m/z* differences corresponding to sialylation were detected in isolates from the MNP protocol that were not present after the EMD enrichment (Figure 3.3).

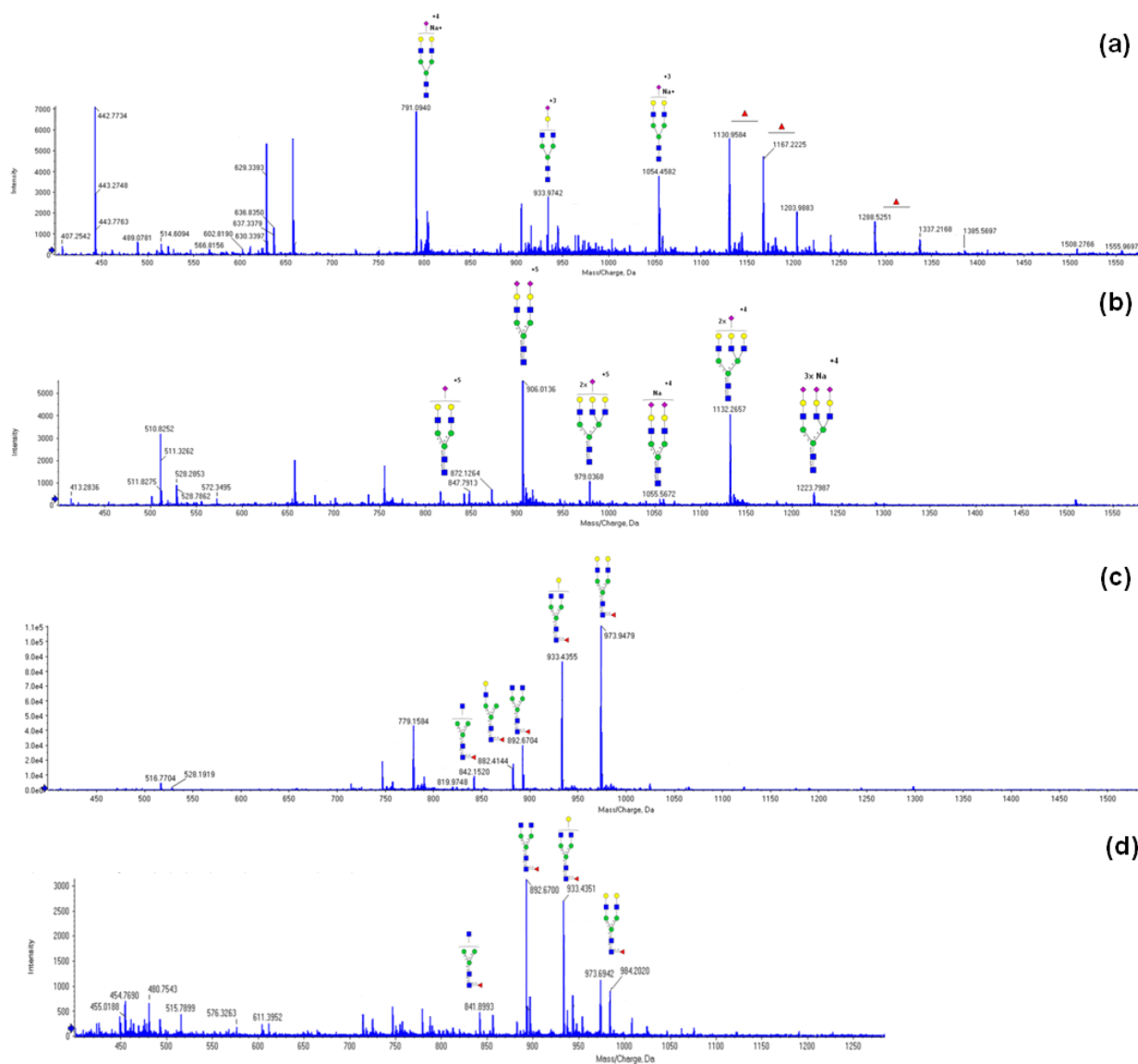
Figure 3.3 – Comparison of commercial kit to MNP method for enhanced sialylation

Linear mode MALDI spectra showing the comparative enrichment of sialylated species for bovine fetuin using the MNP protocol and the commercially available EMD glycopeptide enrichment kit. The rectangle highlights detection of additional sialylated species using MNP protocol.



This helped to validate assumptions on the workflow, allowing us to pursue the study by exploring the relative quantification and efficiency of each method by pooling the samples and analyzing them by HPLC/ESI-MS (Figure 3.4).

Figure 3.4 –HPLC/ESI-MS spectra highlighting glycopeptides from the combined EMD & MNP samples (a)  $\alpha 1$  acid human, (b) fetuin bovine, (c) Eg2 mAb, (d) IgG human



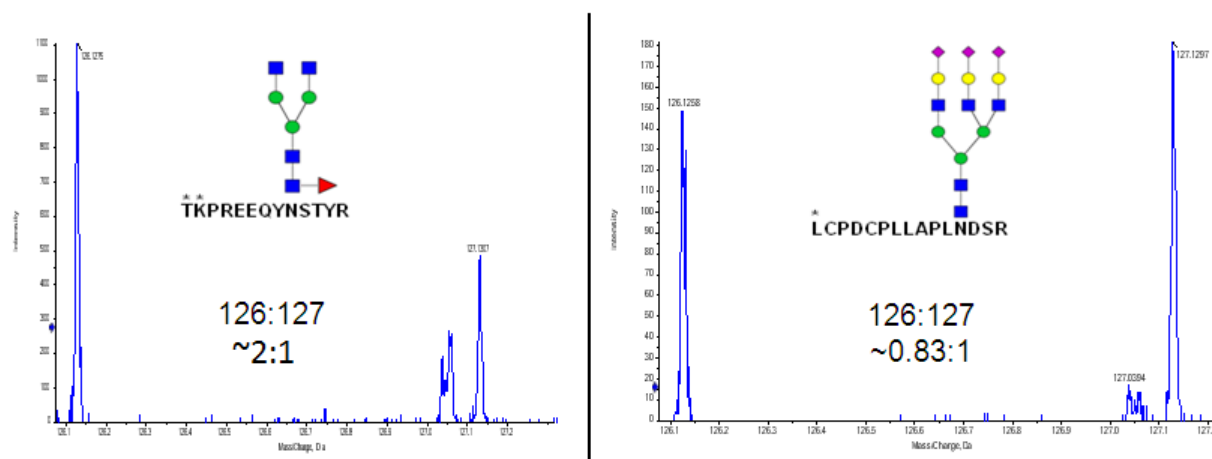
## Data Analysis

All ESI-MS spectra were loaded into Byonic™ and scrutinized for potential glycopeptides. The results were further corroborated by manually checking the MS<sup>2</sup> spectra for a HexNAc oxonium ion, whereby each positive identification was subsequently quantified based on the 126:127 reporter ion ratio abundances (Figure 3.5). Moreover, an overall average ratio was

established for both techniques for each sample, including an average which reflected only those glycopeptides containing sialylation.

### Figure 3.5 – 126:127 TMT Reporter Ion Ratios

The left spectrum is from Eg2 (mAb) demonstrating a higher enrichment for the EMD kit, whereas on the right, the spectrum is a glycopeptide from fetuin (bovine) highlighting the MNP protocol. These ion abundances have been normalized to the m/z 127 ion. An asterisk (\*) indicates the position of TMT labels.



These data are summarized in Table 3.1 . They support the initial idea that the MNP protocol would be more suitable for the enrichment of sialylated glycoproteins, than would the commercial EMD enrichment kit. This was confirmed when comparing the average TMT ratio to the ratio that reflects only those glycopeptides which were sialylated. All of the values in this column suggest that the MNP is a more suitable technique to enrich sialylated glycopeptides as all of the ratios for IgG and Eg2 drop significantly, which is not surprising due to their relative lack of sialylation.

Table 3.1 – 126:127 TMT reporter ion abundance ratio for selected glycopeptides from each sample.

Sample	Peptide	Glycan sequence	m/z observed	Z	TMT ratio (126:127)
<b>α1 acid</b>					
	N*EEY <u>N</u> K*				
		HexNAc <sub>4</sub> Hex <sub>5</sub> Neu5Ac <sub>2</sub>	863.617	4	0.725:1
		HexNAc <sub>3</sub> Hex <sub>4</sub> Neu5Ac <sub>1</sub>	932.402	3	0.634:1
		HexNAc <sub>5</sub> Hex <sub>6</sub> Neu5Ac <sub>3</sub>	1027.676	4	0.570:1
		HexNAc <sub>5</sub> Hex <sub>6</sub> Neu5Ac <sub>4</sub>	1100.454	4	0.737:1
	Q*DQCIY <u>N</u> TTYLNVQR				
		HexNAc <sub>5</sub> Hex <sub>6</sub> Neu5Ac <sub>2</sub>	1178.504	4	3.71:1
<b>Fetuin</b>					
	K*L*CPDCPLLAPL <u>N</u> DSR				
		HexNAc <sub>4</sub> Hex <sub>5</sub> Neu5Ac <sub>2</sub>	905.609	5	2.41:1
		HexNAc <sub>5</sub> Hex <sub>6</sub> Neu5Ac <sub>2</sub>	978.641	5	1.26:1
		HexNAc <sub>5</sub> Hex <sub>6</sub> Neu5Ac <sub>3</sub>	1036.856	5	0.894:1
	L*CPDCPLLAPL <u>N</u> DSR				
		HexNAc <sub>4</sub> Hex <sub>5</sub> Fuc <sub>2</sub> Neu5Ac <sub>2</sub>	1116.476	4	0.667:1
		HexNAc <sub>5</sub> Hex <sub>6</sub> Neu5Ac <sub>3</sub>	1207.509	4	0.682:1
<b>IgG</b>					
	E*EQY <u>N</u> STYR				
		HexNAc <sub>3</sub> Hex <sub>3</sub> Fuc <sub>1</sub>	886.047	3	1:1
		HexNAc <sub>4</sub> Hex <sub>3</sub> Fuc <sub>1</sub>	953.740	3	2:1
		HexNAc <sub>4</sub> Hex <sub>4</sub>	959.072	3	4:1
		HexNAc <sub>4</sub> Hex <sub>4</sub> Fuc <sub>1</sub>	1007.758	3	5.88:1
<b>Eg2</b>					
	E*EQY <u>N</u> STYR				
		HexNAc <sub>3</sub> Hex <sub>3</sub> Fuc <sub>1</sub>	886.048	3	0.575:1
		HexNAc <sub>3</sub> Hex <sub>4</sub> Fuc <sub>1</sub>	940.064	3	2.07:1
		HexNAc <sub>4</sub> Hex <sub>5</sub> Fuc <sub>1</sub>	1061.777	3	4.99:1
	T*K*PREEQY <u>N</u> STYR				
		HexNAc <sub>4</sub> Hex <sub>5</sub> Fuc <sub>1</sub> Neu5Ac <sub>1</sub>	837.176	5	0.645:1
		HexNAc <sub>3</sub> Hex <sub>4</sub> Fuc <sub>1</sub>	882.415	4	1.02:1
		HexNAc <sub>4</sub> Hex <sub>4</sub> Fuc <sub>1</sub>	932.922	4	5.58:1

\* **Note:** This table depicts selected glycopeptides from each of the four standard glycoproteins. The average TMT ratio for each sample (α1, fetuin, Eg2, IgG) is as follows: 1.17:1, 0.98:1, 3.49:1, and 3.70:1 respectively. Considering only those glycopeptides which are sialylated, the ratios are: 0.89:1, 0.98:1, 1.97:1 and 4:1 respectively. The position of TMT labels are indicated by \*



As a whole, it appears that the EMD kit is significantly favorable in both the IgG and Eg2 samples, which would indicate that the latter protocol is more efficient at enriching neutral glycopeptides such as the common G0, G1 and G2 often expressed in these immunoglobulins<sup>56</sup> and generally observed amongst the neutral glycopeptides enriched from  $\alpha$ 1-acid glycoprotein and fetuin. In light of this comparison, the data presented here highlight enriched glycopeptides previously reported by Kuo *et al*, which corroborate and strongly support the use of amine functionalized MNP as a complimentary technique for the enrichment of sialylated glycopeptides. Additively however, the workflow described here not only demonstrates a qualitative aspect for comparing enrichment techniques, as is habitually demonstrated in literature, but it also allows one to support the data quantitatively, providing a true analytical comparison between methodologies.

### 3.6 Conclusions

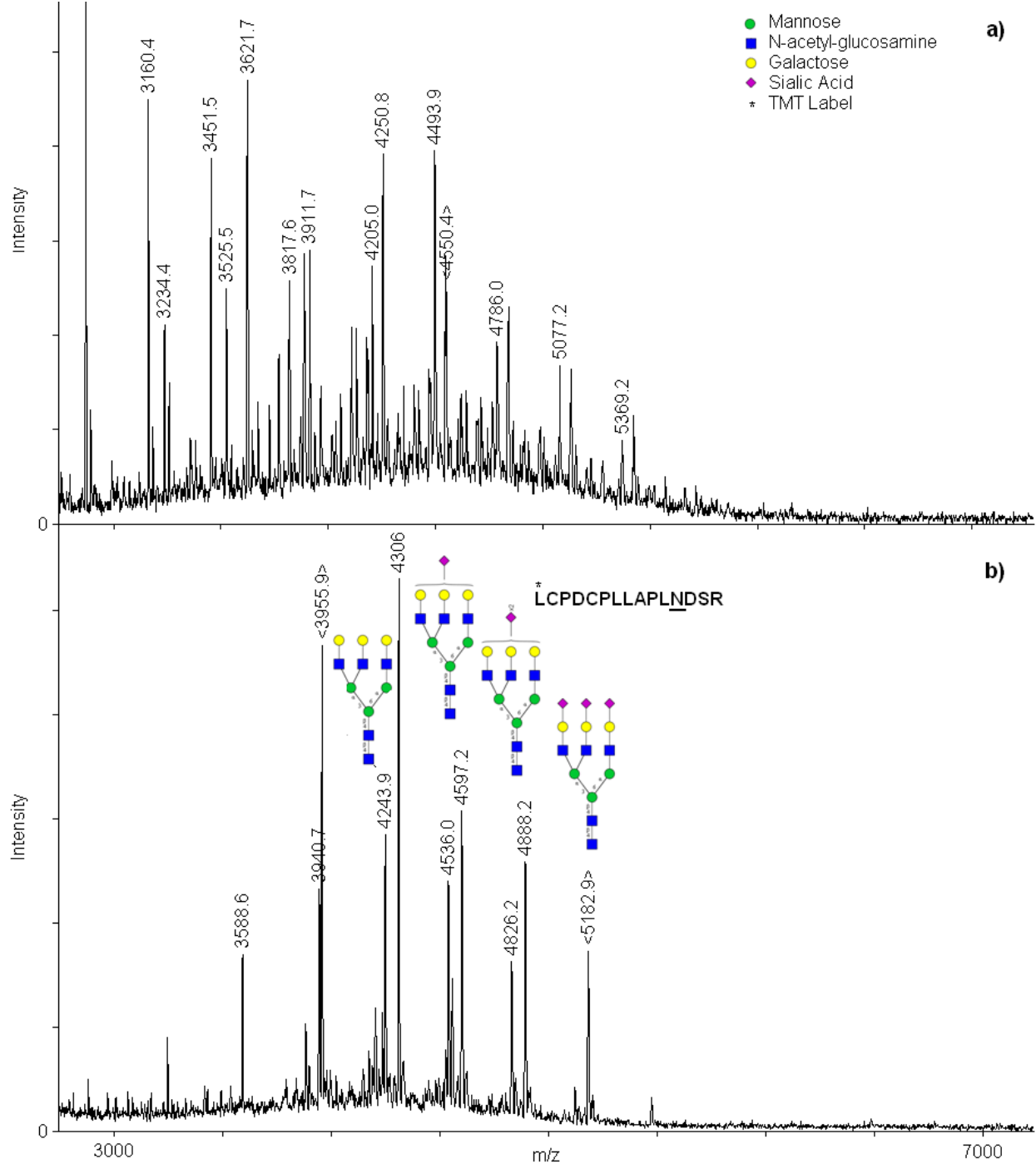
Reported here was a workflow which highlights the ability of using custom-made amine functionalized magnetic nanoparticles to enrich glycopeptides from tryptic digests. This method was compared to a commercially available glycopeptide retention kit and was deemed to enrich more sialylated glycopeptides as was demonstrated both quantitatively and qualitatively. Considering the highly hydrophobic nature of peptides, workflows focusing on the hydrophilic characteristics of glycan moieties must be developed and employed in order to expand the analysis of the glycome. While these experiments focused on the isolation of sialylated glycopeptides, it should be made apparent that amines may also interact with other negatively charged moieties including sulfates and phosphates, which also happen to be integral

modifications on both glycans and peptides. Since this methodology permits analysis at the glycopeptide level, its implications are far reaching including faster analysis, targeted approaches, and minimal sample loss as compared to glycan mediated workflows. In comparison to the commercial kit, it is advantageous both in terms of the time required to perform the enrichment, and its ability to capture sialylated species. Furthermore, the protocol presented here is compatible with streamlined proteomic workflows such as those enabled by electron-transfer dissociation (ETD)-MS. This latter technique has shown considerable benefits for studying glycoproteomics by MS<sup>57,58,59</sup>. As a whole, amine functionalized MNP present themselves as a viable enrichment technique to scientists studying glycobiology and proteomics by mass spectrometry.

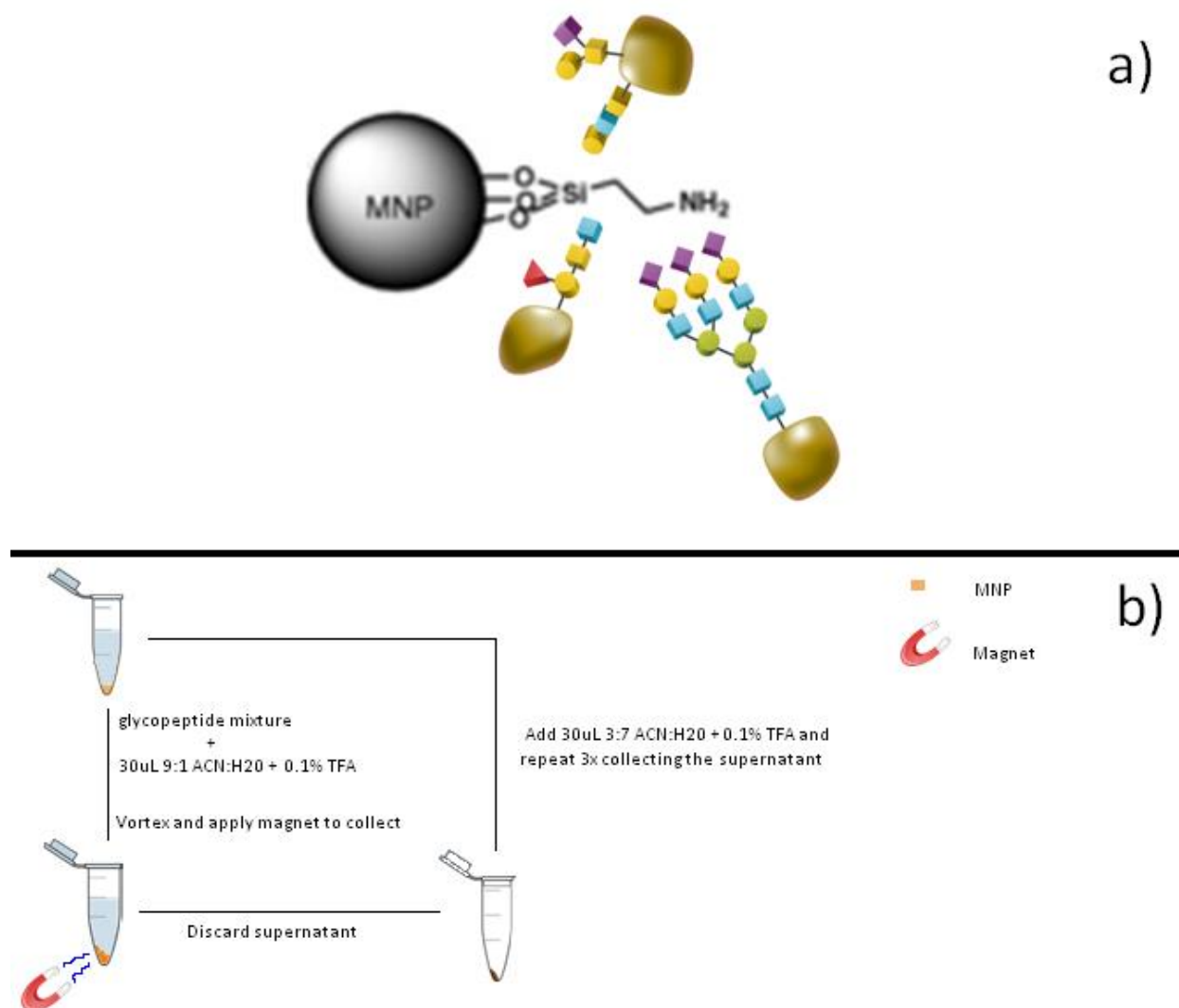
### 3.7 Acknowledgements

The authors would like to express gratitude to Dr. Julian Saba and Dr. Sergei Snovida (Thermo Scientific) for helpful discussions on the use of TMT. The authors thank Vinnith Yathindranath (Chemistry, University of Manitoba) for the synthesis of the MNP. As well, Dr. Oleg Krokhin (Internal Medicine, University of Manitoba) and Dr. Ken Standing's laboratory including Dr. David Shearer and Dr. Vladimir Collado (Physics, University of Manitoba) are thanked for their help and for access to mass spectrometers. Members of MabNet including Dr. Mike Butler's laboratory (Microbiology, University of Manitoba) are recognized for providing monoclonal antibodies for analysis as well as Dr. Chris Becker and Dr. Wildfred Tang (ProteinMetrics) for their help with Byonic. The authors would like to acknowledge the following groups for their funding and support: NSERC, CFI, and MabNet.

### 3.8 Supporting Information



**SI-Figure 1:** MALDI spectra of glycopeptides enriched using the EMD glycopeptide enrichment kit, collected in positive linear mode. a)  $\alpha$ 1-acid glycoprotein, b) bovine fetuin. Each spectrum shows characteristic glycan  $m/z$  differences, and prominent sialylation can be observed.



**SI-Figure 2:** Above represents a more comprehensive view of the magnetic nanoparticles, highlighting (a) the glycopeptides' interactions with the MNPs, and (b) a stepwise protocol for the capture and release of glycopeptides.

### 3.9 References

---

- <sup>1</sup> Cerný, M.; Skalák, J.; Cerna, H.; Brzobohatý, B. *J Proteomics*. **2013**.  
<http://dx.doi.org/10.1016/j.jprot.2013.05.040>
- <sup>2</sup> Lothrop, A.P.; Torres, M.P.; Fuchs, S.M. *FEBS Letters*. **2013**. 587:1247-1257.
- <sup>3</sup> Okuyama, N.; Ide, Y.; Nakano, M.; Nakagawa, T.; Yamanaka, K.; Moriwaki, K.; Murata, K.; Ohigashi, H.; Yokoyama, S.; Eguchi, H.; Ishikawa, O.; Ito, T.; Kato, M.; Kasahara, A.; Kawano, S.; Gu, J.; Taniguchi, N.; Miyoshi, E. *Int. J. Cancer* **2006**. 118, 2803–2808.
- <sup>4</sup> Osório, H.; Reis, C.A. *Meth Mol Bio*. **2013**. 1007, 301-316.
- <sup>5</sup> Cheng, M.; Chen, X.; Cai, Y.; He, Y.; Chen, Z.; Lin, Z.; Zhang, L. *Electrophoresis*. **2013**. 34(8), 1189-1196.
- <sup>6</sup> Kang, P.; Madera, M.; Alley W.R.; Goldman, R.; Mechref, Y.; Novotny, M.V. *Int J Mass Spectrom*. **2011**, 305(2-3):185-198
- <sup>7</sup> Marth, E., Flaschka, G., Steigler, S., Mose, J. *Clin Chim Acta*. **1988**. 176: 251-258.
- <sup>8</sup> Narayanan, S. *Ann. Clin. Lab. Sci*. **1994**. 24, 376–384
- <sup>9</sup> Hakomori, S. *Adv. Exp. Med. Biol*. **2001**. 491, 369–402.
- <sup>10</sup> Zhu, J.; Wang, F.; Cheng, K.; Dong, J.; Sun, D.; Chen, R.; Wang, L.; Ye, M.; Zou, H. *Proteomics*. **2013**. (8): 1306-1313.
- <sup>11</sup> Varki, N.M.; Varki A. *Lab Invest*. **2007**. 87:851–857
- <sup>12</sup> Brown, A.; Higgins, M.K. *Curr Opin Struct Biol*. **2010**. 20:560-566.
- <sup>13</sup> Lee LY,; Hincapie M,; Packer N,; Baker MS,; Hancock WS,; Fanayan S. *J Sep Sci*. **2012**, 35(18), 2445-52.
- <sup>14</sup> Butterfield, D.A.; Owen, J.B. *Proteomics Clin Appl*. **2011**. 5(1-2):50-56.

- 
- <sup>15</sup> Calvano, C.D.; Zambonin, C.G.; Jensen, O.N. *J Proteomics*. **2008**. 71, 304-317.
- <sup>16</sup> Hortin, G.M. *Anal Biochem*. **1990**. 191, 262-267.
- <sup>17</sup> Viner, R. I.; Zhang, T.; Second, T.; Zabrouskov, V. J. *Proteomics* **2009**, 72, 874–885.
- <sup>18</sup> Dayon, L.; Hainard, A.; Licker, V.; Turck, N.; Kuhn, K.; Hochstrasser, D.F.; Burkhard, P.R.; Sanchez, J.C. *Anal. Chem*. **2008**, 80, 2921–2931
- <sup>19</sup> Zhang, Y.; Yin, H.; Lu, H. *Glycoconj J*. 2012 Aug;29(5-6):249-58
- <sup>20</sup> Ongay, S.; Boichenko A.; Goveorukhina, N.; Bischoff, R. *J Sep Sci*. **2012**. 35(18): 2341-2372.
- <sup>21</sup> Ito, S.; Hayama, K.; Hirabaysahi, J. *Meth Mol Biol*. **2009**. 534: 195-203.
- <sup>22</sup> Zhang, Y.; Wang, H.; Haojie, Lu. *Mol. BioSyst*. **2013**. 9: 492-500.
- <sup>23</sup> Zhang, Y.; Kuang, M.; Zhang, L.; Lu, H. *Anal Chem*. **2013**. 85(11):5535-5541.
- <sup>24</sup> Xiong, Z.; Zhao, L.; Wang, F.; Zhu, J.; Qin, H.; Wu, R.; Zhang, W.; Zou, H. *Chem Commun (Camb)*. **2012**. 48(65): 8138-8140
- <sup>25</sup> Lui, M.; Zhang, L.; Xu, Y.; Yang, P.; Lu, H. *Anal chim Acta*. **2013**. Jul 25;788:129-34. doi: 10.1016/j.aca.2013.05.063
- <sup>26</sup> Gao, M.; Deng, C.; Zhang, X. *Expert Rev Proteomics*. **2011**. 8(3):379-90
- <sup>27</sup> Tang, J.; Lui, Y.; Qi, D.; Yao, G.; Deng, C.; Zhang, X. *Proteomics*. **2009**. (9)22: 5046-5055.
- <sup>28</sup> Tang, J.; Lui, Y.; Yin, P.; Yao, G.; Yan, G.; Deng, C.; Zhang, X. *Proteomics*. **2010**. 10(10):2000-2014.
- <sup>29</sup> Wang, L.; Bao, J.; Wang, L.; Zhang, F.; Li, Y. *Chemistry*. **2006**. 12(24): 6341-6347.
- <sup>30</sup> Xiong, Z.; Qin, H.; Wan, H.; Huang, G.; Zhang, Z; Dong, J.; Zhang, L.; Zhang, W.; Zou, H. *Chem Commun (Camb)*. **2013**. doi: 10.1039/c3cc45008b

- 
- <sup>31</sup> Zhou, W.; Yao, N.; Yao, G.; Deng, C.; Zhang, X.; Yang, P. *Chem Commun (Camb)*. **2008**. (43): 5577-5579.
- <sup>32</sup> Abbott, K. L.; Lim, J. M.; Wells, L.; Benigno, B. B.; McDonald, J. F.; Pierce, M. *Proteomics*. **2010**, 10, 470–481.
- <sup>33</sup> Kuo, C-W.; Wu, I-L.; Hsiao, H-H.; Khoo, K-H. *Anal Bioanal Chem*. **2012**. 402: 2765-2776.
- <sup>34</sup> Zhang, J., MacKenzie, R., Durocher, Y. *Methods Mol Biol*. **2009**. 525: 323-336.
- <sup>35</sup> Hongping, Y.; Boyne, M.; Buhse, L.; Hill, J. *Anal Chem*. **2013**. 85, 1531-1539.
- <sup>36</sup> Singh, C.; Zampronio, C.; Creese, A.; Cooper, H.J. *J Proteome Res*. **2012**. 11 (9), 4517-4525.
- <sup>37</sup> Wohlgemuth, J.; Karas, M.; Jiang, W.; Hendriks, R.; Andrecht, S. J. *Sep. Sci*. **2010**, 33, 880–890.
- <sup>38</sup> Wohlgemuth, J.; Andrecht, S.; Schnider, A.; SchweigerHufnagel, U.; Suckau, D. *J. Biomol. Tech*. **2011**, 22, S56.
- <sup>39</sup> Wohlgemuth, J.; Karas, M.; Eichhorn, T.; Hendriks, R.; Andrect, S. *Anal. Biochem*. **2009**, 395, 178–188.
- <sup>40</sup> Monoclonal Antibody Network: [www.mabnet.ca](http://www.mabnet.ca)
- <sup>41</sup> TMT™ Mass tagging Kits and Reagents: <http://www.piercenet.com/instructions/2162073.pdf>
- <sup>42</sup> EMD MILLIPORE [http://www.emdmillipore.com/life-science-research/proteoextract-glycopeptide-enrichment-kit/EMD\\_BIO-72103/p\\_xdCb.s1ORVMAAAEjpxp9.zLX](http://www.emdmillipore.com/life-science-research/proteoextract-glycopeptide-enrichment-kit/EMD_BIO-72103/p_xdCb.s1ORVMAAAEjpxp9.zLX)
- <sup>43</sup> Yathindranath, V.; Sun, Z.; Worden, M.; Donald, L.J., Thliveris, J.A.; Miller, D.W.; Hegmann, T. *Langmuir*. **2013**. 29(34):10850-10858.
- <sup>44</sup> Yathindranath V.; Rebbouh, L.; Moore, D.F.; Miller, D.W.; van Lierop, J.; Hegmann, T. *Adv. Funct. Mater*. **2011**, 21, 1457–1464



- 
- <sup>45</sup> Krokhin, O., Ens, W., Standing, K.G., Wilkins, J., Perreault, H. *Rapid Commun Mass Spectrom.* **2004.** 18(18): 2020-2030.
- <sup>46</sup> Yin, X.; Bern, M.; Xing, Q.; Ho, J.; Viner, R.; Mayr, M. *Mol Cell Proteomics.* **2013.** 12: 956-978.
- <sup>47</sup> McClintock, C.S.; Parks, J.M.; Bern, M.; Ghattyvenkatakrishna P.K.; Hettich, R.L. *J Proteome Res.* **2013.** 12(7): 3307-3316
- <sup>48</sup> Bern, M.; Kil, Y.J.; Becker, C. *Curr Protoc Bioninformatics.* **2012.** Dec; Chapter 13:Unit13.20. doi: 10.1002/0471250953.bi1320s40
- <sup>49</sup> Snovida, S.I.; Bodnar, E.D.; Viner, R.; Saba, J.; Perreault, H. *Carbohydrate Res.* **2010.** 792-801.
- <sup>50</sup> Baenziger, J.U.; Natowicz, M. I *Anal Chem.* **1981.** 112(2): 357-361.
- <sup>51</sup> Bierhuizen, M.F.; De Wit, M.; Gover, C.A.; Ferwerda, W.; Koeleman, C.; Pos, O.; Van Dijk, W. *Eur J Biochem.* **1988.** 175(2): 387-394.
- <sup>52</sup> Shetty, V.; Nickens, Z.; Shah, P.; Sinnathamby, G.; Semmes, O.J.; Philip, R. *Anal Chem.* **2010.** 82(22): 9201-9210.
- <sup>53</sup> Myslting, S.; Palmisano, G.; Højrup, P.; Thaysen-Andersen M. *Anal Chem.* **2010.** 82(13): 5598-5609.
- <sup>54</sup> Sybille, B.; Schwab, I.; Lux, A.; Nimmerjahn, F. *Semin Immunopathol.* **2012.** 34: 443-453.
- <sup>55</sup> Anumula, K.R. *J Immunol Meth.* **2012.** 381(1-2): 167-176.
- <sup>56</sup> Lattová, E., Kapková, P., Krokhin, O., Perreault, H. *Anal Chem.* **2006.** 78(9): 2977-2984.
- <sup>57</sup> Merchref, Y. *Curr Protoc Protein Sci.* **2012.** Chapter 12 – Unit 12.1111
- <sup>58</sup> Alley, W.R.; Mechref, Y.; Novotny, M.V. *Rapid Commun Mass Spectrom.* **2009.** 23(1): 161-170.
- <sup>59</sup> Ye, H.; Boyne, M.T.; Buhse, L.F.; Hill, J. *Anal Chem.* **2013.** 85(3): 1531-1539.

## **Chapter 4 – The Synthesis and Evaluation of Carboxymethyl Chitosan for Glycopeptide Enrichment**

## 4.1 Authors Contributions

All experiments pertaining to this work were designed and performed by Edward D. Bodnar under the guidance of Dr. H. Perreault. Dr. O. Krokhin was responsible for injecting and acquiring data on the AB Sciex 5600 Triple ToF instrument. Edward D. Bodnar was responsible for manuscript drafts and all figures, while Dr. H. Perreault was responsible for editing the final version. All authors contributed equally to the final revision of this chapter.

## 4.2 Abstract

Glycans are known to be involved in a variety of biological processes throughout human physiology. Mass spectrometry has demonstrated itself as powerful analytical tool for quantitative and structural characterization of glycans. Studying these molecules at the glycopeptide level however, offers distinct advantages, namely the ability to characterize both the glycan and peptide fragments simultaneously, and moreover the ability to assign site specific heterogeneity. In light of this, peptides often dominate the spectrum and hinder the ionization efficiency of glycopeptides. For this reason, enrichment protocols prior to downstream MS analysis need to be developed. Here, we discuss the synthesis and use carboxymethyl chitosan (CMCH) to enrich glycopeptides from a 12 protein mixture for MS analysis. This protocol was compared to a commercially available glycopeptide enrichment kit offered by EMD Millipore through the use of tandem mass tags (TMT) for relative quantification. Using this approach, we identified 98 unique *N*-linked glycopeptides and observed, that CMCH was able to enrich more sialylation than the commercial kit. In addition, we observed a trend based on TMT reporter ratios with respect to increasing sialylation. This corroborated that this stationary phase was exhibiting a mixed-mode enrichment through both hydrophilic interaction liquid chromatography (HILIC) and weak anion exchange (WAX) principles.

### 4.3 Introduction

Glycan-modified proteins are involved in a variety of biological and physiological roles throughout the body including cell-cell signaling, cell recognition, pathogenicity and immunology. It has been estimated that on the order of 50-70% of mammalian proteins exhibit glycosylation, and more recently this type of post-translational modification (PTM) has been recognized as an element of disease pathophysiology in areas of cancer, diabetes, Alzheimer's Disease and allergies<sup>1,2</sup>. In light of this, new fields of study have emerged including the 'omic' regimes of phosphoproteomics<sup>3</sup>, and glycoproteomics<sup>4</sup>, both which generally aim to study and understand these PTMs and their involvement in cellular pathways while they are still attached to the peptide. With respect to mass spectrometry, glycopeptides exhibit a lower ionization efficiency compared with their non-glycosylated counterparts, stemming from the micro-heterogeneity component intrinsic to their design, often diluting the overall glycopeptide signal and causing it to be "lost in the noise" of the spectrum. This feature is further magnified when more complex sample sets such as serum are to be studied, and as a result, often call for pre-enrichment steps prior to MS analysis<sup>5,6</sup>.

Hydrophilic interaction liquid chromatography (HILIC) approaches have demonstrated simple, fast and efficient procedures over reversed phase approaches for glycopeptide enrichment<sup>7,8</sup>. In light of this, much emphasis has been placed on designing niche 'glyco-modified' columns which can be used under HILIC conditions including 'click saccharides' onto polymer beads<sup>9</sup>, silica beads<sup>10,11</sup>, and magnetic nanoparticles<sup>12</sup>.

Chitosan is a naturally occurring polymer formed by the de-acetylation of chitin (poly-n-acetyl-glucosamine) typically found in the exoskeleton of many crustaceans<sup>13</sup>. This polymer has

been of significant interest in the areas of human health, drug delivery and agriculture<sup>14,15,16</sup> and derivatives of chitosan have been synthesized for use in the separation of acidic polar compounds<sup>17</sup>. Here, we describe the attachment of carboxymethyl chitosan (CMCH) onto an amino silica particle for use in a multi-stage glycopeptide enrichment approach, exploiting both the hydrophilicity and weak anion exchange characteristics of the stationary phase. To assess and evaluate the ability of CMCH to enrich glycopeptides, this approach is compared to a commercially available glycopeptide enrichment kit through the use of tandem mass tags (TMT) which allow for direct, targeted, and relative quantification using both on-line and off-line MS techniques.

## 4.4 Experimental

### 4.4.1 Materials

$\alpha$ 1-acid glycoprotein (human)/(bovine), fetuin (bovine), IgG (human), ovalbumin (gallus), serotransferrin (human), lysozyme (gallus), cytochrome C (equine), myoglobin (equine),  $\beta$ -casein (bovine), serum albumin (bovine) as well as dithiothreitol (DTT), iodoacetamide (IA), triethyl ammonium bicarbonate (TEAB), trypsin (from bovine), formic acid (FA), trifluoroacetic acid (TFA), acetonitrile (ACN) and methanol (MeOH) were obtained from Sigma (St. Louis, MO) while the Eg2 monoclonal antibody (mAb) was obtained through the Monoclonal Antibody Network (MabNet) (Winnipeg, Manitoba)<sup>18,19</sup>. Carboxymethyl chitosan 90% (CMCH), [O-(benzotriazol-1-yl)-N,N,N',N'-tetramethyluronium tetrafluoroborate] 99% (TBTU) and di-tert-butyl dicarbonate 99% (Boc Anhydride) were purchased from AK Scientific Inc. (Mountain View, CA). Spectra/Por membrane tubing (MWCO: 6000-8000; 23mm flat width, 14.6mm diameter)

was purchased from Spectrum Laboratories (Rancho Dominguez, CA) and Si-amine stationary phase (Si-NH<sub>2</sub>) was purchased from Silicycle (Quebec, QC). TMTs were acquired from Thermo Scientific as part of a TMT<sup>2</sup> Isobaric Mass Tagging Kit and the commercially available Novagen<sup>®</sup> ProteoExtract<sup>®</sup> Glycopeptide Enrichment Kit was purchased from EMD Millipore<sup>™</sup>. All solvents were HPLC-grade and obtained from Sigma (St. Louis, MO, USA). Distilled de-ionized water was obtained using a Milli-Q<sup>™</sup> filtration system supplied by a reverse-osmosis feedstock.

## 4.42 Methods

### 4.421 CMCH Synthesis

Initially, 0.48 g of carboxymethyl chitosan 90% (CMCH) was dissolved in H<sub>2</sub>O, MeOH, triethyl amine (TEA) 1:1:0.05 to a final pH of 12.3. Next, 1 g of di-tert-butyl dicarbonate was added and stirred in a sealed flask overnight for ca. 15 h. The solution was subsequently evaporated to dryness under vacuum, producing a beige/brown film which was removed and crushed with a mortar and pestle. In order to further evaporate excess Boc, the sample remained at room temperature overnight, and was then subjected to a high vacuum for 2 h. The yellow-beige CMCH-Boc was attached to 0.5 g of Si-amine stationary phase (Si-NH<sub>2</sub>) by dissolving the CMCH-Boc in H<sub>2</sub>O:MeOH and adjusting the pH to 7 using 0.5 M HCl where it mixed for ca. 10 min. Next, 1.93 g of TBTU was added and allowed to react overnight where the pH dropped to 5.3. Finally, an additional 1.04 g of TBTU was added and allowed to react for another 4 h, before the solution was filtered, collected, dried and crushed with a mortar and pestle. To remove the Boc-protecting group and any other impurities, the solution was washed extensively with TFA, followed by ACN and finally MeOH.

#### *4.422 Glycopeptide Preparation & Digestion*

Each protein and glycoprotein (1mg) was added to 100  $\mu$ L of [25 mM] TEAB (pH~8) in an Eppendorf™ tube and vortexed until the sample dissolved. Each sample was reduced by adding 500  $\mu$ L DTT [10mM] at 56<sup>0</sup>C for 1 h at which time the sample was alkylated by adding IA 400  $\mu$ L[500mM] and left to react in the dark for 30-60 min. Each sample was dialyzed twice against 4 L of H<sub>2</sub>O for 10 h using 6-8000 MWCO membranes, and lyophilized to dryness. Next, each sample was re-suspended in 250  $\mu$ L of [25 mM] TEAB buffer and a 20  $\mu$ g aliquot of trypsin was added and allowed to react overnight at 37<sup>0</sup>C. To deactivate the trypsin a large volume of acetonitrile + 0.1% TFA was added and this mixture was vortexed, lyophilized and resuspended in 1 mL of Milli-Q™ water to create peptide and glycopeptide standards. The 12 protein mixture, was prepared by pooling 100  $\mu$ g of each sample.

#### *4.423 Tandem Mass Tag (TMT) labeling*

To quantify and compare the enrichment efficiency between techniques, tandem mass tags (TMT) were purchased from Pierce Thermo Scientific (Rockford, IL). The manufacturer's protocols were followed<sup>20</sup>, which in brief involve adding 41  $\mu$ L of acetonitrile to the stock TMT vial, followed by vortexing for ~5 min, at which point the TMT label is sufficient for 100  $\mu$ g of sample. An aliquot of each TMT label was prepared for a 25  $\mu$ g sample followed by a 1 h incubation period at room temperature, at which time the reaction was quenched by adding 2  $\mu$ L of 5% hydroxyquinilone.



#### 4.424 Glycopeptide Enrichment

In order to evaluate the enrichment efficiency between methods, a commercially available glycopeptide kit was purchased from EMD Millipore™. The manufacturer's protocols were followed<sup>21</sup>, which briefly include centrifuging the stationary phase at ~2500 g for 2 min to remove excess storage reagent. This is followed by adding a proprietary binding buffer to the sample then adding it to the stationary phase and allowing it to incubate for up to ca. 20 min with end over-end-mixing. Next, the vial is centrifuged and the supernatant is removed, which is assumed to contain the majority of unbound peptides. The solution is then washed with a proprietary wash solution for ca. 10 min, centrifuged, and the supernatant is once again removed; this is repeated 2 x to aid in removing the remainder of unbound peptides. Finally, to elute the bound glycopeptides, a proprietary elution solution is applied and allowed to react for ca. 2 min, followed by centrifugation and collection of the supernatant, which is then subsequently centrifuged again at 10,000 g to sequester any stationary phase that may have been accidentally transferred.

In comparison to the commercial enrichment kit, 5 mg of Si-CMCH was weighed and added to a 1.5 mL Eppendorf tube. Next, this stationary phase was washed with 3x 0.5 mL of 9:1 ACN:H<sub>2</sub>O, 3 x 0.5 mL of 3:7 ACN:H<sub>2</sub>O + 0.1% TFA, and finally equilibrated with 3 x 0.5 mL of 9:1 ACN:H<sub>2</sub>O whereby each addition of solvent was vortexed and removed after centrifugation. Subsequently, 25 µg of sample was added followed by an equivalent volume to produce a 9:1 ACN:H<sub>2</sub>O + 0.1% TFA and allowed to interact for 10-15 min before the solution was centrifuged and the supernatant was collected; this occurred twice more and was pooled to constitute the

wash or “peptide fraction”. To remove bound glycopeptides, 100  $\mu$ L of 3:7 ACN:H<sub>2</sub>O + 0.1% TFA solution was added and the mixture was vortexed three times, constituting the eluent or “glycopeptide fraction”. These fractions were lyophilized to dryness and TMT labeled where they were once again lyophilized to dryness and re-suspended to 20  $\mu$ L in 3:7 ACN:H<sub>2</sub>O + 0.1% TFA prior to mass spectrometric analysis.

#### **4.425 *Mass Spectrometric Analysis***

For matrix-assisted laser desorption/ionization mass spectrometric (MALDI-MS) and MS/MS analysis an UltrafleXtreme (Bruker Daltonics, Germany) was used, as well as a Manitoba/Sciex prototype quadrupole quadrupole time of flight (MALDI-QqTOF). Unless otherwise stated these instruments were utilized in positive ion mode with a matrix of 2,5 dihydroxybenzoic acid (2,5 DHB) and a scanning range of 600-8000 m/z. Each sample was prepared whereby 0.75  $\mu$ L of matrix was spotted and co-mixed with 0.75  $\mu$ L of sample and then allowed to dry on target before loading it into the MS.

HPLC-MS spectra were acquired on an AB Sciex 5600 Triple TOF™ equipped with a NanoSprayIII source, operated in standard MS<sup>2</sup> data-dependent acquisition mode. The samples were diluted 1:20 with H<sub>2</sub>O+ 0.1% FA. A nano-flow 2D LC Ultra system (Eksigent–Ab Sciex, Dublin, CA) with 10  $\mu$ L injection through a 300  $\mu$ m x 5 mm PepMap100 (Thermo FisherScientific, Rockford, IL) trap-column and 100  $\mu$ m x 200 mm analytical column packed with 5 mm Luna C<sub>18</sub> were used for separation. The gradient employed started at 0% H<sub>2</sub>O + 0.1% FA and went to 30% ACN + 0.1% FA over 45 min.

#### 4.426 ATR-FTIR Analysis

Both Si-NH<sub>2</sub> and Si-CMCH were subjected to attenuated total reflectance (ATR) infrared (IR) measurements with a single bounce diamond crystal using a ThermoScientific Nicolet 6700 FT-IR. In each experiment, the data were collected from 600-4000 nm with a resolution of 4 cm<sup>-1</sup> over 32 scans, followed by background correction.

#### 4.427 TEM Imaging

Silica-NH<sub>2</sub> and CMCH derivatized silica beads were compared using transmission electron microscopy (TEM). A 2 mL volume of 2% uranyl acetate in water was prepared in a culture tube and mixed for ~60 min. The solution was then filtered through a 0.02 µm syringe filter into a separate vial. Silica stationary phases were pre-rinsed with water prior to placement onto the grid. They were then negatively stained with a drop of uranyl acetate and allowed to dry for ca. 1 h prior to imaging. TEM images were acquired with a Hitachi H-7000 transmission electron microscope equipped with a tungsten filter (Dept. Microbiology, University of Manitoba).

#### 4.428 Data Analysis

Glycopeptide MALDI data were analyzed using Bruker's FlexAnalysis, to view and interpret data by hand. In each case, detection of a glycopeptide was further corroborated by the presence of the characteristic MALDI-specific oxonium ion cross ring cleavage (<sup>0,2</sup>X<sub>0</sub>) which occurs between the first HexNAc and the peptide backbone<sup>22</sup>.

To deconvolute and elucidate glycopeptide structures from LC-MS and LC-MS/MS data, the Byonic™ software (Protein Metrics Inc., San Carlos, CA) has been utilized previously<sup>23</sup>. Specific to this analysis, *in silico* lysine and arginine tryptic cleavages with a maximum of 2 missed cleavages were employed. The precursor mass tolerance was set to 20 ppm, and the fragment mass tolerance was 0.1 Da using a QToF/high energy collision dissociation (HCD) type of fragmentation. For the aforementioned sample preparation, the following protein modifications were included in the Byonic™ search: carbamidomethylation for cysteines, N-terminal and lysine TMT<sup>2</sup> tag as fixed modifications, as well as variable methionine oxidation. Moreover, Byonic™ contains a “common human/mammalian” glycan database of 350 N-linked glycans with masses up to 6000 Da for which only one glycan is allowed per peptide sequon. These options were selected for precursor ions with charges 2 to 5, and MS<sup>2</sup> spectra were then ranked in the software from score 0 to 1000, whereby only those entries above 500 (demonstrating a “good match”) were considered. These matches were manually verified in the MS<sup>2</sup> spectra by extracting the total ion chromatogram for the presence of a glycan reporter fragment ion such as the HexNAc oxonium ion at 204.087 Da.

## 4.5 Results and discussion

### *Development and characterization of CMCH*

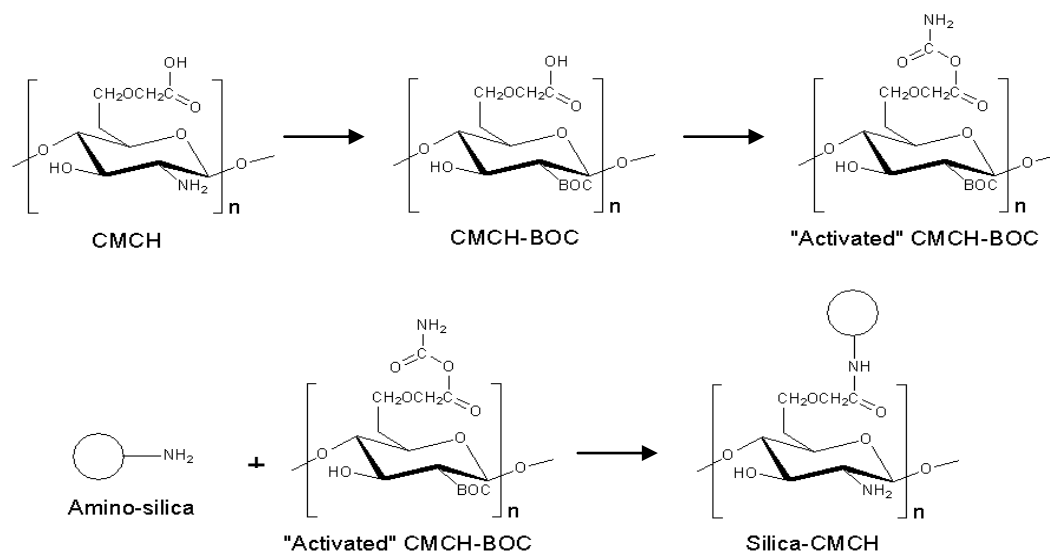
By exploiting Si-CMCH as a stationary phase, it was hypothesized that the CMCH would have increased affinity for glycopeptides, based on hydrophilic interaction liquid chromatography (HILIC) principles. All mammalian N-linked glycans exhibit N-acetylglucosamine, not only in their common penta-glycan core, but also frequently in the

antennary chains of both hybrid and complex glycans. In this regard, chitosan appears as an interesting candidate for the enrichment of glycopeptides through HILIC. In addition, chitosan possesses a free amine on C2 made available upon deacetylation of chitin, allowing it to participate in weak anion exchange (WAX) interactions with other important moieties, including sulfated or sialylated glycans, as well as phosphorylated peptides. Since the pKa of CMCH is ca. 6.5 it may be more adaptable to biological settings.

With respect to the properties of this ligand, a previous attempt of attaching chitosan to Si-NH<sub>2</sub> proved more challenging. Initially, chitosan was chosen as a stationary phase for the extraction of glycopeptides, however its large granular size and tendency to swell and become gelatinous under mildly acidic conditions made it impossible to use under chromatographic conditions, which led to the use of carboxymethyl chitosan (CMCH) as an improved phase. CMCH is a derivative which contains the same molecular framework as chitosan, although in addition it possesses a carboxylic group through which it can covalently link to a free amine (see Figure 4.1, attachment on a Si-NH<sub>2</sub> particle).

Figure 4.1 - Attachment of carboxymethyl chitosan onto an amino silica particle.

This approach was adapted from a previous method <sup>17</sup> by protecting the amine of CMCH with BOC, and subsequently activating it using a carbodiimide. This step is followed by the addition of amino-silica beads which serve as a substrate for CMCH attachment.



To accomplish this, TBTU (a well known peptide coupling reagent) was employed. Uniquely, CMCH possesses both carboxylic and amine groups, and to ensure that it would not couple with itself under these conditions, the amine on CMCH was BOC protected and BOC was removed following the synthesis. To characterize this preparation, ATR-FTIR measurements were taken both before and after the addition of CMCH (Figure 4.2).

Figure 4.2 – ATR-FTIR spectra of Si-NH<sub>2</sub> and Si-CMCH

Three characteristic regions correlate with the presence of CMCH, namely with a band at ca. 700 cm<sup>-1</sup> which indicates the presence of primary amines, another one at ca. 1650 cm<sup>-1</sup> which is a signature for carbonyl amides, and with a broad stretching band around ~3300 cm<sup>-1</sup> attributed to H bonding of –OH and NH<sub>2</sub> groups<sup>24</sup>. Furthermore, samples of both Si-NH<sub>2</sub> and Si-CMCH particles were imaged using transmission electron microscopy (TEM, Figure 4.3). These images depict A) native silica-NH<sub>2</sub> in comparison to B) Si-CMCH. In B), there are noticeable sphere-like inclusions at the surface, corroborating the ATR-FTIR results that the surface was modified.

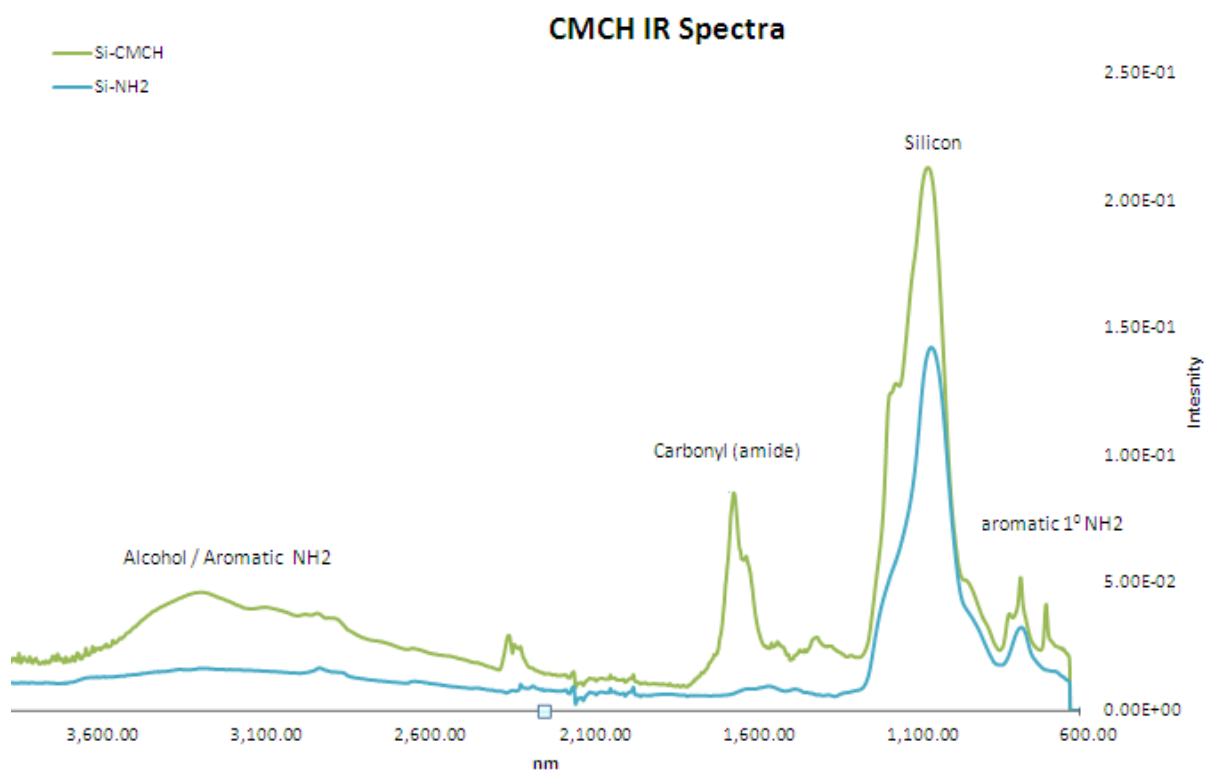


Figure 4.3 - TEM Images at 40,000x magnification of Si-NH<sub>2</sub> and Si-CMCH.

TEM images suggest a noticeable ‘film-like’ surface as indicated by the arrows (A) Si-NH<sub>2</sub> (B) Si-CMCH. Paler background lines are due to the TEM grid holding the sample.



#### *Preliminary enrichment using CMCH*

CMCH was first assessed for its ability to enrich glycopeptides from the tryptic digests of individual glycoproteins (Eg2 antibody, human IgG, human  $\alpha$ 1-acid glycoprotein, bovine fetuin). MALDI-MS spectra of the enriched fractions were acquired in the positive reflector mode and are shown in Figure 4.4. No labeling was used here. Qualitatively, these data showed significant enhancement of glycopeptide signals after enrichment, relative to the spectra of crude tryptic digests (not shown). CMCH enrichment also favored the retention of sialylated species vs. neutral glycopeptides, compared with the EMD commercial protocol (not shown). This agrees with our design hypothesis that Si-CMCH would be beneficial for targeting sialylated glycoforms using a ‘mixed-mode’ (HILIC-WAX) approach. For a more quantitative assessment, each of  $\alpha$ 1-acid glycoprotein, Eg2 and IgG was then digested individually and subjected to glycopeptide enrichment with comparative TMT labeling. In this procedure each crude tryptic digest sample was enriched in parallel by two protocols, (Si-CMCH and EMD kit), labeled with a separate TMT,



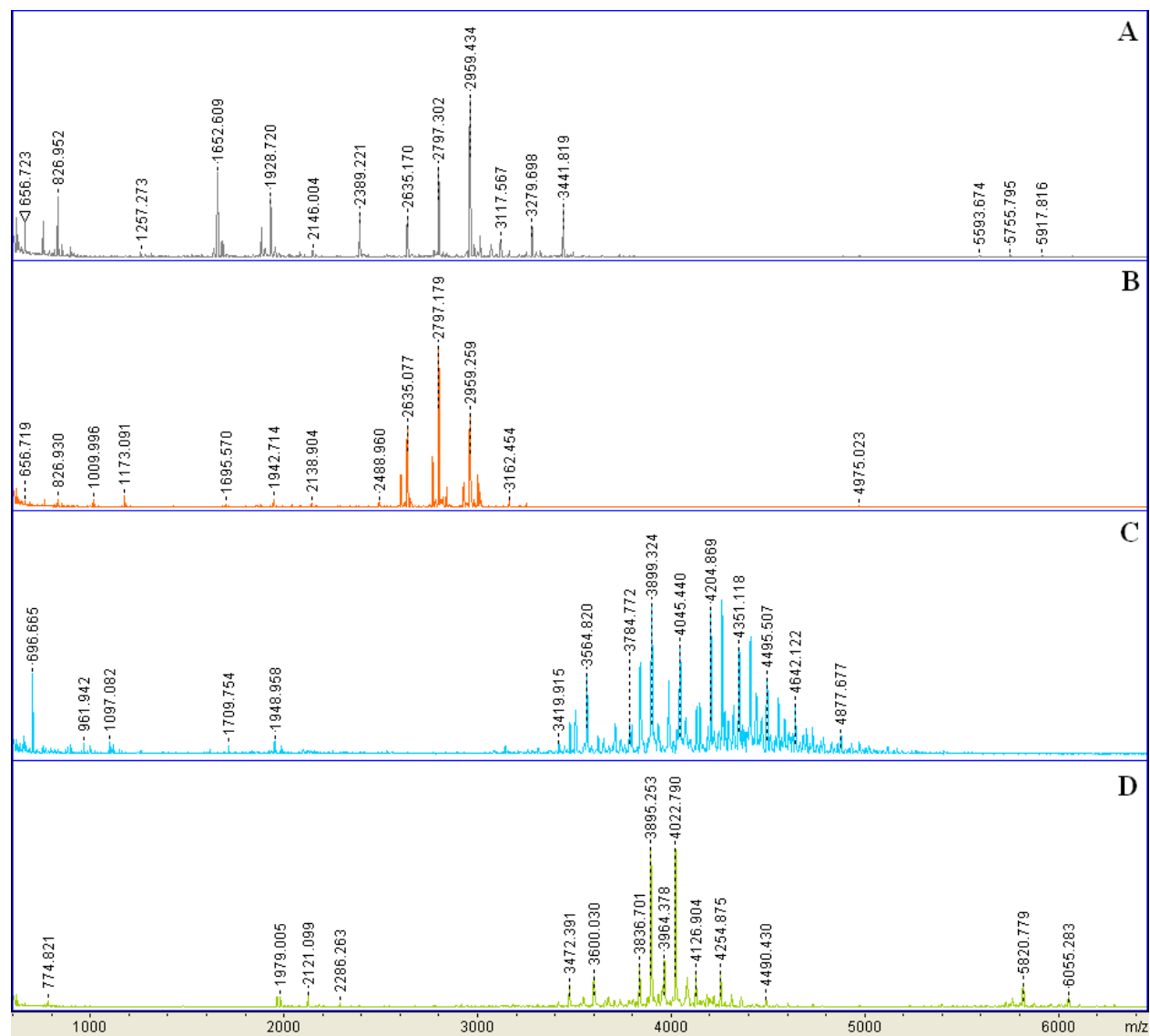
mixed and subjected to LC-MS/MS analysis. Since each TMT label only differs by the relative location(s) of the  $^{13}\text{C}$  isotope(s) on its backbone, isobaric labeled glycopeptides co-elute and have the same physicochemical properties, e.g. ionization efficiency. It is only when fragmentation occurs<sup>25</sup> that a mass difference in reporter ions can be observed, whereby the ratio between these reporter ions can be directly correlated to the enrichment efficiencies of the two methodologies. This workflow for glycopeptide enrichment has been previously demonstrated by our group using amine functionalized magnetic nanoparticles (MNP)<sup>26</sup>. From this work, and other published glycomic studies, a standard library of glycoproteins has been generated for reference<sup>7,27,28,29</sup>. The results (Table 4.1) demonstrated enhanced enrichment ratios of sialylated glycoproteins for the Si-CMCH protocol vs. the commercially available EMD approach, still corroborating the selectivity of the new mixed-mode design. This experiment was successful, although not representative of a more complex sample containing multiple proteins and glycoproteins.

Table 4.1 - Average TMT Ratios for three individual glycoproteins and number of observed glycopeptides.

<b><i>Protein</i></b>	<b>Observed Glycopeptides</b>	<b>EMD : CMCH</b>
<i><math>\alpha</math>1 acid glycoprotein (human)</i>	38	0.4 : 1
<i>IgG (human)</i>	17	2.6 : 1
<i>Eg2 (mAb)</i>	27	2.3 : 1

Figure 4.4 - MALDI spectra of Si-CMCH enriched tryptic glycopeptides

These spectra were collected in positive reflector mode A) Eg2 antibody B) human IgG, C) human  $\alpha$ 1-acid glycoprotein D) bovine fetuin.

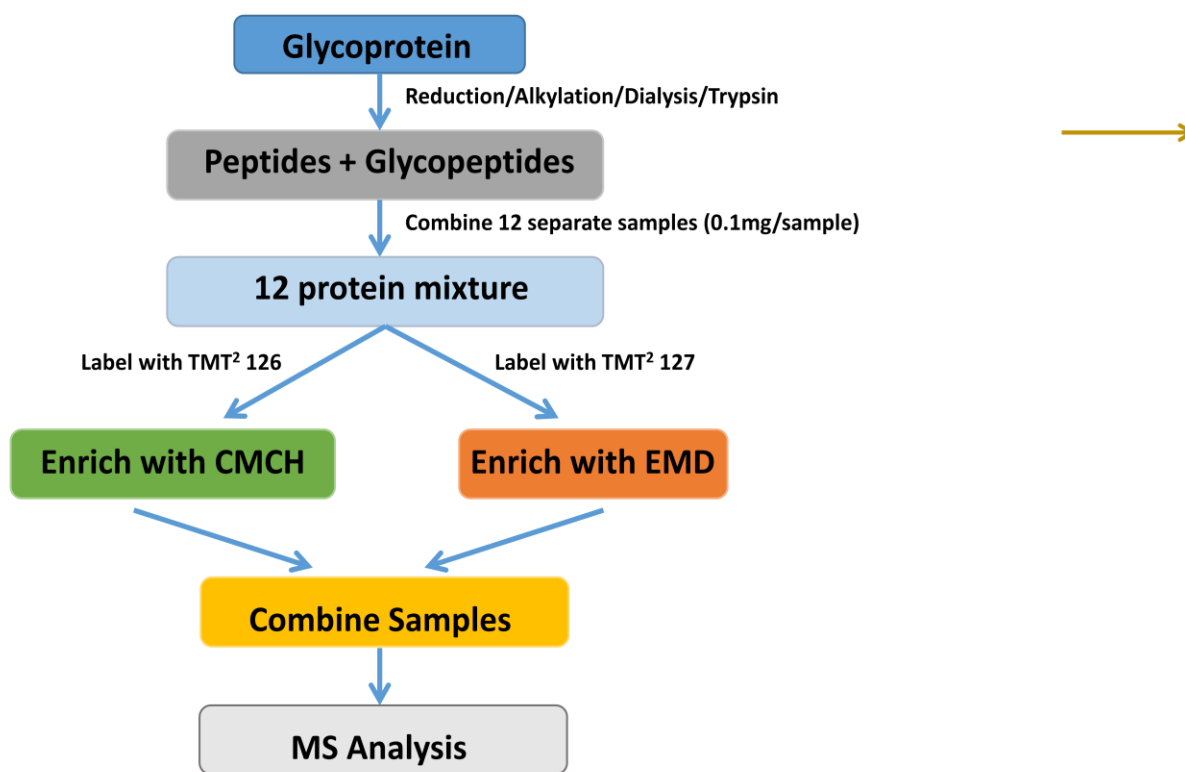


### *Enrichment of 12 proteins using CMCH*

The next step was to apply this enrichment scheme to a more complex sample, and for this a mixture of 12 proteins/glycoproteins was used (Figure 4.5). See the experimental sections (materials) for the specific proteins in the mixture. Proteins were chosen with respect to varying ranges of glycosylation, and more importantly sialylation. The 12 protein mixture was digested with trypsin, then two aliquots of the digest (25 µg each) were enriched in parallel with Si-CMCH and EMD. They were then TMT labeled and recombined for MS and MS/MS analysis (Figure 4.6). All glycoproteins were identified with varying sequons containing glycosylation, with the exception of ovalbumin. This is presumably due to the larger mass associated with the glycopeptide at Asn<sub>292</sub> (YNLTSVLMAMGITDVFSSSA NLSGISSAESLK; 3293.6279 m/z without glycans), in conjunction with the limited detection range for data dependent acquisition which could likely be improved by digesting this sample into smaller peptides using a combination of enzymes such as trypsin + proteinase K<sup>30</sup>.

Figure 4.5 – Workflow used to compare the enrichment efficiency between Si-CMCH and EMD on a 12 protein mixture

Individually, 12 separate tryptic digests are prepared and co-mixed to create a 12 protein mixture. Equal aliquots are labeled separately with a unique TMT<sup>2</sup> and enriched by their respective method. The enriched samples are then pooled and subjected to mass spectrometric analysis.



#### *Data analysis using Byonic*

LC-MS spectra were elucidated using Byonic™ software and identification of glycosylated species was further confirmed manually by tracking the presence of diagnostic ions (N-acetylglucosamine, 204.087 m/z) in the MS<sup>2</sup> spectra. Subsequently, TMT ratios were tabulated and normalized against TMT-126 (Table 4.2). TMT 126 corresponds to the reporter

ions obtained for glycopeptides isolated using the Si-CMCH, and TMT 127 characterizes those enriched by the EMD method. Glycoproteins bearing complex glycans with moderate to higher levels of sialylation ( $\alpha$ 1 acid, fetuin, and serotransferrin) demonstrated enrichment ratios which on average favoured the Si-CMCH protocol (1.15:1; 126:127) by 15%, whereas proteins with

Figure 4.6 - (A) Selected LC-MS spectrum highlighting the elution of various enriched glycopeptides. Molecular ions of each glycopeptide triggered (B) MS<sup>2</sup> analysis as demonstrated at 1057.92 *m/z* (4+), where (C) reporter ions 126 and 127 peak areas were compared.

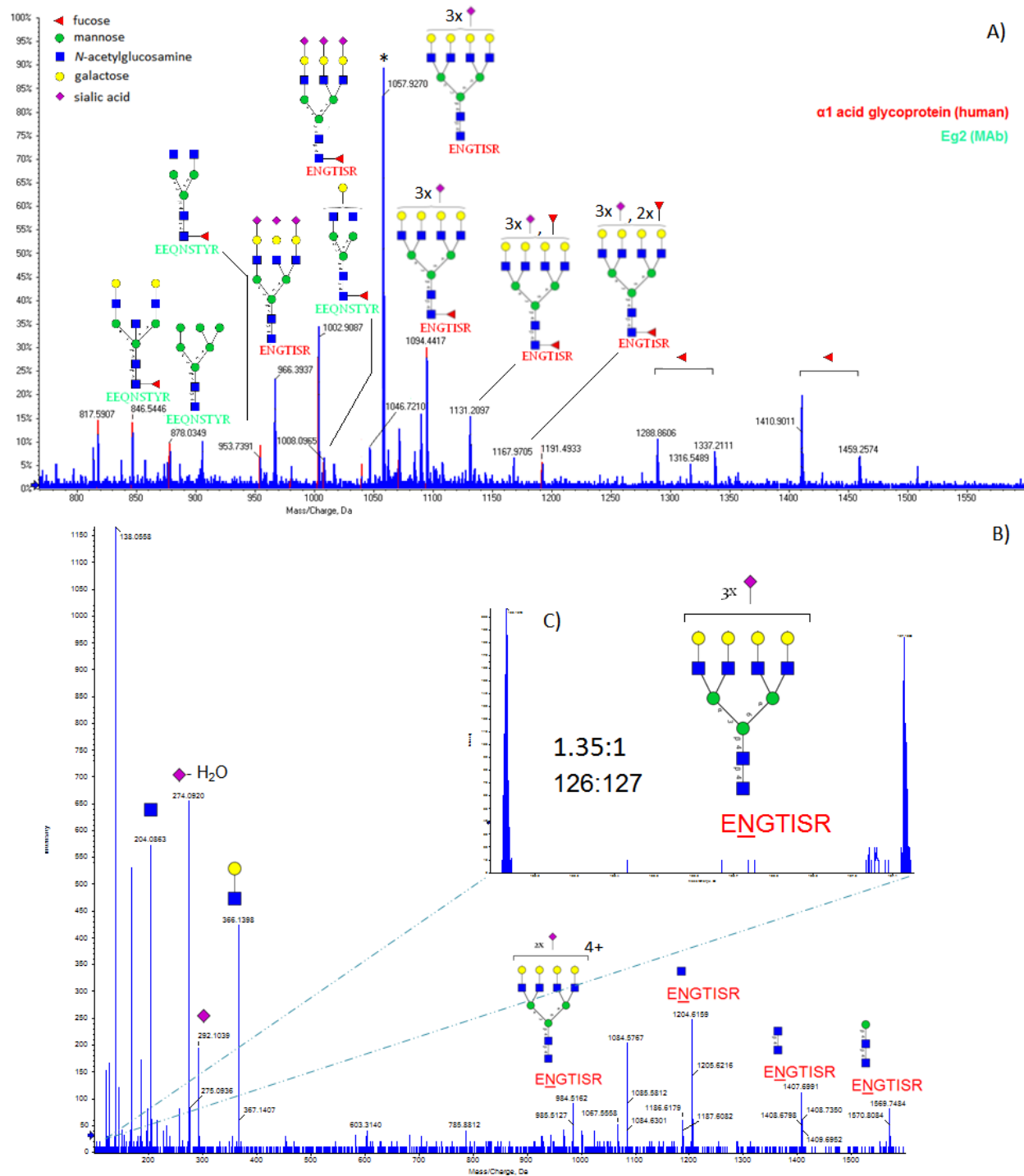


Table 4.2 - Average TMT Ratios for all glycoproteins in the mixture and number of observed glycopeptides.

<b>Protein</b>	<b>Observed Glycopeptides</b>	<b>EMD : CMCH</b>
<i><math>\alpha</math>1 acid glycoprotein (human)</i>	37	1.1 : 1
<i><math>\alpha</math>1 acid glycoprotein (bovine)</i>	26	0.9 : 1
<i>Fetuin (bovine)</i>	14	0.74 : 1
<i>IgG(human)/Eg2(mAb)*</i>	14	2.8 : 1
<i>Serotransferrin (human)</i>	7	0.75 : 1

little or no sialylation (IgG, Eg2) favoured the ZIC-HILIC EMD method (1:2.8; 126:127).

Moreover, several series of glycoforms from the same sequon with increasing sialylation levels showed corresponding increments in their 126:127 TMT ratios (Figure 4.7). While this trend is still under investigation, this suggests an increased affinity of sialylation for Si-CMCH using this mixed-mode approach. Sialylation on wild type human immunoglobulin is considered low in general, with reports suggesting A2G2FS1 glycoforms constitute up to 10-12% of the total glycan pool, whereas A2G2FS2 glycoforms exist only in trace amounts<sup>31,32</sup>. With this considered, the ratios calculated for singly and doubly charged sialylated glycans favour Si-CMCH enrichment, where A2G2FS1 and A2G2FS2 ratios are 1.10 and 1.13, respectively. This attests to the ability of this protocol to capture low abundance sialylated glycans and shows as discussed above a trend of CMCH to interact more efficiently with higher sialylated glycoforms.

### **Method Comparison**

Upon comparing Si-CMCH (Method 1) with the EMD commercial kit likely developed based on a report by Wohlegmuth *et al.*<sup>33</sup> (Method 2), some comments can be made. Both enrichment materials were tested on glycopeptides from protein mixtures in which  $\alpha$ 1 acid glycoprotein, bovine fetuin, BSA and human IgG were in common. The enrichment procedure

optimized by Wohlegmuth *et al.* in Method 2 aimed at extracting glycopeptides from a 6 protein mixture. In contrast, the method presented here (Method 1) doubles the complexity of the sample, enriching for glycopeptides from a 12 protein digest. The commercial kit is presumed to use 'wash buffers' consisting of ammonium salts as reported in Method 2. These were introduced in order to help reduce electrostatic interactions between analytes and the zwitterionic stationary phase, therefore enhancing the retention of hydrophilic sialylated glycopeptides. In contrast, Method 1 does not use any buffers. Instead, it aims to exploit the hydrophilic character of CMCH and the weak anion exchange capabilities of its primary amine in order to enrich for sialylated glycopeptides. This is seen as advantageous with respect to clean up procedures often necessary prior to MS analysis.

In order to determine the enrichment efficiency of Method 2, Wohlegmuth *et al.* collected their flow-through fractions and deglycosylated them using *N-glycosidase F* (PNGaseF), noting that no further glycans could be detected. Here, for Method 1 we performed a subsequent enrichment of flow-through fractions on Si-CMCH followed by MS analysis, and no glycopeptides could be detected (data not shown). Through a systematic comparison of both methodologies, Si-CMCH appears dominant for the enrichment of sialylated glycopeptides. The use of TMT labels for Method 1 also supports this finding.

### Summary

Using this approach, we identified glycopeptides with 98 different sequences from the 12 protein mixture, which is on the same scale of enrichment as obtained from other protocols reported in the literature using these glycoproteins<sup>34,35</sup>. The enrichment of glycopeptides from the same glycoproteins as used in this work has been discussed. In a first example, Takakura *et*

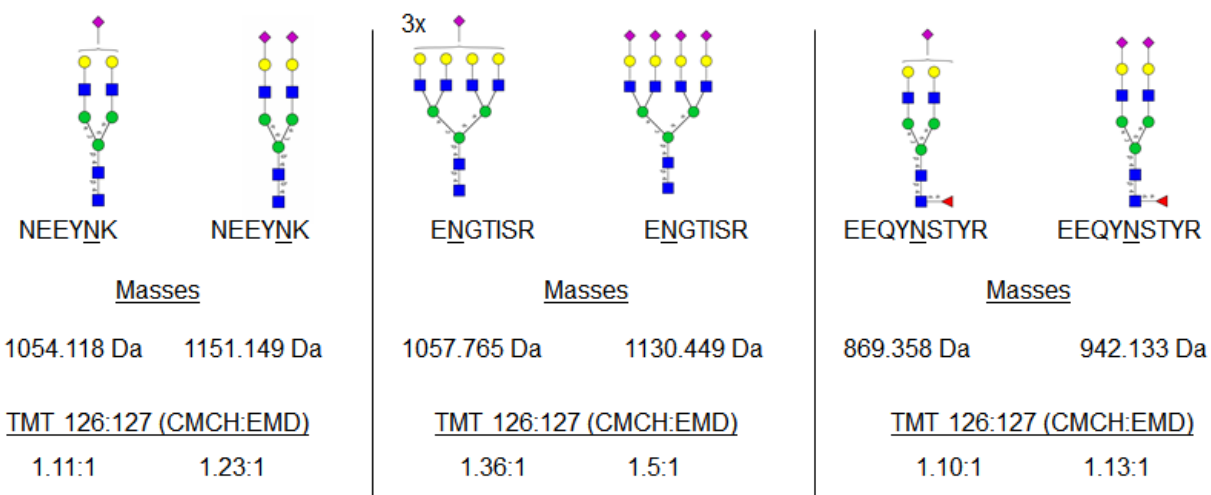


*al.* employed acetone enrichment for bulk precipitation of glycopeptides from  $\alpha 1$  acid glycoprotein and identified 9 distinct N-linked glycoforms<sup>36</sup>. In another report, Selman *et al.* proposed a HILIC SPE enrichment technique using cotton wool for fetuin and IgG samples<sup>37</sup> which produced similar enrichment yields as the CMCH approach, but with no enrichment of the A2G2FS2 glycoform. Overall, the CMCH method combines the positive attributes of these alternative ways of enrichment, as using Si-CMCH does enrich the bulk of glycopeptides from a sample and is advantageous over the EMD method when targeting sialylated glycopeptides.

Figure 4.7 - Enrichment ratios for selected glycoforms of the same sequon determined using

TMT-based quantitation

These pairs of glycans exhibit increasing levels of sialylation. A systematic trend is observed between sialylation level and affinity for CMCH vs. EMD ( *$\alpha 1$ -acid NEEYNK, ENGTISR; Eg2 EEQYNSTYR*).



## 4.6 Conclusion

This goal of this chapter presented a proof of principle of the preparation and use of Si-CMCH for glycopeptide enrichment of tryptic digestion mixtures. This solid phase, when used in the bulk for pull down, shows a higher affinity for sialylated glycopeptides than for peptides bearing neutral glycans. Through the incorporation of tandem mass tags in a 12 protein mixture digest, it was determined quantitatively that Si-CMCH enriched sialylated glycopeptides with a 13% higher yield than the glycopeptide enrichment kit offered by EMD Millipore. The ability of Si-CMCH to enrich sialylated species was further validated for the isolation of sialylated glycopeptides from antibody species (low sialylation levels). As the degree of sialylation increased on the glycopeptide, TMT ratios favored Si-CMCH enrichment. This suggests that Si-CMCH interacts both in HILIC and WAX modes, expanding the ability for retention of these analytes.. In the search for a fast, efficient and robust glycopeptide enrichment protocol which is crucial prior to MS analysis, the use of Si-CMCH has shown these three positive aspects. Approaches such as this, which aim to target glycans using niche 'glyco-like' stationary phases, are excellent additions to the repertoire of currently available enrichment strategies, and it would not be surprising to see additional workflows designed around these principles. Future work with this stationary phase will aim to investigate the observed trend regarding increases in sialylation which may be accomplished by employing either released N-linked glycans or polysialic acid ladders for relative retention capacities. Furthermore, a more complex sample such as human serum will be investigated to assess the quantity and enrichment of sialylated species.

## 4.7 Acknowledgments

The authors express sincere gratitude to the group of Dr. Frank Schweizer (Chemistry, University of Manitoba) for a variety of helpful discussions regarding protecting groups and synthesis. Dr. Oleg Krokhin (Internal Medicine, University of Manitoba) is sincerely thanked for granting access to electrospray mass spectrometers. Dr. Mike Butler (Microbiology, University of Manitoba) as well as the Monoclonal Antibody Network (MabNet) are thanked for supplying monoclonal antibodies for analysis. The authors would also like to thank Mr. Andre Dufresne (Microbiology, University of Manitoba) for his analysis with the transmission electron microscope. Lastly, the funding agencies including MabNet, as well the Natural Sciences and Engineering Research Council (NSERC), Canadian Foundation for Innovation (CFI) and Manitoba Research & Innovation Fund are thanked.

## 4.8 References

---

- <sup>1</sup> Patrie, S.M.; Roth, M.J.; Kohler, J.J. *Methods in Molecular Biology*. **2013**, 951, 1-17.
- <sup>2</sup> Novotny, M.V.; Alley, W.R.; Mann, B.F. *Glycoconjugate Journal*. **2013**, 30(2): 89-117.
- <sup>3</sup> Schmelzle, K.; White, F.M. *Curr Opin Biotechnol*. **2006**, 17(4): 406—414.
- <sup>4</sup> Novotny, M.V.; Mechref, Y. *J Sep Sci*. **2005**, 28(15): 1956-1968.
- <sup>5</sup> Wuhrer, M.; Catalina, M. I.; Deelder, A. M.; Hokke, C. H. *J. Chromatography B*. **2007**, 849, 115–128.
- <sup>6</sup> Pasing, Y.; Sickmann, A.; Lewandrowski, U. *Biol Chem*. **2012**, 393, 249-258.
- <sup>7</sup> Snovida, S.I.; Bodnar, E.D.; Viner, R.; Saba, J.; Perreault, H. *Carbohydrate Res*. **2010**, 345, 792-801.
- <sup>8</sup> Jensen, P.H.; Mysling, S.; Højrup, P.; Jensen, O.N. *Methods Mol Biol*. **2013**, 951, 131-44.
- <sup>9</sup> Gong, T.; Adzime, B.J.; Baker, N.H.; Bowman, C.N., *Adv. Mater*. **2013**, **25**, 2024-2028.
- <sup>10</sup> Huagn, H.X.; Jin, Y.; Xue, M.Y.; Yu, L.; Fu, Q.; Ke, Y.X., Chu, C.H., Liang, X.M. *Chem. Chommun*. **2009**, 6973-6975.
- <sup>11</sup> Moni, L.; Ciogli, A.; Acquarica, I.D.; Dondoni, A.; Gasparrini, F.; Marra, A. *Chem. Eur. J*. **2010**, 16, 5712-5722.
- <sup>12</sup> Jian, G.Q.; Liu, Y.X.; He, X.W.; Chen, L.X.; Zhang, Y.K. *Nanoscale*, **2012**, 4, 6336-6342.
- <sup>13</sup> Rampino, A.; Borgogna, M.; Blasi, P.; Bellich, B.; Cesàro, A. *Int J Pharm*. **2013**, doi: 10.1016/j.ijpharm.2013.07.034.
- <sup>14</sup> Shelma, R.; Sharma, C.P. *J Biomed Nanotechnol*. **2013**, (1), 129-138.
- <sup>15</sup> Elsaid, N.; Jackson, T.L.; Gunic, M.; Somavarapu, S. *Invest Ophthalmol Vis Sci*. **2012**, (13), 8105-8111.

- 
- <sup>16</sup> Nagpure, A.; Choudhar, B.; Gupta, R.K. *Crit Rev Biotechnol*. **2014**, 34(3): 215-232.
- <sup>17</sup> Lü, Z.; Zhang, P.; Jia, L. *J. Chromatography A*, **2010**, 1217, 4958-4964
- <sup>18</sup> Monoclonal Antibody Network: [www.mabnet.ca](http://www.mabnet.ca)
- <sup>19</sup> Zhang, J.; Liu, X.; Bell, A.; To, R.; Baral, T.N.; Azizi, A.; Li, J.; Cass, B.; Durocher, Y. *Protein Expr Purif*. **2009**, 65(1):77-82.
- <sup>20</sup> TMT™ Mass tagging Kits and Reagents: <http://www.piercenet.com/instructions/2162073.pdf>
- <sup>21</sup> EMD MILLIPORE [http://www.emdmillipore.com/life-science-research/proteoextract-glycopeptide-enrichment-kit/EMD\\_BIO-72103/p\\_xdCb.s1ORVMAAAEjpxp9.zLX](http://www.emdmillipore.com/life-science-research/proteoextract-glycopeptide-enrichment-kit/EMD_BIO-72103/p_xdCb.s1ORVMAAAEjpxp9.zLX)
- <sup>22</sup> Krokhin, O.; Ens, W.; Standing, K.G.; Wilkins, J.; Perreault, H. *Rapid Commun Mass Spectrom*. **2004**;18(18):2020-30.
- <sup>23</sup> Yin, X.; Bern, M.; Xing, Q.; Ho, J.; Viner, R.; Mayr, M. *Mol Cell Proteomics*. **2013**, 12, 956-978.
- <sup>24</sup> Zou, X.; Liu, D.; Zhong, L.; Yang, B.; Lou, Y.; Yin, Y. *Carbohydrate Polymers*. **2012**, 90, 799-804.
- <sup>25</sup> Dayon, L.; Hainard, A.; Licker, V.; Turck, N.; Kuhn, K.; Hochstrasser, D.F.; Burkhard, P.R.; Sanchez, J.C. *Anal. Chem*. **2008**, 80, 2921–2931
- <sup>26</sup> Bodnar, E.D.; Perreault, H. *Anal. Chem*. **2013**, 85(22), 10895-903.
- <sup>27</sup> Snovidá, S.I.; Rak-Banville, J.M.; Perreault, H. *Jam Soc Mass Spectrom.* **2008**, 19(8), 1138-1146.
- <sup>28</sup> Snovidá, S.I.; Chen, V.C.; Perreault, H. *Anal Chem*. **2006**, 78(24), 8561-8568.
- <sup>29</sup> Snovidá, S.I.; Chen, V.C.; Krokhin, O.; Perreault, H. *Anal. Chem*. **2006**, 78(18), 6556-6563.
- <sup>30</sup> Thaysen-Andersen, M.; Myslning, S.; Højrup, P. *Anal Chem*. **2009**, 81(10):3933-43.
- <sup>31</sup> Stadlmann, J.; Weber, A.; Pabst, M.; Anderle, H.; Kunert, R.; Ehrlich, H.J.; Peter Schwarz, H.; Altmann, F. *Proteomics*. **2009**, 9: 4143–4153.

- 
- <sup>32</sup> Böhm, S.; Schwab, I.; Lux, A.; Nimmerjahn, F. *Semin Immunopathol.* **2012**, 34(3):443-53.
- <sup>33</sup> Wohlgemuth, J.; Karas, M.; Eichhorn, T.; Hendriks, R.; Andrecht, S. *Anal Biochem.* **2009**, 395(2), 178-188.
- <sup>34</sup> Ji, Y.; Xiong, Z.; Huang, G.; Liu, J.; Zhang, Z.; Liu, Z.; Ou, J.; Ye, M.; Zou, H. *Analyst.* 2014 Aug 11. [Epub ahead of print]
- <sup>35</sup> Huang, G.; Sun, Z.; Qin, H.; Zhao, L.; Xiong, Z.; Peng, X.; Ou, J.; Zou, H. *Analyst.* **2014**, 139(9):2199-206.
- <sup>36</sup> Takakura, D.; Harazono, A.; Hashii, N.; Kawasaki, N. *J Proteomics.* **2014**, 101:17-30.
- <sup>37</sup> Selman, M.H.; Hemayatkar, M.; Deelder, A.M.; Wuhrer, M. *Anal Chem.* **2011**, 83(7):2492-9.

## **Chapter 5 – Metabolic Glycan Engineering for the Recovery and Analysis of Sialic Acids**

## 5.1 Authors Contributions

Edward D. Bodnar is responsible for the design of this experiment, including the synthesis of the sugar precursor based on a published method, mass spectrometric analysis and interpretation while under the guidance of Dr. H. Perreault. Céline Raymond was responsible for cell culturing and monitoring for monoclonal antibodies production using the modified azido sugar while under the guidance of Dr. Y. Durocher. Edward D. Bodnar was responsible for the draft of this chapter, while Dr. Y. Durocher, Céline Raymond and Dr. H. Perreault all contributed to its final version.



## 5.2 Abstract

Metabolic engineering of glycans present on antibodies and other glycoproteins is becoming an interesting research area for improving our understanding of the glycome. With knowledge of the sialic acid biosynthetic pathways, the experiments described in this report involved the addition of a synthesized azido-mannosamine sugar into cell culture media and evaluation of downstream expression as azido-sialic acid. This unique bioorthogonal sugar has the potential for a variety of 'click-chemistry' reactions through the azide linkage, which allow for it to be isolated and quantified given the choice of label. In this report, mass spectrometry was used to investigate and optimize the cellular absorption of peracetylated *N*-azidoacetylmannosamine (Ac<sub>4</sub>ManNAz) to form *N*-azidoacetylneuraminic acid (SiaNAz) in a CHO cell line transiently expressing a double mutant Trastuzumab (TZMm2), human galactosyltransferase 1 (GT) and human  $\alpha$ -2,6-sialyltransferase (ST6). This *in vivo* approach is compared to *in vitro* enzymatic addition SiaNAz onto TZMm2 using soluble  $\beta$ -galactosamide  $\alpha$ -2,6-sialyltransferase 1 and CMP-SiaNAz as donor. The *in vivo* results suggest that for this mAb, concentrations above 100  $\mu$ M of Ac<sub>4</sub>ManNAz are necessary to allow for observation of terminal SiaNAz on tryptic peptides of TZMm2 by MALDI mass spectrometry.

## 5.3 Introduction

Glycosylation is a commonly studied post-translational modification (PTM) of proteins known to influence both their physical and functional properties, participating in a variety of biological functions including protein-protein interactions, cell communication, protein folding, and immunogenicity<sup>1,2</sup>. Recently, glyco-engineering of therapeutic monoclonal antibodies (Mabs) based on the immunoglobulin G (IgG) structure has become of interest and as a result, nearly 30 Mabs are currently available on the market<sup>3</sup>. Many functional roles of mAbs can be directly correlated to the specific glycan structures present in the Fc domain. Some examples include the absence of core fucosylation for enhanced FcγRIIIA binding and the presence or absence of sialylation which affects inflammatory properties<sup>4,5,6</sup>. In light of this, new methodologies must be employed for stringent quality control of the Mab.

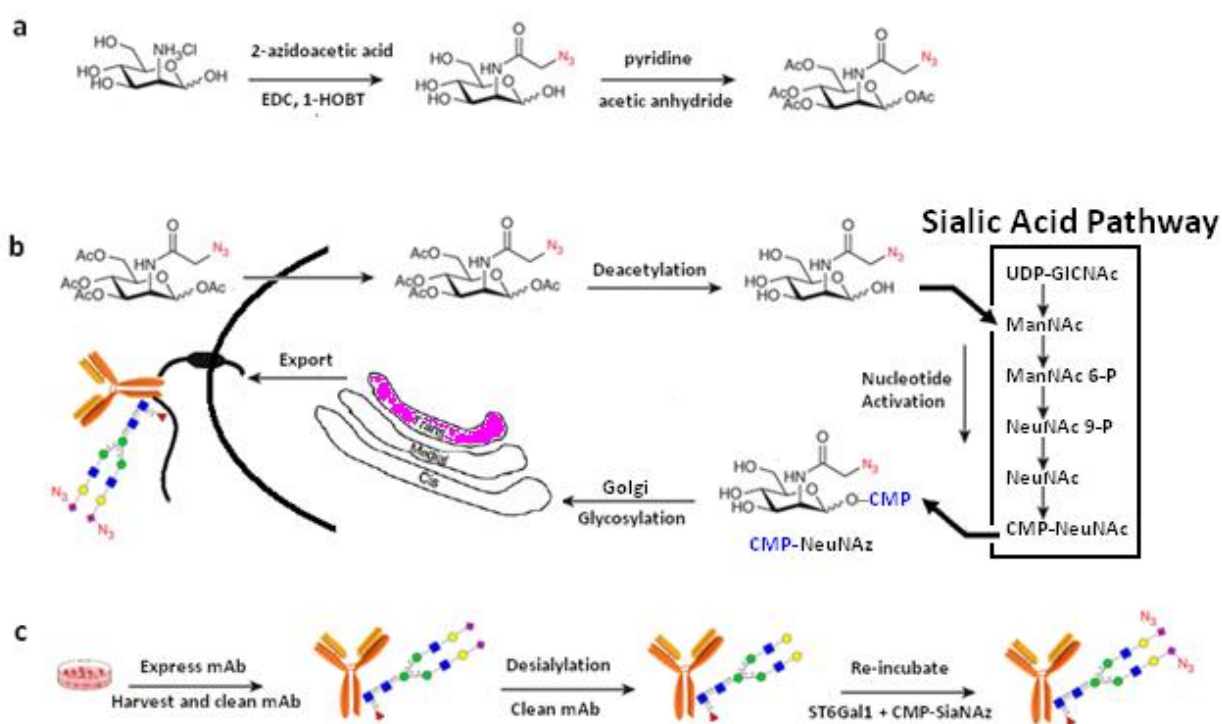
Routinely, mAb glycosylation analysis can be performed based on a “bottom-up” strategy by enzymatically detaching glycans and labeling them with fluorophores that can be detected after separation with high performance liquid chromatography (HPLC)<sup>7</sup>. An alternative and valuable approach consists of studying glycosylation at the glycopeptide level using a variety of robust mass spectrometric (MS) techniques which afford high sensitivity, minimal sample use and extensive characterization<sup>8,9,10</sup>. The need for enrichment of glycopeptides from peptides prior to MS analysis is crucial and can be addressed through a variety of established techniques<sup>11,12,13</sup>. These protocols aim to enrich the bulk of glycopeptides, and are not aimed at enriching specific glycoforms such as those containing fucosylation or sialylation which are often crucial modifiers of mAb efficacy.

One novel approach which can circumvent this issue was designed for the purpose of real-time *in vivo* glycan imaging. This methodology was developed by Bertozzi *et al.* and involves labeling sugar precursors with a bioorthogonal azido group for subsequent metabolic incorporation, which will be specifically detected upon reaction with a fluorescent label through rapid copper free click chemistry<sup>14,15,16</sup>. The sialic acid pathway is of most interest due to many of the aforementioned properties regarding its role in mAbs. As both *N*-acetylated D-mannosamine and D-glucosamine are known to be precursors to sialylation, *N*-azido versions of these sugars have also been incorporated in cell cultures and expressed as azido glycan residues in glycoproteins<sup>17,18</sup>.

This platform serves as a unique approach for investigating the sialylation of a Mab in more detail. Here, we synthesize peracetylated *N*-azidoacetylmannosamine (Ac<sub>4</sub>ManNAz) and investigate its metabolic incorporation onto a double mutant Trastuzumab monoclonal antibody (TZMm2) as *N*-azidoacetylneuraminic acid (SiaNAz) in Chinese hamster ovary (CHO) cells (Figure 5.1)<sup>19</sup>. This mAb has been engineered with two important amino acid substitutions (F241A and F243A). These substitutions have previously been shown to improve terminal galactosylation and sialylation<sup>20</sup>. This approach was further compared to the *in vitro* enzymatic addition of SiaNAz in terminal position using CMP-SiaNAz and soluble  $\beta$ -galactosamide  $\alpha$ -2,6-sialyltransferase 1.

Figure 5.1 - Synthesis & Metabolic Workflow for Introducing an azido functionality onto Monoclonal Antibodies

a) Preparation of azide modified mannosamine (ManNAz) and its peracetylated analogue ( $\text{Ac}_4\text{ManNAz}$ )<sup>21</sup>, which was subsequently b) fed into CHO cells where it was de-acetylated by non-specific esterases, and converted to an azido sialic acid (SiaNAz), then expressed on the monoclonal antibody (mAb). Alternatively, c) T2M2 mAbs were cultured and expressed under normal conditions, then desialylated and reincubated with ST6Gal1 and CMP-SiaNAz to promote sialylation by the bioorthogonal SiaNAz. Adapted from <sup>19,21</sup>.



## 5.4 Experimental

### 5.41 Materials

Triethyl ammonium bicarbonate (TEAB), formic acid (FA), 2-azidoacetic acid (2-AzAc), 1-ethyl-3-(3-dimethylaminopropyl)carbodiimide (EDC), hydroxybenzotriazol (1-HOBt), dichloromethane (DCM), methanol (MeOH), ethyl acetate (EtAc), ethanol (EtOH), deuterated chloroform (CDCl<sub>3</sub>), formic acid (FA) and tri-fluoroacetic acid (TFA) were obtained from Sigma (St. Louis, MO) while mannosamine hydrochloride was purchased from Carbosynth (San Diego, CA). Sequencing grade Trypsin was purchased from Promega (Madison, WA) and C<sub>18</sub> solid phase extraction (SPE) tubes were acquired from Biotage (Charlotte, NC). Biotinylated SNA and ECL lectins were purchased from Vector Laboratories (Burlington, Ontario). All solvents were HPLC-grade and obtained from Sigma (St. Louis, MO, USA). Distilled de-ionized water was obtained using a Milli-Q™ filtration system supplied by a reverse-osmosis feedstock.

### 5.42 Methods

#### 5.421 Preparation of Azidomannosamine

The synthesis of azidomannosamine (ManNAz) was carried out using a previously published protocol<sup>21</sup> (Figure 5.1a). In brief, this involved reacting 2-azidoacetic acid with mannosamine hydrochloride overnight in the presence of 1-HOBt and EDC to produce ManNAz. This product was then cleaned using flash chromatography and eluted with 9:1 dichloromethane:methanol; ManNAz fractions were pooled and dried on a rotary evaporator. To produce the acetylated analogue (Ac<sub>4</sub>ManNAz), ManNAz was re-suspended in dry pyridine and acetic anhydride where

it was left to react for 24h with stirring. Ac<sub>4</sub>ManNAz was next extracted into ethyl acetate and washed with 1 M HCl, followed by saturated sodium bicarbonate and finally saturated sodium chloride. Subsequently, Ac<sub>4</sub>ManNAz was cleaned on flash chromatography eluting with 7:3 hexanes:EtAc. Fractions were pooled, and further cleaned using C<sub>18</sub> HPLC where the desired product eluted with 15-20% ACN. Ac<sub>4</sub>ManNAz was subsequently collected and lyophilized until it became oily. It was then analyzed using <sup>13</sup>C NMR and ESI-MS.

#### **5.422 Plasmids and Proteins**

TZMm2 is a mutated version of Herceptin<sup>®</sup> where F<sub>241</sub> and F<sub>243</sub> are substituted by alanines. Herceptin<sup>®</sup> is a humanized mouse IgG1 used in HER2-breast cancer treatments. The heavy and light chain genes were cloned separately in pTT5 vectors as described elsewhere<sup>22</sup>. The membrane-bound human  $\beta$ 1,4-galactosyltransferase 1 (b4GT1) and galactoside- $\alpha$ 2,6-sialyltransferase 1 (ST6Gal1) were also cloned into pTT5 vectors. GFP was used as a reporter protein to evaluate the transfection efficiency and was cloned into the pTTo vector as described elsewhere<sup>22</sup>.

#### **5.423 Cell Culture and Ac<sub>4</sub>ManNAz incorporation**

The incorporation of Ac<sub>4</sub>ManNAz into Chinese hamster ovary cells stably expressing truncated Epstein-Barr virus Nuclear Antigen-1 (CHO3E7) was essentially performed as described by Laughlin-Bertozzi et al <sup>21</sup>. CHO3E7 cells were grown in suspension in F17 medium supplemented with 4 mM glutamine and 0.1% Kolliphor to a cell density of 1.5 x 10<sup>6</sup> cells/mL (>99% viability) in ventilated flasks (SF) shaken at 120 rpm in a humidified incubator at 37°C with 5% CO<sub>2</sub>. The day of transfection, a solution of 100 mM Ac<sub>4</sub>ManNAz in ethanol was prepared and the required volume to reach 5, 10 , 50, 100, 200  $\mu$ M was introduced in empty

125 mL SF for 20 mL cultures or 5 L glass bottles for 1 L cultures, where the ethanol was allowed to evaporate prior to the addition of the cells. After 6 h, DNA plasmids coding for double mutant trastuzumab (TZMm2), human  $\beta$ -1,4-galactosyltransferase 1(GT), and human  $\alpha$ -2,6-sialyltransferase (ST6) were introduced into cells by transient transfection<sup>23</sup>.

#### **5.424 Transfection**

Linear 25 kDa polyethylenimine (PEIpro, Poly plus Transfection, Illkirch, France) and plasmid DNA solutions were prepared in F17 for a final concentration of 2.5  $\mu$ g/mL of culture and 1  $\mu$ g/mL of culture respectively. The DNA mix was composed of 2% in weight of b4GT1 plasmid, 19% of ST6Gal1 plasmid, 45% of LC plasmid, 30% of HC plasmid and 5% of pTToGFPq. When b4GT1 and ST6Gal1 were not required, the mix comprised 21% of salmon sperm DNA (inert DNA). The solution of PEIpro was added to the DNA solution to form polyplexes, which were added to the cells after 5 min of incubation at room temperature. The transfection was realized 6 h after the cells were put in contact with Ac<sub>4</sub>ManNAz.

#### **5.425 mAb Production**

1 day post-transfection, the cells were fed with peptone TN1 (1% final) to enhance productivity. 6 days post-transfection, the supernatants containing the secreted antibodies were collected and loaded on 2.5 mL or 5 mL MabSelect SuRe columns (GE Healthcare, Mississauga, ON) equilibrated in PBS. The column was washed with PBS and mAbs were eluted with 100 mM citrate buffer pH 3.0. The fractions containing mAbs were pooled and the citrate buffer was exchanged against water on illustra NAP-10 columns (GE Healthcare) for 20 mL cultures or Econo-Pac 10DG columns (Bio-Rad, Mississauga, ON) for 1 L cultures.

#### 5.426 Synthesis of CMP-N-azidoacetylneuraminic acid (CMP-SiaNAz)

ManNAz was synthesized according to the methods described above. In general, starting with this *N*-azido precursor, CMP-SiaNAz was enzymatically prepared using a sialic acid aldolase from *Pasteurella multocida* and CMP-sialic acid synthetases from either *Neisseria meningitidis* or *Campylobacter jejuni*<sup>24,25,26</sup>. Initially, a 19 ml aldolase reaction was performed containing 100 mM Tris pH 8.6, 100 mM pyruvate and 20 mM ManNAz with sufficient quantities of *P. multocida* aldolase to obtain optimal conversion in 24 h at 37 °C. Next, CMP-sialic acid synthetase (CSAS) was added to these 24 h reactions in addition to CTP and MgCl<sub>2</sub>, at 12.7 mM and 63 mM final concentrations, respectively. This 30 ml reaction was left at 37 °C for an additional 1.5 h. The CMP-SiaNAz enzymatic reaction was then passed through an Amicon Ultra-15 (10,000 molecular weight cut-off) filter membrane before purification. The filtered CMP-SiaNAz sample was then diluted 29 fold in water and purified using a HiTrap Q (GE Healthcare) column with a 0-0.25 M ammonium bicarbonate gradient over 20 CV. Quantification of CMP-SiaNAz was determined using the molar extinction coefficient of CMP ( $\epsilon_{260}=7,400$ ). The pure fractions were diluted with water, and NaCl was added to give approximately 3 molar equivalents of NaCl for every mole of CMP-SiaNAz preparation, prior to lyophilization.

#### 5.427 Enzymatic Addition of SiaNAz on TzMm2

TMZm2 was produced in the absence of Ac<sub>4</sub>ManNAc and purified as described above. It was subsequently de-sialylated at 37°C for 20 h with the neuraminidase from *Arthrobacter ureafaciens*. Next, the sample was purified on a Protein A resin in order to eliminate the



neuraminidase and any cleaved sialic acids. Following this, the purified sample was re-incubated with soluble ST6Gal1 and CMP-SiaNAz for 3 days at 37°C, where every 24 h the sample was filtered to remove excess CMP, following which, fresh soluble ST6Gal1 and CMP-SiaNAz were added. Lastly, this mAb was purified on a protein A resin and stored in H<sub>2</sub>O prior to digestion and analysis.

#### **5.428 Preparation & Digestion of Monoclonal Antibodies**

Each intact monoclonal antibody (mAb; 200 µg) was prepared to a final concentration of [50 mM] with TEAB where the Eppendorf™ tube was vortexed until the sample dissolved. As any expressed azide (N<sub>3</sub>) would be susceptible to reduction by dithiothreitol (DTT), the mAb was not reduced nor alkylated. Instead, 4 µg of trypsin were added and the mixture was allowed to react at 37°C for approximately 18 h. To deactivate the trypsin a large volume of acetonitrile (ACN) + TFA was added and this mixture was vortexed.

#### **5.429 HPLC Separation of Glycopeptides**

Separation of glycopeptides was performed using a previously reported method<sup>27</sup> using a Waters 1525 binary pump equipped with a Waters 2707 autosampler and a Waters 2998 photodiode array detector. In brief, this involved equilibrating the column (Vydac 218 TP54 Protein & Peptide C18 analytical column; Separation Group, Hesperia, Ca, USA), with 95:5 H<sub>2</sub>O:ACN + 0.1%TFA, for roughly 10 min. After injection of the sample (25 µL), the gradient that was used is as follows: 95:5 H<sub>2</sub>O:ACN + 0.1%TFA for (5 min), then increased to 90:10 H<sub>2</sub>O:ACN + 0.1%TFA (over 5 min), and finally increased to 70:30 H<sub>2</sub>O:ACN + 0.1%TFA (over 10 min). Prior to injection, the column was cleaned for 10 min using 50:50 H<sub>2</sub>O:ACN + 0.1%TFA, 10 min using

5:95 H<sub>2</sub>O:ACN + 0.1%TFA, and finally re-equilibrated with 95:5 H<sub>2</sub>O:ACN + 0.1%TFA, with a flow rate of 0.7 ml/min. Fractions were collected manually, pooled, and dried completely prior to further analysis.

#### **5.430 Mass Spectrometric Analysis**

For MALDI-MS and MS/MS analysis an UltrafleXtreme (Bruker Daltonics, Germany) was used. Unless otherwise stated this instrument was utilized in positive ion mode with a matrix of 2,5 dihydroxybenzoic acid (2,5 DHB) and a *m/z* range of 700-4500. Each sample was prepared whereby 0.75 µL of matrix was mixed with 0.75 µL of sample and then allowed to dry on target before loading it into the MS.

ESI-MS analysis of synthesized Ac<sub>4</sub>ManNAz was performed on a Varian 500 Ion Trap-MS (Santa Clara, CA, USA). This sample was dissolved in acetonitrile + 0.1% formic acid for a direct injection in positive mode with a scanning range of 200-2000 *m/z*. Loading RF was set to 54% and the capillary voltage was set to 80.0 V.

#### **5.431 Nuclear Magnetic Resonance Analysis**

The <sup>13</sup>C NMR spectrum of the purified Ac<sub>4</sub>ManAz was performed on a 300MHz Bruker AC 300 (Fällenden, Switzerland) in CDCl<sub>3</sub> at the University of Manitoba (Department of Chemistry). This spectrum was compared to a theoretical spectrum generated using the Advanced Chemistry Development (ADC) (Toronto, Canada) program, Algorithm Version: v12.1.0.33936<sup>28</sup>.

## 5.5 Results & Discussion

### *Enzymatic addition of CMP-SiaNAz*

An in vitro method was first investigated for the production of azido glycans on TZMm2 that was produced in CHO cells without labeling. It consisted of producing high levels of sialylated antibodies under normal metabolic expression conditions, then desialylating the sample, cleaning it, and re-attaching SiaNAz from a donor (CMP-SiaNAz), under the action of a sialyltransferase. This was seen as an efficient way of generating a control sample containing SiaNAz. CHO cells were chosen as they are a well-established cell line for monoclonal antibody production<sup>29,30</sup> which contains the same essential metabolic features as humans, yet demonstrate different features in their glycome<sup>1</sup>. CHO cells are not known to express *N*-acetylglucosaminyltransferase III (Gn TIII), the enzyme responsible for producing a bisecting *N*-acetylglucosamine, which consecutively, is known to inhibit core fucosylation and ultimately increase FcγRIIIa binding<sup>31</sup>. Additionally, CHO cells have the ability to express both *N*-acetylneuraminic acid (Neu5Ac) and low levels of the potentially immunogenic *N*-glycolylneuraminic acid (Neu5Gc)<sup>32</sup>. For these reasons, CHO cells are a suitable choice for exploring SiaNAz expression, but require strong quality control in regards to protein glycosylation.

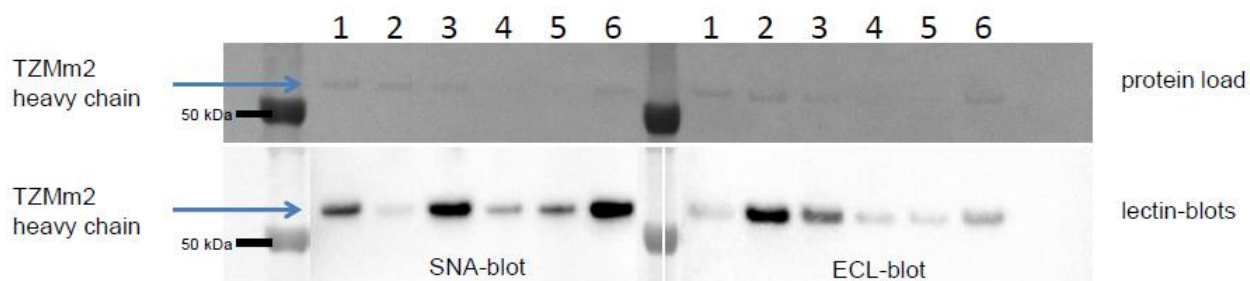
### *Monitoring sialylation with lectins*

To monitor levels of sialylation using this approach, lectin-blots were performed using two biotinylated lectins: *sambucus nigra* (SNA) and *erythrina cristagalli* lectins (ECL), specific for binding α2,6 sialic acids<sup>33</sup> and terminal galactoses respectively<sup>34</sup>. Production of TZMm2 yielded high levels of sialylation, as observed through the comparison of SNA and ECL lectin stains

(Figure 5.2). Next, TZMm2 was desialylated and cleaned to prepare it for the addition of CMP-SiaNAz. Figure 5.2-2 shows the expected opposite trend, with a dark band on the ECL blot but only a faint band on the SNA blot. This suggests that the mAb was desialylated. At this stage, the desialylated mAb was incubated with CMP-SiaNAz for over three days, and aliquots from production were compared (Figure 5.2-3,4,5). There was a strong staining with the SNA lectin after 24 h, and an even more noticeable difference between SNA and ECL after cleaning TZMm2 on a Protein A column (Figure 5.2-6). Since the purified and desialylated TZMm2 was incubated solely with CMP-SiaNAz, this suggests that the mAb should contain no endogenous neuraminic acids.

#### Figure 5.2 – Monitoring sialylation using Western Blot analysis

Comparison of SNA lectin known to bind  $\alpha$ 2,6 sialic acids (bottom left), to ECL lectin known to bind terminal galactose (bottom right), taken after TZMm2 production (1), after desialylation of TZMm2 (2), after 24 h of incubation with CMP-SiaNAz (3), 48 h of CMP-SiaNAz (4), 72 h of CMP-SiaNAz (5), and finally after Protein A purification (6).



#### *Isolating glycopeptides*

A sample of TZMm2 corresponding to that of Figure 5.2 lane 1 (i.e. not sialylated with azido sialic acids) was first digested with trypsin, followed by isolation of glycopeptides, which produced the spectrum of Figure 5.3, for reference. TZMm2 is an antibody based on the

structure of IgG and also contains one site of glycosylation in the Fc region at Asn<sub>297</sub>.

Glycoforms of EEQYNSTYR that characterize the Fc region are core fucosylated biantennary G0F, G1F, G2F, and G2FS1<sup>22</sup> as seen in Figure 5.3. In azide-modified TZMm2, if azido residues are successfully incorporated, predicted mass shifts corresponding to +42.01 *m/z* will be observed and this can be further verified using tandem MS. Figure 5.4 shows the structures of a) N-acetyl and b) N-azido neuraminic acid.

Figure 5.3 – Mass Spectrum of Commonly Observed Fc typtic Glycopeptides from TZMm2

MALDI-ToF spectrum of glycopeptides from TZMm2 collected in positive mode after HPLC separation. This depicts four commonly observed glycopeptides G0F, G1F, G2F, G2FS1.

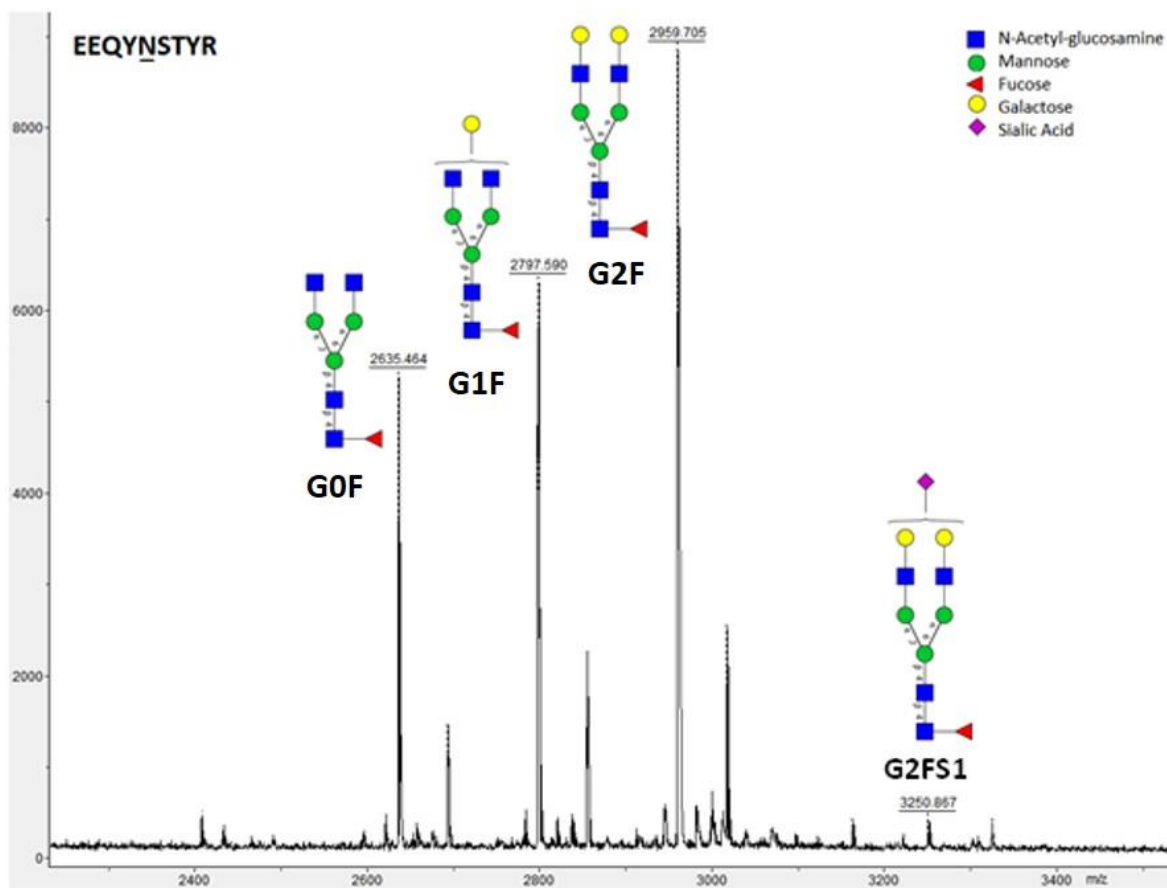
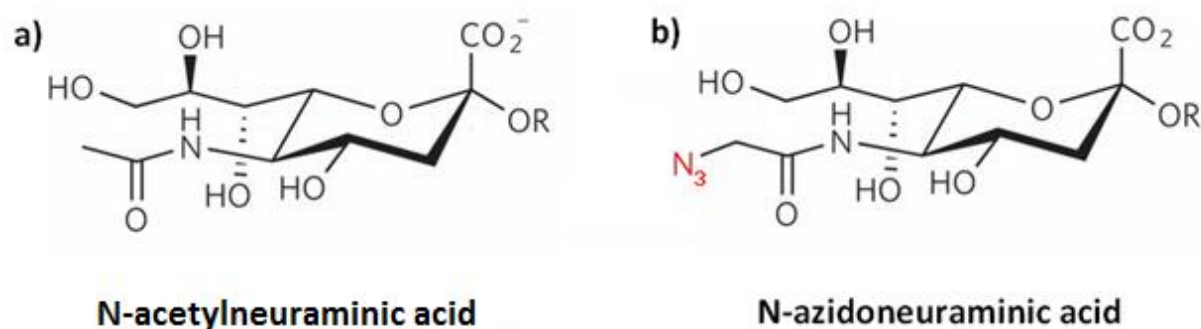


Figure 5.4 – N-acetyl and N-azidoneuraminic acids

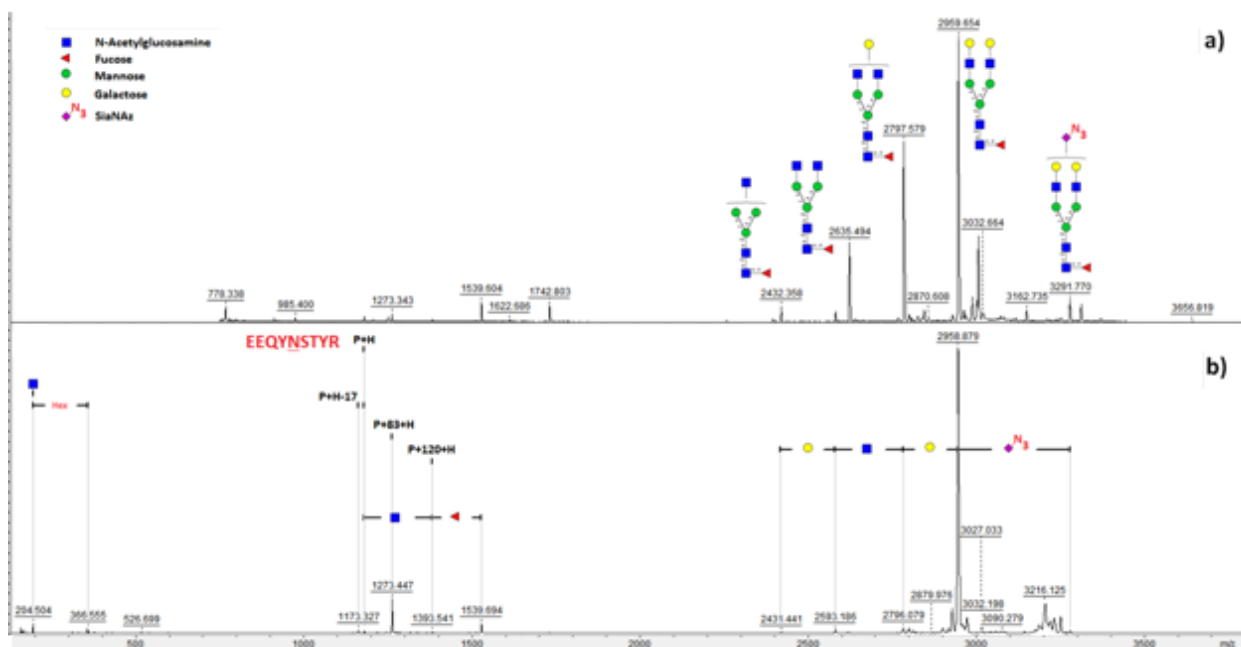


#### *MS Analysis of Enzymatically attached SiaNAz*

In Figure 5.5a), the spectrum of isolated glycopeptides from modified TZMm2 indeed shows differences of +42  $m/z$  on sialylated glycoforms of EEQYNSTYR. No endogenous sialylated glycopeptides were detected. Azido analogues were profiled manually by tabulating potential azido shifts. One peak at 3291.770  $m/z$ , indicating an azide addition to G1FS was subjected to MS<sup>2</sup> analysis (Figure 5.5b)). Upon MS/MS fragmentation, these precursors easily lost the azido-sialic acid moiety leading to product ions at 2959  $m/z$ . This was a good indication that the modification was located on sialic acid and not elsewhere in the glycopeptide molecule, as  $m/z$  2959 ions correspond to the G2F asialo glycoform. At  $m/z$  1273, a <sup>1,3</sup>GlcNAc cross ring cleavage ion peak was observed, which constitutes the marker peak “peptide+83+H”<sup>35</sup>. Other fragment ions observed were namely the GlcNAc<sup>+</sup> ( $m/z$  204) and GlcNAc-Hex<sup>+</sup> ( $m/z$  366) marker ions. Experiments conducted using specific lectins and MALDI-TOF mass spectrometry showed a successful incorporation of SiaNAz into TZMm2 antibodies. The product generated and analyzed through these steps can therefore serve as a benchmark for the second portion of this investigation.

Figure 5.5 – MALDI-ToF and MALDI-ToF/ToF spectra of SiaNAz introduced enzymatically

Spectra of SiaNAz introduced enzymatically: (a) MALDI-ToF spectrum of glycopeptides isolated from azido modified TZMm2. b) MALDI-ToF/ToF tandem spectrum of parents ions at  $m/z$  3291.770, corresponding to G2FSiaNAz1. P denotes the mass of the bare peptide.



### *Synthesis and characterization of Ac<sub>4</sub>ManNAz*

In an alternative approach, Ac<sub>4</sub>ManNAz was synthesized as a sialic acid biosynthetic pathway precursor for azide incorporation. Ac<sub>4</sub>ManNAz was analyzed by <sup>13</sup>C-NMR and ESI-MS (Figure 5.6 and Figure 5.7) prior to metabolic expression. With respect to the <sup>13</sup>C-NMR data, a theoretical spectrum was generated and compared to that of the experimental sample. Similarities between the spectra suggest that the product is fully acetylated and furthermore contains the azide as evident by the distinct shift occurring on the carbon next to the azide (~52 ppm). Moreover, an ESI-MS spectrum showed a pure product ionizing as both Ac<sub>4</sub>ManNAz + Na<sup>+</sup> and Ac<sub>4</sub>ManNAz + K<sup>+</sup> adducts.

Figure 5.6 –  $^{13}\text{C}$  NMR spectrum of synthesized  $\text{Ac}_4\text{ManNAz}$  acquired on a 400mHZ NMR compared to a theoretically generated spectrum

$^{13}\text{C}$  NMR spectra of  $\text{Ac}_4\text{ManNAz}$ . A) Theoretical carbon shifts of  $\text{Ac}_4\text{ManNAz}$  compared to the B) experimental sample in  $\text{CDCl}_3$ , acquired on a 400 MHz NMR. Clusters of peaks at  $\sim 20$  ppm,  $\sim 52$  ppm,  $\sim 91$  ppm, and  $\sim 169$  ppm are observed in both spectra. Positions of carbon atoms are labeled for identification in the theoretical spectrum.

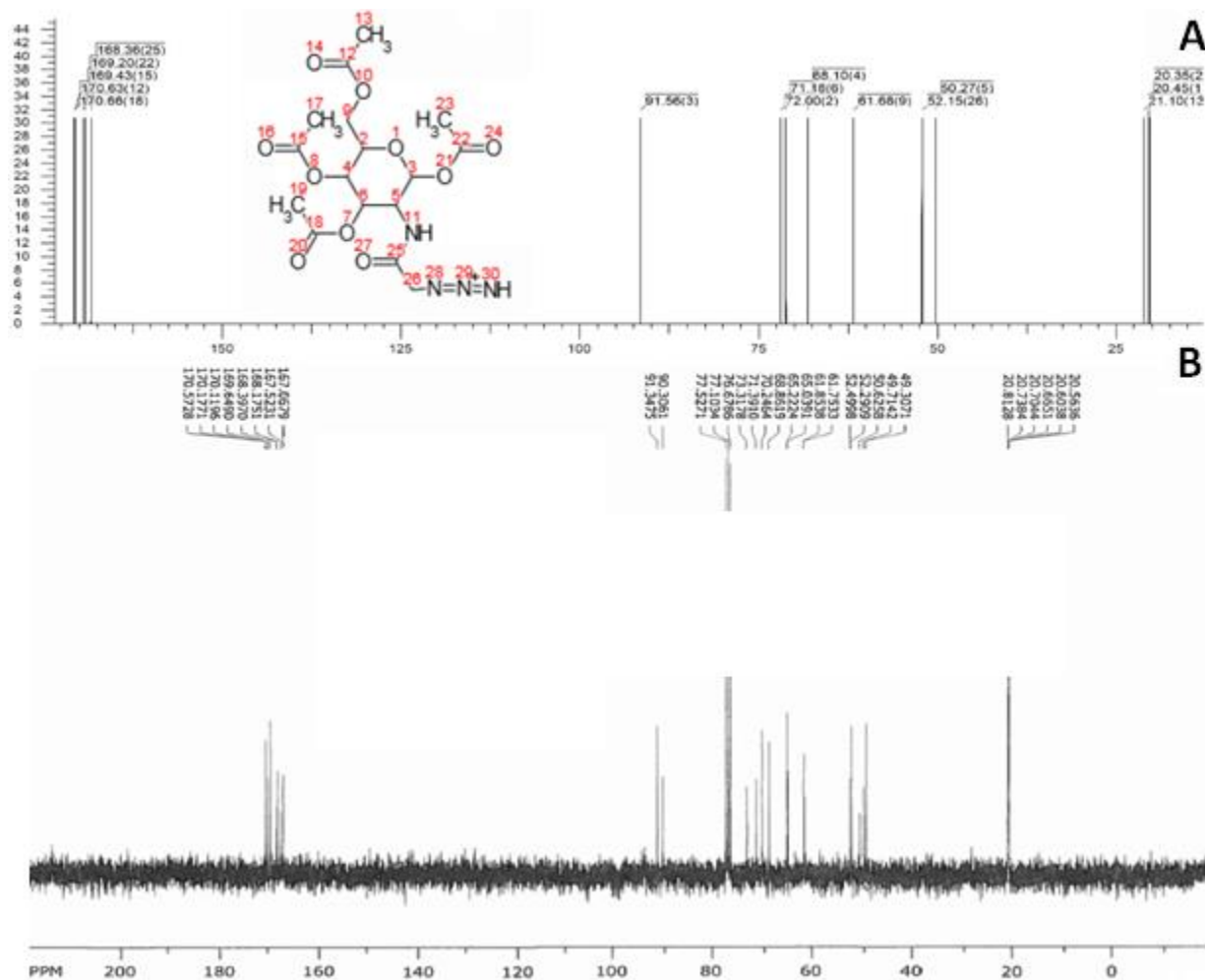
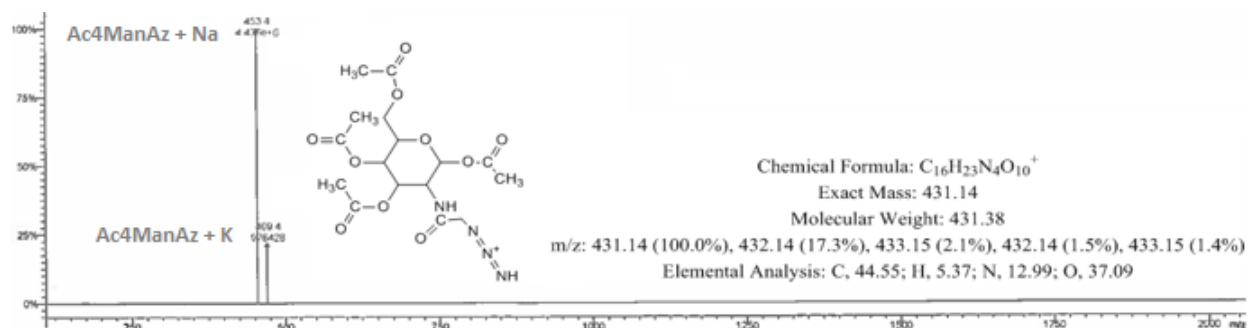




Figure 5.7 – ESI-MS spectrum of synthesized Ac<sub>4</sub>ManNAz precursor

Direct injection ESI-MS spectrum of synthesized Ac<sub>4</sub>ManNAz precursor, showing ionization with sodium and potassium adducts at 453.4 and 469.4 *m/z*, respectively.

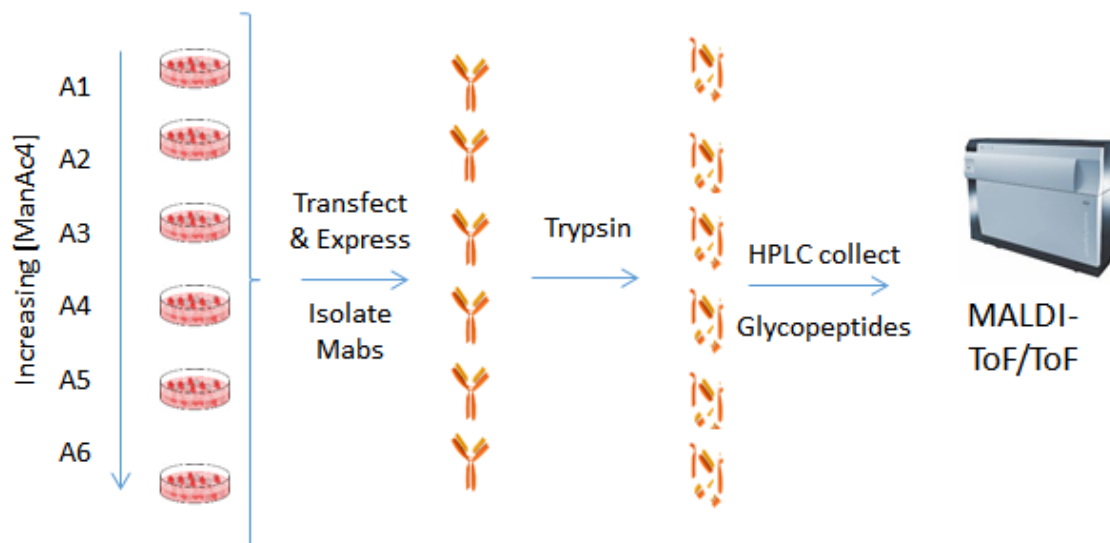


### *Metabolic incorporation of Ac<sub>4</sub>ManNAz*

In order to determine the amount of peracetylated ManNAz necessary for detectable metabolic incorporation of *N*-azidoacetylneuraminic acid (SiaNAz) in mAbs, increasing concentrations of Ac<sub>4</sub>ManNAz (0, 5, 10, 50, 100, 250 μM) were added to six flasks of CHO cells transfected with plasmids expressing double mutant trastuzumab (TZMm2), β-1,4-galactosyltransferase 1 (GT), and human α-2,6-sialyltransferase 1 (Figure 5.8). Each cell batch (A1-A6) was incubated with increasing amounts of Ac<sub>4</sub>ManNAz to determine the metabolic expression of SiaNAz. After mAb purification and tryptic digestion, glycopeptides were isolated on RP-HPLC, and these fractions were subjected to MALDI-MS analysis.

### Figure 5.8 - Workflow to Compare SiaNAz expression

Workflow to Compare SiaNAz expression: CHO cell cultures were fed increasing amounts of Ac<sub>4</sub>ManNAz. These samples were worked up independently, by digesting each mAb and isolating its glycopeptides, which were subsequently analyzed using MALDI-ToF/ToF for differences in azide expression.



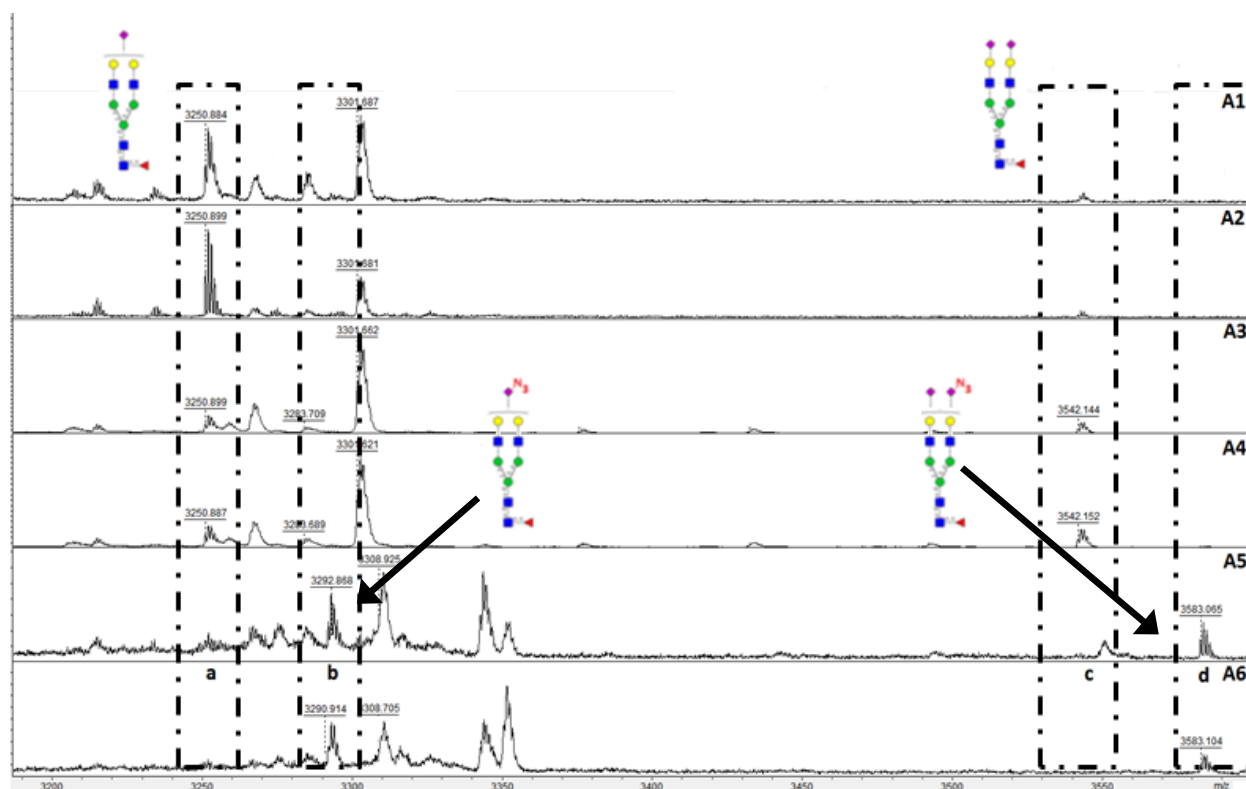
### MS Analysis of metabolically cultured SiaNAz mAbs

Figure 5.9 shows the MALDI-ToF spectra obtained for all six experiments (top: no Ac<sub>4</sub>ManNAz precursor, bottom 250  $\mu$ M Ac<sub>4</sub>ManNAz precursor). In a),  $m/z$  3250 peaks correspond to the singly sialylated glycopeptides EEQYNSTYR (G2FS1), where no incorporation of Ac<sub>4</sub>ManNAz is observed in samples A1-A4. This trend changes at sample A5, in which 100  $\mu$ M of Ac<sub>4</sub>ManNAz was introduced, producing a +42  $m/z$  shift in G2FS1 as indicated by b), where peaks at  $m/z$  3292 represent G2FSiaNAz1, a glycopeptide containing a single SiaNAz glycan. This same trend is observable for the disialylated glycopeptide. In c),  $m/z$  3542 peaks correspond to G2FS2, where ions highlighted in d) show the presence of G2FS1SiaNAz1. This suggests that concentrations near 100  $\mu$ M of Ac<sub>4</sub>ManNAz are necessary to express SiaNAz analogues, without

however producing the transformation of both sialic acids, which would have led to the glycopeptide G2FSiaNAz2.

Figure 5.9 – MALDI-ToF spectra of glycopeptides from TZMm2, expressed in the presence of Ac<sub>4</sub>ManNAz in increasing concentration

MALDI-ToF spectra of glycopeptides from TZMm2, expressed in the presence of Ac<sub>4</sub>ManNAz in increasing concentration. Six samples (A1-A6) were grown with increasing concentrations of Ac<sub>4</sub>ManNAz [0, 10, 20, 50, 100, 250 mM]. Four areas are highlighted containing  $\alpha$ -2,6 forms of sialylation: (a) G2FS1 containing one underivatized sialic acid, (b) G2FSiaNAz1 containing one SiaNAz, (c) G2FS2 containing two underivatized sialic acids and (d) G2FS1SiaNAz1 containing one underivatized sialic acid and one derivatized SiaNAz.



The results obtained by this experiment reconfirm that SiaNAz expression by CHO cells is achievable, however expression is limited<sup>36,37</sup>. Through the comparison of data presented in Chapter 2 and the data generated by this experiment, similar expression of the G0F, G1F and G2F glycoforms were observed, while lower amounts of sialylation were present when using the modified precursor. Reasons for this may include lower tolerance for the bioorthogonal compound by the sialyltransferases, or even lower tolerance by the CMP-sialic acid golgi transporter for CMP-SiaNAz. Moreover, the endogenous form of ManNAc may compete with ManNAz, limiting the expression of SiaNAz. Also, the enzymes involved in the conversion of ManNAz to SiaNAz may be less tolerant to azide analogues<sup>38</sup>. For example, the ManNAc 6-kinase required to convert the ManNAc taken up by cells to ManNAc-6-phosphate has been reported to be rate-limiting with various ManNAc analogs<sup>39</sup>. Without this 6-phosphorylation, the ManNAz accumulating within the cytosol will not be able to proceed in the next sialic acid biosynthetic step, which is condensation with pyruvate to form 9-phosphorylated-SiaNAz. Subsequent steps involve the actions of a phosphatase to form SiaNAz, transport to the nucleus and CMP-activation to CMP-SiaNAz by the CMP-sialic acid synthetase, transport across the golgi membrane by a specific transporter and various sialyltransferases that will decorate glycan chains with the SiaNAz. As can be appreciated, there are several potential 'roadblocks' for efficient SiaNAz expression.

In original experiments of this kind using ManNAz (unacetylated) as a precursor, it was estimated that around 30-50 mM, or approximately  $10^6$  precursors were required to express one SiaNAz molecule on the cell surface<sup>40</sup>. At that stage cell permeability was considered an important factor in this low yield, ManNAz precursors were peracetylated into Ac<sub>4</sub>ManNAz.

More recently, *O*-butanoyl derivatization was used instead of acetylation, and this resulted the need of ~5x lower precursor concentrations (12-25  $\mu\text{M}$ ; 1,3,4-*O*-Bu<sub>3</sub> ManNAz). Under these conditions, no apoptotic cell death with precursor concentrations up to 400  $\mu\text{M}$  was observed<sup>41</sup>. However, neither approach has yet to yield glycoforms which solely contain azido analogues, therefore quantitative studies using a “click-chemistry” approach may not be feasible.

The metabolic expression of SiaNAz in recombinant glycoproteins has been reported previously<sup>38</sup>. Here, Bertozzi *et al.* explored whether SiaNAz would perturb sialylation in a variety of cell lines by quantifying sialylation through enzymatic de-sialylation at the glycan level. This approach however forfeits sialic acid linkage information, such as the implication of SiaNAz on  $\alpha$ -2,3 or  $\alpha$ -2,6 branching, site specific heterogeneity, as well as the occurrence of singly or doubly sialylated glycoforms as in the case of recombinant IgG's. A similar approach using *N*-azidoacetyl galactosamine (GalNAz) has also been reported by Wu *et al.*<sup>42</sup>, where enrichment at the glycoprotein level occurs through “click chemistry” to a biotin tag which is later enriched by NeutrAvidin beads. This approach however also involved deglycosylation and analysis at the glycan level.

The method we present takes into account these limitations by analyzing samples at the glycopeptide level. To our knowledge it is the first MS based systematic concentration dependence study of Ac<sub>4</sub>ManNAz metabolism into SiaNAz which uses mass spectrometry as the main detection method. Moreover, enzymatic addition of SiaNAz to the TZMm2 construct demonstrated two important conclusions: noticeably higher levels of SiaNAz expression and substitution of natural sialic acids. Since reduction and alkylation were not performed prior to protein digestion, the potential for missed cleavages is noted, however none was observed in

this study around the mAb's Fc portion. No alternative forms of sialylation including *N*-glycolylneuraminic acid were observed.

## 5.6 Conclusion

The results from these preliminary experiments have demonstrated that it is possible to introduce SiaNAz into a monoclonal antibody (mAb) both metabolically and enzymatically. Using metabolic expression, azide linkages in SiaNAz were incorporated in both mono and disialylated species of TZMm2 mAb. In contrast, only singly sialylated glycoforms (G2FSiaNAz1) were found to contain an azide linkage resulting from enzymatic addition, and no native sialic acids were observed. This study presents a lucrative approach to studying the sialylation of this mAb in more detail. Future work will investigate if SiaNAz incorporation results in a bias for  $\alpha$ -2,3 or  $\alpha$ -2,6 linkages because of donor preferences by the corresponding sialyltransferases. Furthermore, we are currently testing higher metabolic concentrations of Ac<sub>4</sub>ManNAz to determine the limit of SiaNAz expression in the case of this construct while performing cell viability measurements. "Click" labeling experiments will also be attempted on samples containing azido-glycopeptide. This will be useful for the capture and isolation of those species by a "pull down" process, enabling site specific sialylation analysis.

## 5.7 Acknowledgements

Dr. Mike Butler (Microbiology, University of Manitoba) as well as the Monoclonal Antibody Network (MabNet) are thanked for supplying monoclonal antibodies as models for analysis. Dr. Miloslav Sailer (Chemistry, University of Manitoba) is thanked for acquiring NMR spectra. We thank Dr Michel Gilbert and Marie-France Goneau for the synthesis of CMP-SiaNAz. Funding agencies including the Monoclonal Antibody Network (MabNet; Winnipeg), as well the National Sciences and Engineering Research Council (NSERC), Canadian Foundation for Innovation (CFI) and Manitoba Research & Innovation Fund are thanked for their funding. This is NRC publication #53294.

## 5.8 References

---

- <sup>1</sup> Butler, M.; Spearman, M. *Current opinion in biotechnology*. **2014**, 30, 107-12.
- <sup>2</sup> Ko, K.; Ahn, M. H.; Song, M.; Choo, Y. K.; Kim, H. S.; Ko, K.; Joung, H. *Molecules and cells* **2008**, 25, 494-503.
- <sup>3</sup> Reichert J.M. *MAbs*. **2012**. 4(3): 413–415.
- <sup>4</sup> Gornik, O.; Pavic, T.; Lauc, G. *Biochim Biophys Acta*. **2012**. 1820, 1318-1326.
- <sup>5</sup> Kaneko, Y.; Nimmerjahn, F.; Ravetch, J.V. *Science*. **2006**. 313, 670-673.
- <sup>6</sup> Iida, S.; Kuni-Kamochi, R.; Mori, K.; Misaka, H.; Inoue, M.; Okazaki, A.; Shitara, K.; Satoh, M. *BMC Cancer*. **2009**. 9, 7.
- <sup>7</sup> Uçaktürk, E. *J Sep Sci*. **2012**. 35(3), 341-350.
- <sup>8</sup> Furlong, M.T.; Titsch, C.; Xu, W.; Jiang, H.; Jemal, M.; Zeng, J. *Bioanalysis*. **2014**. [ahead of print]
- <sup>9</sup> Shah, B.; Jiang, X.G.; Chen, L.; Zhang, Z. *J Am Soc Mass Spectrom*. **2014**. 25(6), 999-1011.
- <sup>10</sup> Stadlmann, J.; Pabst, M.; Kolarich, D.; Kunert, R.; Altmann, F. *Proteomics*. **2008**. 8(14), 2858-2871.
- <sup>11</sup> Bodnar, E.D.; Perreault, H. *Anal. Chem*. **2013**, 85(22): 10895-10903
- <sup>12</sup> Snovidá, S.I.; Bodnar, E.D.; Saba, J.; Viner, R.; Perreault, H. *Carbohydrate Research*, **2010**. 345(6), 792-801.
- <sup>13</sup> Tajiri, M.; Yoshida, S.; Wada, Y. *Glycobiology*. **2005**. 15(12), 1332-1340.
- <sup>14</sup> Laughlin, S.T.; Bertozzi, C.R. *Proc. Natl. Acad. Sci. USA*. **2009**. 106(1), 12-17.
- <sup>15</sup> Dehnert, K.W.; Baskin, J.M.; Laughlin, S.T.; Beahm, B.J.; Naidu, N.N.; Amacher, S.L.; Bertozzi, C.R. *ChemBiochem*. **2012**. 13(3), 353-357.



- 
- <sup>16</sup> Baskin, J.M.; Dehnert, K.W.; Laughlin, S.T.; Amacher, S.L.; Bertozzi, C.R. *Proc. Natl. Acad. Sci. USA*. **2010**. 107(23),10360-10365.
- <sup>17</sup> Keppler, O.T.; Stehling, P.; Herrmann, M.; Kayser, H.; Grunow, D.; Reutter, W.; Pawlita, M. *J. Bio. Chem.* **1995**. 270, 1308-1314.
- <sup>18</sup> Charter, N.W.; Mahal, L.K.; Koshland, D.E.; Bertozzi, C.R. *Glycobiology*. **2000**. 10(10), 1049-1056.
- <sup>19</sup> Rochefort, M. M.; Girgis, M. D.; Ankeny, J. S.; Tomlinson, J. S. *Glycobiology*. **2014**, 24, 62-9.
- <sup>20</sup> Lund, J.; Takahashi, N.; Pound, J.D.; Goodall, M.; Jefferis, R.; *J Immunol*. 1996. 1;157(11):4963-4969.
- <sup>21</sup> Laughlin, S.T.; Bertozzi, C.R. *Nat Protoc*. 2007. 2, 2930-2944.
- <sup>22</sup> Raymond, C.; Robotham, A.; Kelly, J.; Lattová, E.; Perreault., H.; Durocher, Y. **2012**. Production of highly sialylated monoclonal antibodies , p. 397. *In* Stefana Petrescu (ed.), Glycosylation. InTech.
- <sup>23</sup> Zhang, J.; Liu, X.; Bell, A.; To, R.; Nath, T.; Azizi, A.; Li, J.; Cass, B.; Durocher, Y. *Protein Expression and Purification*. **2009**. 65, 77-82.
- <sup>24</sup> Guerry, P.; Ewing, C. P.; Hickey, T. E.; Prendergast, M. M.; Moran, A. P. *Infect Immun*. **2000**, 68, 6656-62.
- <sup>25</sup> Karwaski, M. F.; Wakarchuk, W. W.; Gilbert, M. *Protein expression and purification*. **2000**, 25, 237-40.
- <sup>26</sup> Li, Y.; Yu, H.; Cao, H.; Lau, K.; Muthana, S.; Tiwari, V. K.; Son, B.; Chen, X. *Applied microbiology and biotechnology*, **2008**, 79, 963-70.
- <sup>27</sup> Lattová, E.; Perreault, H. *Methods Mol Biol*. **2009**, 534:65-77.

- 
- <sup>28</sup> <https://ilab.acdlabs.com/iLab2/>
- <sup>29</sup> Kim, J.Y.; Kim, Y.G.; Lee, G.M. *Appl Microbiol Biotechnol.* **2012**, 93, 917-930.
- <sup>30</sup> Durocher, Y.; Butler, M. *Curr Opin Biotechnol.* **2009**, 20, 700-707.
- <sup>31</sup> Schachter, H. *Biochem. Cell Biol.* **1986**, 64(3), 163-181.
- <sup>32</sup> Spearman, M.; Bodnar, E.D.; Perreault, H.; Butler, M. *Pharmaceutical Bioprocessing.* **2014**, 2(5), 449-468.
- <sup>33</sup> Shibuya, N.; Goldstein, I.J.; Broekaert, W.F.; Nsimba-Lubaki, M.; Peeters, B.; Peumans, W.J. *J Biol Chem.* **1987**, 262(4), 1596-1601.
- <sup>34</sup> Brennan, M.J.; David, J.L.; Kenimer, J.G.; Manclark, C.R. *J Biol Chem.* **1988**, 263(10), 4895-9.
- <sup>35</sup> O. Krokhin, W. Ens, K. G. Standing, J. Wilkins, H. Perreault. *Rapid Commun Mass Spectrom.* **2004**, 18, 2020-2030.
- <sup>36</sup> Baskin, J. M.; Prescher, J. A.; Laughlin, S. T.; Agard, N. J.; Chang, P. V.; Miller, I. A.; Lo, A.; Codelli, J. A.; Bertozzi, C. R. *Proceedings of the National Academy of Sciences of the United States of America.* **2007**, 104, 16793-7.
- <sup>37</sup> Mbua, N.E.; Guo, J.; Wolfert, M.A.; Steet, R.; Boons, G.J. *Chembiochem.* **2011**, 12(12), 1912-21.
- <sup>38</sup> Luchansky, S.J.; Argade, S.; Hayes, B.K.; Bertozzi, C.R. *Biochemistry.* **2004**, 43(38):12358-66.
- <sup>39</sup> Jacobs, C. L.; Goon, S.; Yarema, K. J.; Hinderlich, S.; Hang, H. C.; Chai, D. H.; Bertozzi, C. R. *Biochemistry*, **2001**, 40, 12864-74.
- <sup>40</sup> Yarema, K.J.; Mahal, L.K.; Bruehl, R.E.; Rodriguez, E.C.; Bertozzi, C.R. *J Biol Chem.* **1998**, 273:31168–31179.

---

<sup>41</sup> Almaraz, R.T.; Aich, U.; Khanna, H.S.; Tan, E.; Bhattacharya, R.; Shah, S.; Yarema, K.J.

*Biotechnol Bioeng.* **2012**. 109(4):992-1006.

<sup>42</sup> Smeekens, J.M.; Chen, W.; Wu, R. *J. Am. Soc. Mass Spectrom.* **2014**, ahead of print, doi:

10.1007/s13361-014-1016-7.

## **Chapter 6 –Considerations & Future Work**

## 6.0 Conclusions

### 6.01 General Overview

The understanding of the field of Glycobiology is quickly expanding in part, due to the sensitive methods developed for improved analysis of glycans by MS. These methods serve as tools which allow researchers to probe deeper into the glycome, generating a better understanding of the role of glycoproteins in cell biology and medicine. For example, two closely related sialic acids Neu5Ac and Neu5Gc (which differ by a single oxygen), have been studied with their relationship towards malignancies such as cancer<sup>1,2</sup>. The conclusion from this research is that the latter glycan Neu5Gc is acquired endogenously through diet and may serve to promote chronic inflammation and cancer progression. Results such as this provide insight for clinicians, dieticians, oncologists and researchers alike who work concertedly to understand the information which has been generated. Given a thorough understanding and analysis of a certain glycoprotein, these individuals can further modify various aspects of its synthesis in order to promote a desired effect. For example, immunoglobulins (Ig) are glycoproteins known to be involved in the immunological processes which help remove antigens from the immune system. One such commercial example is known as Herceptin (Trastuzumab) which is a humanized mouse IgG that has been modified to bind to the HER2 receptor shown to be upregulated on breast cancers. The ability to target glycoproteins in order to analyze and understand their structure, therefore, can answer questions about their function and provide developments which will enhance our understanding of modern medicine.

Over the past 5 years, many workflows for MS-based glycoproteomics and glycomic analyses have been developed. These techniques, and the ones presented in this dissertation, were performed as “bottom-up” procedures involving the use of normal-phase separation approaches such as HILIC<sup>3,4</sup> and protocols using TiO<sub>2</sub> particles<sup>5,6,7</sup> to enrich N-linked glycosylated peptides from proteolytic digests for improved MS analysis. During this time period, many improvements have been made on commercial mass spectrometers which have aided in better analytical sensitivity for glycan analysis; namely advancements in mass analyzers such as ion traps, and improved fragmentation options such as higher-energy collision dissociation (HCD)<sup>8</sup> and electron transfer dissociation (ETD)<sup>9</sup>. Through the combination of HILIC based separations and these improved fragmentation methods for MS, researchers are now able to probe deeper into the glycome<sup>10,11</sup>.

ETD fragmentation is known to preserve labile modifications such as glycosylation, and therefore has extended direct site mapping to O-linked glycans<sup>12,13</sup>. This approach is based on the random transfer of electrons from a donor molecule to form radicals which induce cleavage in no specific manner. This results in longer stretches of peptides with c/z ion fragmentation patterns that allow for simultaneous site-specific characterization.

In addition, newer fragmentation methods have allowed researchers to begin studying glycoproteins from a “top-down” perspective<sup>14</sup>. Top down methods refer to the introduction of an intact glycoprotein into the mass spectrometer without enzymatic or chemical digestion and instead rely on the fragmentation patterns produced by the MS as the first step of characterization. This methodology offers many advantages including a lower sample

consumption, and the fingerprinting of all glycoforms in mass if the MS resolution is sufficient. The major drawback of this approach is that there is limited information in relation to the site-specific characterization of glycans generated on intact proteins. If MS/MS is performed at the top-down level, the average size of fragments obtained is still too large to yield detailed sequence characterization, for the glycan as much as for the peptide<sup>15</sup>. For this reason, researchers still employ “bottom-up” experiments combining the complementary information obtained from glycan and glycopeptide analysis.

Even with these improvements, key challenges still need to be addressed. These include the ability to separate structural isomers, as well as analysis of negatively charged glycans such as sialic acids and sulfate moieties which currently involve switching MS polarity, or specialized derivatization protocols for improved MS analysis<sup>16</sup>. Recently, some chromatographic stationary phases have been presented by industry at the past American Society for Mass Spectrometry conference (ASMS, 2014), which are based on carbohydrate polymers with nearly identical structure to those developed in Chapter 4 (personal communication, Thermo Fisher, 2014). Four general topics have surfaced for future considerations in the field:

- 1) The need for improved enrichment and separation techniques at the glycopeptide level. These have been dramatically improved through a variety of enrichment techniques using cellulose, amine magnetic nanoparticles, TiO<sub>2</sub>, etc. However, future work in this area needs to address absolute enrichment values in order to have a better understanding of the entire glycome which is being analyzed, as well as the efficiency of each technique if they are to be implemented in routine analysis. These

enrichment protocols should also include unique multi-mixed mode approaches for targeting sialylation and sulfation.

- 2) As enrichment techniques are improving, the ability to separate structural isomers has lagged behind. Future researchers may choose to explore niche glyco materials, including carbohydrate polymers, uniquely synthesized stationary phases, or derivatization protocols for cleaner, selective isolation of desired glycoforms. Alternatively or in parallel, groups may focus on MS<sup>n</sup> acquisition workflows<sup>17</sup> which probe deeper into the glycome observing unique cleavage patterns on select portions of molecules in order to create a so-called MS glycan fragmentation library which may also aid in understanding and comparing these isomers.
- 3) Quantification is an important analytical area which allows the researcher to compare expression of a particular component(s) between multiple experiments. Since isobaric tags have been introduced and implemented for relative quantification of glycopeptides, as well as the recent introduction of isobaric tags at the glycan level, these tools have flourished in both proteomic and glycomic workflows<sup>18,19</sup>, offering duplex kits, 6-plex kits and 10-plex kits which allow for 10 unique samples to be compared in a single run. Expanding beyond this however has been challenging presumably due to the “linker/expansion” region of the molecule and the cleavage sites of the reporter ions. This comes at a cost of both sensitivity and structural elucidation, as expanding the ability to multiplex creates more molecules to isotopically manipulate and also creates more competing fragment



ions<sup>20</sup>. Research groups are currently working on this problem and it will be interesting to see what is developed.

- 4) With many improvements in the realm of MS over the past few years, this has also generated larger data sets. As even more improvements are made in points 1, 2 and 3, the ability to organize and process this data both efficiently and accurately will need to be addressed. Some bioinformatic programs are currently addressing this which include: SimGlycan™ (Primier Biosoft)<sup>21</sup> and Byonic (Protein Metrics)<sup>22</sup>. These two programs have been highlighted as they are capable of elucidating spectra from a variety of instrumentation at both the glycan and glycopeptide levels, as well as interpreting for N and O-linked fragmentation patterns. As new improvements and tools are made in the field, changes need to be made to the software including new fragmentation options, unique moieties, and even better organizational options which may include probing output files for select information such as TMT (personal communication, ProteinMetrics Inc., 2014). Since Glycobiology is an extremely diverse field, glycobiologists will need to work alongside computer programmers in order to fully address this issue. It will not be surprising to see a large push from the community for better programs in the near future.

## 6.02 Analysis of Highly Sialylated Glycoproteins

Chapter 2 of the dissertation focused on optimizing an adapted HPLC procedure to isolate glycopeptides of mAbs followed by an on-target derivatization of glycans using phenylhydrazine for improved MS analysis<sup>23,24</sup>. This workflow aimed to measure the degree of sialylation on mutant vs. non-mutant monoclonal antibodies at the glycopeptide and glycan levels. Using this methodology, glycopeptides were isolated and characterized in both the positive and negative modes. In light of this, multiple adducts of each glycoform were produced making quantification of a single species difficult at the glycopeptide level. To overcome this, glycans were detached from the antibodies which made qualitative spectral interpretation much simpler. Through MS comparison of the mutant mAbs to their non-mutant counterparts, higher levels of both the FG2S1 and FG2S2 glycoforms were observed as suggested from a previous report<sup>25</sup> indicating that the goal of this experiment was achieved. Currently, the analysis of sialylation appears to be migrating towards the use of ESI based instruments as MALDI-MS is known to cleave labile sialic acids and underestimate their expression as shown through a recent comparison using a HILIC approach<sup>26</sup>.

Since this work was completed, our group has conducted further experiments at the glycopeptide level to investigate the source and location of overalkylation adducts<sup>27</sup>. Our preliminary results suggest that the adduct at  $M+39^+$  occurs as a result of dehydration of +57 adducts between the first glutamic acid and N-terminal backbone which has also been reported in literature<sup>28</sup>. Two major adjustments to alleviate this complication have since been introduced to this workflow. Firstly, the concentration of iodoacetamide has been reduced and secondly a

fast clean up procedure has been implemented to remove excess iodoacetamide. This clean up procedure can be performed using multiple approaches. One such example that has shown improvement was the use of MWCO spin filters to retain the alkylated protein and filter out excess iodoacetamide<sup>29</sup>. This approach is fast (15 mins) and highly reproducible with high recovery yields, however it is costly especially if it is to be implemented in a high throughput environment due to the single-use of the MWCO filters. Alternatively, one can 'desalt' the protein on a solid-phase extraction cartridge (or custom made 'stage tip'), which generally hail lower costs and the added benefit of multiple uses provided they are well maintained. This latter approach has been implemented into our workflow and provides remarkably cleaner spectra with single peaks for each glycosylated species.

With the exception of excess iodoacetamide, the workflow presented here is easily reproducible, efficient and fast, providing results in approximately 22 hours with >95% of this consumed by enzymatic digestion. In light of this, one may want to optimize the optimal time-frames for reduction, alkylation and trypsinization, as newer methods based on microwave digestion have significantly reduced preparation time<sup>30,31,32</sup>. In addition, one may want to investigate whether detaching glycans at the protein level provide the same quantifiable data as detachment at the peptide level, since this would dramatically reduce handling steps and increase the speed of this protocol. In conjunction with automated acquisition methods, this demonstrates itself as a useful workflow for glycan characterization of mAbs.

### 6.03 Magnetic Nanoparticles for Glycopeptide Enrichment

The work presented here along with similar protocols using functionalized nanoparticles<sup>33,34</sup> has shown great promise for enriching glycopeptides from a variety of samples as outlined in Chapter 3. More specifically, this experiment aimed to enrich sialylated glycopeptides and to compare this approach to that of a commercially available glycopeptide enrichment kit through the use of tandem mass tags (Figure 1.19) for relative quantification by MS.

As demonstrated by the data presented in this chapter, this method allows a higher level of sialylated glycopeptides to be detected as compared to that of a commercially available glycopeptide kit. This ultimately leads to improved sensitivity through mass spectrometry, and the possibility to study this unique glycan in more detail.

This method however is not a single approach for enriching glycopeptides as two key concerns should be addressed. Firstly, this approach was applied to a sample set in which only 2 of the 4 glycoproteins were highly sialylated ( $\alpha$ 1 acid and fetuin). While, these 2 glycoproteins suggest a trend in which the amine functionalized magnetic nanoparticles outperform the commercial kit, a larger sample size of sialylated glycoproteins should be tested for confirmation. Secondly, while this method out-performed the commercial kit regarding sialylation, glycopeptides which were non-sialylated were enriched on average ~2.7x more by the commercial kit, suggesting that this approach may be an application for targeted glycopeptides.

Important features of this work include the smaller size of the magnetic nanoparticles (5-8 nm) compared to others used for similar purposes<sup>35,36</sup>, which increases the surface area for interactions. In addition, the speed of the overall technique is comparable to that of a similar approach in literature<sup>37</sup>. All things considered, it would be interesting to test this method on a larger more complex sample such as a serum, which contains a more diverse mixture of glycoproteins. Here, further studies could evaluate the aforementioned trend, as well as further optimize the loading capacity of the magnetic nanoparticles compared to that of the commercial kit, and explore the cost-to-benefit ratio.

#### **6.04 Carboxymethyl Chitosan for Glycopeptide Enrichment**

The work presented in Chapter 4 of this dissertation was an expansion on a previous methodology using cellulose to enrich glycopeptides for downstream mass spectrometry<sup>38</sup>. Here, a novel mixed-mode stationary phase was designed (Figure 4.1) which aimed to exploit the hydrophilicity of the glycan (HILIC), as well as any electrostatic interactions (WAX) of glycans through a carbohydrate polymer known as chitosan. Using tandem mass tags for relative quantification (Figure 1.19), this niche mixed-mode approach demonstrated on average ~13% more recovery of sialylated glycopeptides as compared to a commercially available glycopeptide enrichment kit. Unique trends were observed in multiple samples which demonstrated that as the sialylation on the glycan increased, so did its propensity to bind to the stationary phase.

These trends were observed on a digest containing 12 proteins, 7 of which were glycosylated, 3 of which contained relatively high amounts of sialylation. In nearly all sialylated

samples, this method demonstrated improved enrichments over the commercial kit. The ability of this method to enrich sialylated species was also extended to immunoglobulin samples which typically contain low amounts of sialylation<sup>39,40</sup>. Of the sialylated glycoforms recovered for comparison from these constructs, CMCH yielded on average ~17% higher recovery of sialylated glycopeptides than the commercially available kit despite it recovering 2.7x more total glycopeptides than CMCH.

Since chitosan is a naturally occurring carbohydrate polymer, this makes its attachment onto stationary phases very affordable. Furthermore, it quantitatively demonstrated the ability to enrich sialylated glycopeptides over a commercially available enrichment kit. Notwithstanding these advantages, this methodology should be further investigated with more complex samples which contain a wider variety of sialylation in order to assess its affinity in full. This may include using a polysialic acid ladder to confirm whether or not there is a linear relationship in the binding affinity, and if so, this approach should also be tested on a sample such as human serum.

## 6.05 Glyco-Engineering using ManAz for the Analysis of Sialylation in Mabs

The goal of the research in this chapter was to use mass spectrometry to investigate a unique workflow on IgG constructs which are applicable to the biotherapeutic industries<sup>41,42</sup>. These preliminary experiments synthesized an azide-modified sialic acid precursor (Ac<sub>4</sub>ManAz) and stepwise increased its concentration introduced into each mAb culture. These experiments were performed in an attempt to determine the optimal concentration of precursor necessary for expression of SiaNAz. As a standard reference for comparison, mAbs were cultured without introducing Ac<sub>4</sub>ManAz. They were then desialylated, cleaned, and reincubated with CMP-SiaNAz plus galactoside- $\alpha$ 2,6-sialyltransferase 1 (ST6Gal1). Enzymatically, SiaNAz was observed as a singly sialylated mAb with no endogenous sialylation detected. Through mass spectrometric comparison, it was determined that concentrations of around 100  $\mu$ M of the Ac<sub>4</sub>ManAz precursor were necessary for expression of azide containing sialic acids, which were observed in both the singly and doubly sialylated glycoforms. The results obtained from this experiment are on the order as those reported in literature using similar methods<sup>43,44</sup>.

Future experiments regarding this workflow should investigate higher concentrations of Ac<sub>4</sub>ManAz precursor to determine if higher yields of SiaNAz can be obtained. This approach can also be extended to fucosylation to see whether it has the same expression as sialic acids in CHO cells. Moreover, unique 'click' labels can be explored both for UV or fluorescent detection, either online or offline with HPLC.

Another interesting experiment regarding site-specific glycosylation of mAbs may involve fluorescent labeling the mAb to determine if sialylation or fucosylation is present on

both glycans within the Fc region of the molecule. Furthermore, this approach may also be used as a quantitative method for determining absolute amounts of sialylation or fucosylation provided that an appropriate UV or fluorescent 'click' label is chosen. This would be beneficial for quantification, as the removal of the glycan or monosaccharide from the mAb is no longer required, in effect reducing the number of steps in the workflow.

Lastly, as both fucosylation and sialylation are important regulators of mAb efficacy, quantification by this approach in an array of different cell lines would easily allow the researcher to systematically choose the cell types and variables which provide the desired levels of expression.

## 6.1 Closing Summary

Future work should strongly focus on improving the enrichment yields of glycopeptides as well as targeted enrichment of specific glycoforms for downstream MS analysis, namely sialylation and sulfation. Techniques need to be developed that are facile and economically viable which also can be easily adapted to high-throughput workflows without compromising qualitative or quantitative information. The use of cellulose as a stationary phase has demonstrated these qualities and cellulose is an appropriate material that can be easily adapted into any workflow. For more selective enrichments, the use of functionalized magnetic nanoparticles and carboxymethyl chitosan have demonstrated facile methods for improved enrichment of sialylated glycopeptides with minimal handling and cleaning. This constitutes an improvement over some currently employed methods.



Interestingly, glyco-engineering has also become an important area for detection and isolation of glycans using a bio-orthogonal azide moiety capable of downstream specific 'click' chemistry<sup>45</sup>. This approach offers numerous improvements for targeted analysis both by way of unique labeling options or for specific enrichment options such as 'click'-able magnetic nanoparticles, stationary phases, etc. In each case, these methods need to be compared in terms of their ability for absolute enrichment. I anticipate that many of these aims will materialize in the near future as I can see them being of great benefit to those who partake in their study. I look forward to further developing techniques that are related to this field.

## 6.2 References

---

- <sup>1</sup> Samraj, A.N.; Pearce, O.M.; Läubli, H.; Crittenden, A.N.; Bergfeld, A.K.; Banda, K.; Gregg, C.J.; Bingman, A.E.; Secrest, P.; Diaz, S.L.; Varki, N.M.; Varki, A. *Proc Natl Acad Sci U S A*. 2015, 112(2), 542-7.
- <sup>2</sup> Samraj, A.N., Läubli, H.; Varki, N.; Varki A. *Front Oncol*. **2014**, 19; 4, 33.
- <sup>3</sup> Wohlgemuth, J.; Karas, M.; Eichhorn, T.; Hendriks, R.; Andrecht, S. *Anal Biochem*. 2009, 395(2), 178-88.
- <sup>4</sup> Hernandez-Hernandez, O.; Lebron-Aguilar, R.; Quintanilla-Lopez, J.E.; Sanz, M.L.; Moreno, F.J. *Proteomics*. 2010, 10(20), 3699-711.
- <sup>5</sup> Palmisano, G.; Lendal, S.E.; Engholm-Keller, K.; Leth-Larsen, R.; Parker, B.L.; Larsen, M.R. *Nat Protoc*. **2010**, (12), 1974-82.
- <sup>6</sup> Zhang, B.; Sheng, Q.; Li, X.; Liang, Q.; Yan, J.; Liang, X. *J Sep Sci*. **2011**, 34(19) , 2745-50.
- <sup>7</sup> Palmisano, G.; Lendal, S.E.; Larsen, M.R. *Methods Mol Biol*. **2011**, 753, 309-22.
- <sup>8</sup> Olsen, J.V.; Macek, B.; Lange, O.; Makarov, A.; Horning, S.; Mann, M. *Nat Methods*. **2007**, 4(9), 709-12.
- <sup>9</sup> Syka, J.E.; Coon, J.J.; Schroeder, M.J.; Shabanowitz, J.; Hunt, D.F. *Proc Natl Acad Sci U S A*. **2004**, 101(26), 9528-33.
- <sup>10</sup> Zhao, P.; Viner, R.; Teo, C.F.; Boons, G.J.; Horn, D.; Wells, L. *J Proteome Res*. **2011**,10(9), 4088-104.
- <sup>11</sup> Singh, C.; Zampronio, C.G.; Creese, A.J.; Cooper, H.J. *J Proteome Res*. **2012**, 11(9), 4517-25.
- <sup>12</sup> Kjeldesen, F.; Giessing, A.M.B.; Ingrell, C.R.; Jensen, O.N. *Anal Chem*.2007, 79, 9243-52.

- 
- <sup>13</sup> Housley, M.P.; Rodgers, J.T.; Udeshi, N.D.; Kelly, T.J.; Shabaowitz, J.; Hunt, D.F.; Puigserver, P.; Hart, G.W. *J Biol Chem.* **2008**, 283(24), 16283-92.
- <sup>14</sup> Hanisch, F.G. *Methods Mol Bio.* **2012**, 842, 179-189.
- <sup>15</sup> Zhang, Z.; Pan, H.; Chen, X. *Mass Spectrom Rev.* **2009**, 28(1), 147-76.
- <sup>16</sup> Toyoda, M.; Ito, H.; Matsuno, Y.; Narimatsu, H.; Kameyama, A. *Anal Chem.* 2008, 80, 5211-5218.
- <sup>17</sup> McAlister, G.C.; Nusinow, D.P.; Jedrychowski, M.P.; Wühr, M.; Huttlin, E.L.; Erickson, B.K.; Rad, R.; Haas, W.; Gygi, S.P. *Anal Chem.* **2014**, 86(14), 7150-8.
- <sup>18</sup> Viner, R.I.; Zhang, T.; Second, T.; Zabrouskov, V. *J Proteomics.* **2009**, 72(5), 874-85.
- <sup>19</sup> Ye, H.; Boyne, M.T. 2nd; Buhse, L.F.; Hill, J. *Anal Chem.* **2013**, 85(3), 1531-9.
- <sup>20</sup> McAlister, G.C.; Huttlin, E.L.; Haas, W.; Ting, L.; Jedrychowski, M.P.; Rogers, J.C.; Kuhn, K.; Pike, I.; Grothe, R.A.; Blethrow, J.D.; Gygi, S.P. *Anal Chem.* **2012**, 84(17), 7469-78.
- <sup>21</sup> Apte, A.; Meitei, N.S. *Methods Mol Biol.* **2010**, 600, 269-81.
- <sup>22</sup> Bern, M.; Kil, Y.J.; Becker, C. *Curr Protoc Bioinformatics.* **2012**, Dec;Chapter 13:Unit13.20.
- <sup>23</sup> Lattová, E.; Perreault H. *Methods Mol Biol.* **2009**, 534, 65-77.
- <sup>24</sup> Lattová, E.; Perreault H. *J Chromatogr B Analyt Technol Biomed Life Sci.* **2003**, 793(1), 167-79.
- <sup>25</sup> Jassal, R.; Jenkins, N.; Charlwood, J.; Camilleri, P.; Jefferis, R.; Lund, J. *Biochem Biophys Res Commun.* **2001**, 286(2), 243-249.
- <sup>26</sup> Raymond, C.; Durocher, Y.; *et al. Mabs*, **2015**; in submission.
- <sup>27</sup> Oliveira, A.; Roy, R.; Raymond, C.; Bodnar, E.; Tayi, V.; Butler, M.; Durocher, Y.; Perreault, H. *Rapid Commun Mass Spectrom.* **2015**; in submission.

- 
- <sup>28</sup> Yu, L.; Vize, A.; Huff, M.B.; Young, M.; Remmele Jr., R.L.; He, B. *J Pharm Biomed Anal.* **2006**, 42, 455.
- <sup>29</sup> Manza, L.L.; Stamer, S.L.; Ham, A.J.; Codreanu, S.G.; Liebler, D.C. *Proteomics.* **2005**, 5(7), 1742-5.
- <sup>30</sup> Zhou, H.; Froehlich, J.W.; Briscoe, A.C.; Lee, R.S. *Mol Cell Proteomics.* **2013**, (10), 2981-91.
- <sup>31</sup> Chen, Z.; Li, Y.; Lin, S.; Wei, M.; Du, F.; Ruan, G. *Biochem Biophys Res Commun.* **2014**, 445(2), 491-6.
- <sup>32</sup> Taverna, D.; Norris, J.L.; Caprioli, R.M. *Anal Chem.* **2015**, 87(1), 670-6.
- <sup>33</sup> Zhang, Y.; Wang, H.; Lu, H. *Mol Biosyst.* **2013**, 9(3), 492-500.
- <sup>34</sup> Yeh, C.H.; Chen, S.H.; Li, D.T.; Lin, H.P.; Huang, H.J.; Chang, C.I.; Shih, W.L.; Chern, C.L.; Shi, F.K.; Hsu, J.L. *J Chromatogr A.* **2012**, 1224, 70-8.
- <sup>35</sup> Tang, J.; Lui, Y.; Yin, P.; Yao, G.; Yan, G.; Deng, C.; Zhang, X. *Proteomics.* **2010**, 10(10):2000-2014.
- <sup>36</sup> Wang, L.; Bao, J.; Wang, L.; Zhang, F.; Li, Y. *Chemistry.* **2006**, 12(24): 6341-6347.
- <sup>37</sup> Kuo, C.W.; Wu, I.L.; Hsiao, H.H.; Khoo, K.H. *Anal Bioanal Chem.* **2012**, 402(9), 2765-76.
- <sup>38</sup> Snovid, S.I.; Bodnar, E.D.; Viner, R.; Saba, J.; Perreault, H. *Carbohydr Res.* **2010**, 345(6), 792-801.
- <sup>39</sup> Sybille, B.; Schwab, I.; Lux, A.; Nimmerjahn, F. *Semin Immunopathol.* **2012**, 34, 443-453.
- <sup>40</sup> Anumula, K.R. *J Immunol Meth.* **2012**, 381(1-2), 167-176.
- <sup>41</sup> Baselga, J.; Norton, L.; Albanell, J.; Kim, Y.M.; Mendelsohn, J. *Cancer Res.* **1998**, 58(13), 2825-31.
- <sup>42</sup> Robertson, D. *Nat Biotechnol.* **1998**, 16(7), 615.

---

<sup>43</sup> Baskin, J.M.; Prescher, J.A.; Laughlin S.T.; Agard, N.J.; Chang, P.V.; Miller I.A.; Lo, A.; Codelli, J.A.; Bertozzi, C.R. *Proc Natl Acad Sci USA*. **2007**. 104(43), 16793-16797.

<sup>44</sup> Mbua, N.E.; Guo, J.; Wolfert, M.A.; Steet, R.; Boons, G.J. *Chembiochem*. **2011**. 12(12), 1912-21.

<sup>45</sup> Smeekens, J.M.; Chen, W.; Wu, R. *J. Am. Soc. Mass Spectrom*. **2014**, ahead of print, doi: 10.1007/s13361-014-1016-7.